1988

Fast transport of cobalt in thorium

Steven C. Axtell
Iowa State University

Order Number 8825899

Fast transport of cobalt in thorium

Axtell, Steven C., Ph.D.

Iowa State University, 1988

U·M·I
300 N. Zeeb Rd.
Ann Arbor, MI 48106

PLEASE NOTE:

In all cases this material has been filmed in the best possible way from the available copy. Problems encountered with this document have been identified here with a check mark __✓__.

1. Glossy photographs or pages _____
2. Colored illustrations, paper or print _____
3. Photographs with dark background _____
4. Illustrations are poor copy _____
5. Pages with black marks, not original copy __✓__
6. Print shows through as there is text on both sides of page _____
7. Indistinct, broken or small print on several pages __✓__
8. Print exceeds margin requirements _____
9. Tightly bound copy with print lost in spine _____
10. Computer printout pages with indistinct print _____
11. Page(s) _____ lacking when material received, and not available from school or author.
12. Page(s) _____ seem to be missing in numbering only as text follows.
13. Two pages numbered _____. Text follows.
14. Curling and wrinkled pages _____
15. Dissertation contains pages with print at a slant, filmed as received _____
16. Other _____

_____

_____

Fast transport of cobalt in thorium

by

Steven C. Axtell

A Dissertation Submitted to the

Graduate Faculty in Partial Fulfillment of the

Requirements for the Degree of

DOCTOR OF PHILOSOPHY

Department: Materials Science and Engineering
Major: Metallurgy

Approved:

Signature was redacted for privacy.

In Charge of Major Work

Signature was redacted for privacy.

For the Major Department

Signature was redacted for privacy.

For the Graduate College

Iowa State University
Ames, Iowa

1988

TABLE OF CONTENTS

	Page
GENERAL INTRODUCTION	1
Explanation of Thesis Format	12
REFERENCES CITED	13
SECTION I. AN INVESTIGATION OF A METASTABLE $ThCo_x$ PHASE AND THE SOLID SOLUBILITY OF COBALT IN THORIUM IN DILUTE THORIUM-COBALT ALLOYS	15
INTRODUCTION	16
EXPERIMENTAL PROCEDURES	19
RESULTS	21
Solid Solubility Studies	21
Metastable Plate Phase	28
Quenching Studies	28
Aging Studies	36
DISCUSSION	44
CONCLUSIONS	47
REFERENCES CITED	48
SECTION II. A STUDY OF THE MECHANISM OF FAST DIFFUSION OF COBALT IN THORIUM USING DIFFUSION AND INTERNAL FRICTION EXPERIMENTS	49
INTRODUCTION	50
EXPERIMENTAL PROCEDURES	55
Materials and Sample Preparation	55
Method	56
Diffusion	56

Internal friction 57

RESULTS 60

Diffusion Studies 60

Internal Friction Studies 60

DISCUSSION 73

Substitutional-interstitial Pairs 78

CONCLUSIONS 84

REFERENCES CITED 85

SECTION III. A STUDY OF THE THERMOTRANSPORT BEHAVIOR OF COBALT IN THORIUM 87

INTRODUCTION 88

THEORY 91

EXPERIMENTAL PROCEDURES 93

Materials and Sample Preparation 93

Mass Transport Studies 93

Two-Phase Nonsteady-State Technique 97

RESULTS 100

Thermotransport in Single-Phase Alloys 100

Thermotransport in Two-Phase Alloys 104

Q* Versus Temperature 110

DISCUSSION 112

CONCLUSIONS 116

REFERENCES CITED 117

SUMMARY AND DISCUSSION 119

ACKNOWLEDGEMENTS 121

APPENDIX 122

GENERAL INTRODUCTION

Just before the turn of the century, Roberts-Austen discovered that gold diffuses rapidly in lead (1). This was the first observation of the phenomenon that has become known as "fast diffusion". Over the past twenty years several reviews have been written on this subject (2-5). Fast diffusion is associated with metal-metal systems in which the solute migrates at a much faster rate than the solvent. In general, it is observed that the solute diffusivity is at least one order of magnitude greater than the self-diffusivity of the solvent and the activation energy for solute diffusion is significantly less than that for self-diffusion of the host metal. It is interesting to note that, although the diffusion properties of these systems are similar to those involving the interstitial elements carbon, oxygen and nitrogen, the ratio between the solute and solvent atom sizes generally exceeds the Hägg limit for the formation of interstitial solutions (2).

The number of systems in which fast diffusion has been observed has grown substantially over the past thirty years. It has been generally found that 1) elements of Groups I and II, including the late transition elements, i.e., transition elements located on the right side of the Periodic Table, are fast diffusing in In, Sn, Tl and Pb as well as some lanthanide and actinide elements, 2) late transition elements diffuse fast in some early transition elements, i.e., transition elements located on the left side of the Periodic Table, and 3) Group IB elements are fast diffusing in the alkaline metals (5). More recently, fast diffusion has been observed in several systems involving thorium as the host metal.

These include iron, nickel and cobalt (6) and molybdenum, tungsten and rhenium (7).

The primary concern of researchers in this field has been the identification of the mechanism responsible for fast diffusion. At one time it was believed that this phenomenon might be due to grain boundary or dislocation short-ciruiting. Later, it was shown by Ascoli that gold diffuses as fast in single as in polycrystalline lead specimens (8). In addition, Kidson observed that the introduction of dislocations into a single-crystal lead specimen did not have any significant effect on the diffusivity of gold (9). Therefore, it was concluded that fast diffusion was proceeding by a bulk diffusion mechanism, which at that time was believed to be either a vacancy or an interstitial mechanism.

An experimental technique that has been used to establish whether a vacancy mechanism is operating in fast diffusing systems is the measurement of the linear enhancement factor, b, for the self-diffusion of the solvent metal (10). For small solute concentrations, i.e., <2 at.%, this factor is described by

$$D_H(x) = D_H(o)\ (1 + bx) \qquad (1)$$

where $D_H(x)$ and $D_H(o)$ are the diffusion coefficients of the solvent metal in the alloy and in the pure solvent and x is the solute concentration in the alloy (11). The enhancement of the self-diffusion of the host metal is the result of interactions between solute atoms and vacancies which can alter the equilibrium fraction of vacancies and from solute-solvent

interactions which can change neighboring solvent-vacancy exchange frequencies (10). Experimentally, the self-diffusivity of the solvent is measured in the pure solvent metal and in several dilute alloys which contain different amounts of the fast diffusing solute. The linear enhancement factor is then obtained from the slope of a plot of $D_H(x)/D_H(o)$ versus x according to equation (1). Based on the five frequency model of Howard and Manning (11), the minimum value of b that is consistent with a vacancy mechanism is given by

$$b_{min} = -18 + 1.9448 \left[D_S/D_H(o)\right] \qquad (2)$$

where D_S is the solute diffusivity and $D_H(o)$ is the self-diffusivity in the pure solvent (10). Therefore, for a given system, a comparison between the value of b_{min} calculated from equation (2) and the value of b determined experimentally may indicate whether a vacancy mechanism is operating.

Calculated values for b_{min} and experimentally determined values of b have been reported for gold, silver, cadmium and mercury in lead (10,12-14). For silver and gold in lead, b is about a factor of 12 and 40, respectively, less than b_{min}. For cadmium in lead b was found to be about a factor of 1.1 to 1.5 less than b_{min} over the temperature range 198.7 to 300.5°C, whereas for mercury in lead b was observed to be about a factor of 1.3 to 2.3 greater than b_{min} over the temperature range 225.5 to 294.6°C. Therefore, on the basis of this self-diffusion enhancement

criterion, the vacancy mechanism can be rejected for the Pb-Au, Pb-Ag and possibly Pb-Cd system, but may be admitted for the Pb-Hg system (5).

Having ruled out a vacancy mechanism, it was believed that many of the fast diffusing systems form partially or wholly interstitial solutions with the solute diffusing interstitially (2). Frank and Turnbull proposed a dissociative model in which the solute occupies both substitutional and interstitial sites and migrates predominantly by an interstitial mechanism (15). According to this model, the solute diffusivity, D, is described by

$$D = \frac{c_i}{c_i + c_s} D_i + \frac{c_s}{c_i + c_s} D_s \qquad (3)$$

where c_i and c_s are the solute concentrations in interstitial and substitutional sites, respectively, and D_i and D_s are the corresponding diffusivities. Since it is expected that D_i is much greater than D_s, it was assumed that solute diffusion would be dominated by the interstitial mechanism even for small fractions of interstitials. Although it appeared that fast diffusion proceeds by an interstitial process in many fast diffusing systems, conclusive experimental evidence had not yet been obtained. Such evidence can be aquired from the measurement of the isotope effect (16).

Measurements of the isotope effect E have been made for copper, gold silver, mercury and cadmium in lead in order to determine the mechanism associated with fast diffusion in these systems (5,17-19). Isotope effect measurements can provide information about the value of the

correlation factor for tracer diffusion. The correlation factor is the fraction of jumps that is effective in causing random diffusion and is different for different diffusion mechanisms. E may be expressed as

$$E \equiv \left[(D_\alpha/D_\beta) - 1\right] / \left[(m_\alpha/m_\beta)^{\frac{1}{2}} - 1\right] = f_\alpha \Delta K \qquad (4)$$

where D_α and D_β are the diffusivites of isotopes α and β, m_α and m_β are the corresponding masses of the isotopes, f_α is the correlation factor of isotope α and ΔK is the fraction of the kinetic energy at the saddle point, associated with motion in the jump direction, that belongs to the diffusing atom (16). Both f_α and ΔK are bounded by zero and unity, therefore, E will be a value between zero and one. For an interstitial mechanism, involving the random jumping of single solute atoms between the interstices of a crystal, E is expected to be close to one (4). Experimentally it is observed that E is 0.25 at 300°C and 0.32 at 178°C for silver in lead, 0.23 at 319°C for copper in lead, 0.12 at 249°C for cadmium in lead, 0.26 over the temperature range 289 - 297°C for gold in lead and 0.25 at 225 and 297°C for mercury in lead. These relatively small values of E are not consistent with an interstitial mechanism and may indicate that, for these systems, solute diffusion is dominated by a highly correlated or multi-atom jump process (4). Two mechanisms that involve such processes are the interstitial-vacancy and host-solute diplon mechanisms (3).

In order to explain the diffusivity of cadmium in lead and the linear enhancement of the self-diffusion of lead due to additions of

cadmium, Miller (20) proposed a model in which cadmium diffusion is dominated by the migration of tightly-bound interstitial-vacancy pairs. The possibility of such defects was argued on the basis that a strong electrostatic interaction might occur between vacancies and cadmium ions located in interstitial sites. The proposed interstitial-vacancy pair, shown in Fig. 1, consists of an interstitially-sited solute atom and a vacancy which is located on one of the lattice sites nearest to the interstitial. The migration of these pairs is assumed to proceed by two steps: 1) interstitial jumps around the vacancy with the frequency k_2 (solid arrow in Fig. 1(a)) and 2) solvent jumps into the vacancy with the frequency w_2 (Fig. 1(b)) with $k_2 \gg w_2$. Long range diffusion by this process would be strongly correlated, which is consistent with the small value of the isotope effect parameter that was observed experimentally.

Warburton later modified this model to account for the self-diffusion enhancement of lead in the Pb-Hg system (3,13). In this version of the model it is assumed, from geometrical considerations, that the interstitial jumps (solid arrow in Fig. 1(a)) do not occur. Rather, it is suggested that the solute is mobile only through v_1 and v_2 jumps (broken arrows in Fig. 1(a)). Also, it is considered that the solvent jumps (shown in Fig 1(b)) occur at a much greater frequency than the v_2 jumps, i.e., $w_2 \gg v_2$. Although this variation of the interstitial-vacancy model can explain the observed enhancement of the self-diffusion of lead in the Pb-Hg and Pb-Cd systems and the isotope effect of cadmium in lead (4), it can not explain the isotope effect of mercury in lead which has recently been measured (5).

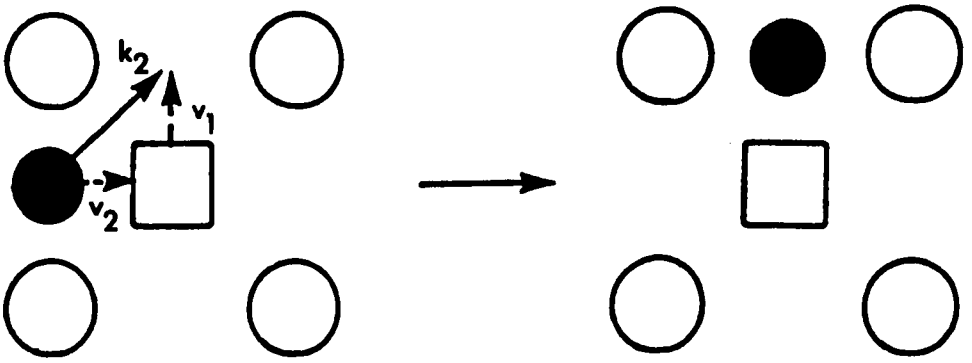

(a)

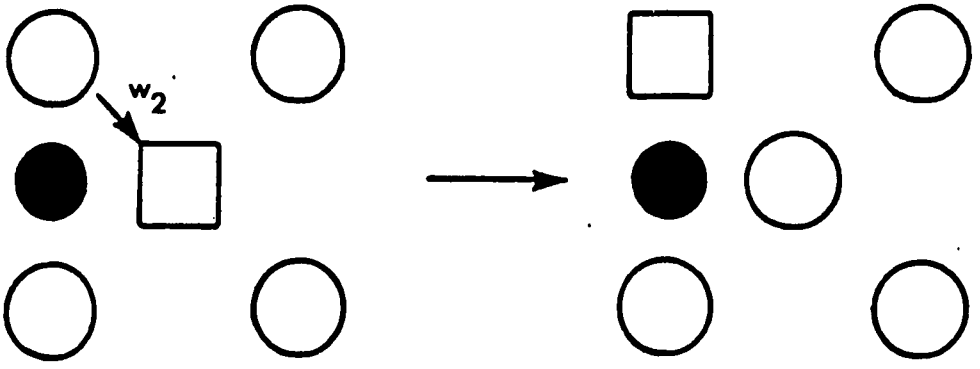

(b)

Figure 1. Schematic drawing of proposed interstitial-vacancy pair models showing the possible (a) solute jumps and (b) solvent jump

Based on the results of diffusion, self-diffusion enhancement and internal friction experiments on gold, copper and silver in lead, Warburton and Turnbull (3) proposed that, in these systems, fast diffusion proceeds by the migration of host-solute diplons. This defect, which has also been referred to as a host-solute split interstitial, consists of a solute atom and a solvent atom which share a lattice site. The host-solute diplon mechanism involves two jump processes, both of which are required for long-range diffusion. These jump processes are illustrated in Fig. 2 and include 1) the rotation of the defect pair about the lattice site (Fig. 2(a)) and 2) translation of the solute atom from one host atom to an adjacent one (Fig. 2(b)). Since the rotation jump involves two atoms, (one solute and one solvent atom) the value of the isotope effect corresponding to the diplon mechanism is expected to be significantly less than one, which is in qualitative agreement with that observed experimentally (3). The host-solute diplon mechanism, therefore, appears to provide a plausible explanation for the diffusion behavior of copper, gold and silver in lead.

On the basis of the work performed on the Pb-based fast diffusing systems, it is generally accepted that fast diffusing solutes dissociate into substitutional and interstitial-type defects upon dissolution in the host metal where diffusion is dominated by the migration of the interstitial-type defects (3). Here, interstitial-type defects refer to single interstitial atoms, interstitial-vacancy pairs or host-solute diplons. Evidence for solute-solute diplons has been reported (21-27),

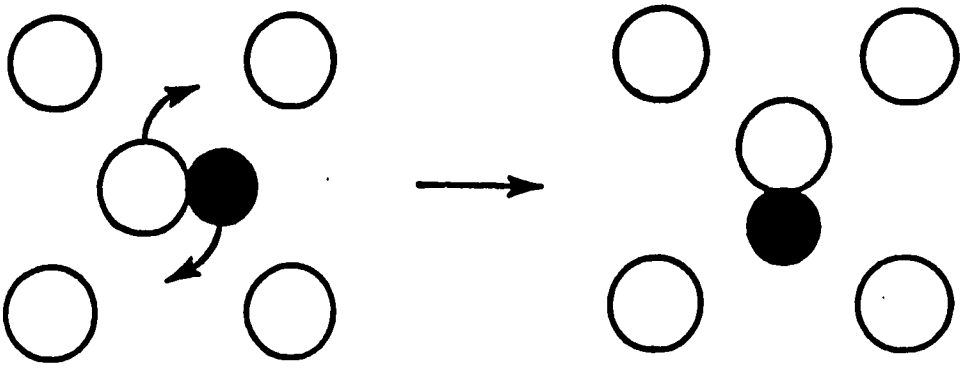

(a)

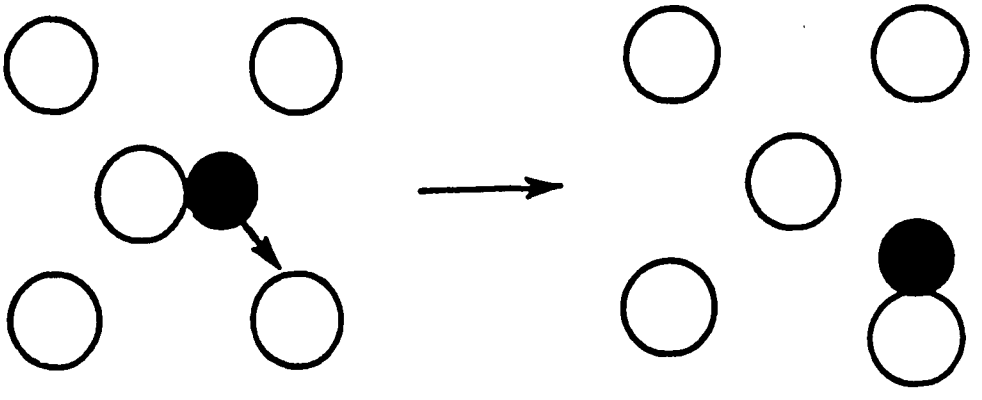

(b)

Figure 2. Schematic drawing of proposed host-solute diplon model showing the possible diplon motions of (a) rotation and (b) translation

although such defects are not expected to be responsible for fast diffusion (3).

Attempts to characterize the nature of the solute defects present in various fast diffusing systems have been made. Channeling experiments on gold in tin (28), X-ray and neutron diffraction studies on gold in lead (25,26) and possibly Mössbauer measurements on iron in yttrium (29) appear to indicate that a substantial fraction of the solute atoms are present as substitutionals, which suggest that a dissociative mechanism is operating. Internal friction experiments on copper, gold and silver in lead (30) appeared to indicate that these solute atoms may be associated with solute-solute or host-solute pairs, although the results of these experiments were not confirmed by Sagues and Nowick (31). Electron channeling experiments on gold in lead (32), centrifuge experiments on gold in sodium (33), indium (34) and lead (35), Mössbauer measurements on cobalt in indium (36) and quasielastic neutron scattering measurements on cobalt in zirconium (37) appear to indicate that the solute atoms in these systems are at least partially associated with interstitial-type defects. Although various experiments have provided information about the nature of the solute defects present in many fast diffusing systems, they have not established the exact nature and configuration of the defect responsible for fast diffusion.

Recently, Weins and Carlson (38) used internal friction to investigate the defects responsible for the fast diffusion of iron, nickel and cobalt in thorium. Two internal friction peaks were observed in each system suggesting that these solutes are associated with two

different types of defects that can be characterized as elastic dipoles. For iron and nickel, the similarity between the activation energy for relaxation for the high temperature peak and the activation energy for diffusion suggested that the defect producing this peak is responsible for diffusion. However, the data for cobalt was somewhat anomalous in that the two energies were quite different. The concentration dependence of the magnitude of the high temperature peak in the Th-Fe system was investigated and found to be linear suggesting that one iron atom is associated with the defect producing this peak. A similar investigation in the Th-Ni and Th-Co systems was not attempted, however. The analysis of the lower temperature peaks, including a study of the concentration dependence of the peak magnitude in the Th-Fe system, did not reveal any conclusive evidence as to the nature of this peak.

The present studies were undertaken to 1) characterize the defect responsible for the fast diffusion of cobalt in thorium using internal friction, 2) characterize the transport behavior of cobalt in thorium in the presence of a temperature gradient and 3) develop an understanding of the stable and metastable phases present at the thorium-rich end of the Th-Co system.

Initially it was planned to investigate the mechanism of fast diffusion of cobalt in thorium. The goals of this study were to determine the activation energies for diffusion and relaxation more accurately than was done in the previous investigation (20) and to investigate the cobalt concentration dependence of the magnitude of both the high and low temperature internal friction peaks. Later, it was

realized that very few studies of the thermotransport behavior of fast diffusing systems had been conducted. Therefore, it was decided to include a study of the thermotransport behavior of cobalt in thorium. This particular study is special in that a new technique for investigating thermomigration is introduced. The phase study was essentially an outgrowth of the other two studies, which required a knowledge of the amount of cobalt that could be quenched into a supersaturated solid solution as well as the solid solubility of cobalt in thorium.

Explanation of Thesis Format

This thesis has been written in the alternate format as outlined in The Graduate College Thesis Manual. The main body of this thesis consists of three papers which are designated as Sections I, II and III. The papers designated as Section I and Section II were presented at the 1988 TMS-AIME Annual Meeting at Phoenix, Arizona on February 27, 1988. The paper designated as Section III was presented at the 1986 TMS-AIME Fall Meeting at Orlando, Florida on October 9, 1986. The paper designated as Section I is the work of Dr. O. N. Carlson, Dr. A. J. Bevolo and myself. The papers designated as Sections II and III are the sole work of Dr. O. N. Carlson and myself. All three papers will be submitted for publication shortly.

REFERENCES CITED

1. W. C. Roberts-Austen, Proc. Roy. Soc. 59, 281 (1896); Phil. Trans. Roy. Soc. 187, 404 (1896).

2. T. R. Anthony, in Vacancies and Interstitials in Metals, edited by A. Seeger (North-Holland, Amsterdam, 1970), p. 935.

3. W. K. Warburton and D. Turnbull, in Diffusion in Solids: Recent Developments, edited by A. S. Nowick and J. J. Burton (Academic Press, New York, NY, 1974), p. 171.

4. A. D. Le Claire, J. Nuc. Mater. 69 & 70, 70 (1978).

5. C. Herzig, in Diffusion in Metals and Alloys, edited by F. J. Kedves and D. L. Beke (Trans Tech Publications, Switzerland, 1983) p. 23.

6. W. N. Weins and O. N. Carlson, J. Less-Common Metals 66, 99 (1979).

7. F. A. Schmidt, M. S. Beck, D. K. Rehbein, R. J. Conzemius and O. N. Carlson, J. Electrochem. Soc. 131, 2169 (1984).

8. A. A. Ascoli, J. Inst. Metal. 89, 218 (1960-1961).

9. G. V. Kidson, Philos. Mag. 13, 247 (1966).

10. J. W. Miller, Phys. Rev. 181, 1095 (1969).

11. R. E. Howard and J. R. Manning, Phys. Rev. 154, 561 (1967).

12. J. W. Miller, Phys. Rev. 2, 1624 (1970).

13. W. K. Warburton, Phys. Rev. 7, 1330 (1973).

14. B. F. Dyson, T. R. Anthony and D. Turnbull, J. Appl. Phys. 37, 2370 (1966).

15. F. C. Frank and D. Turnbull, Phys. Rev. 104, 617 (1956).

16. N. L. Peterson, in Diffusion (American Society for Metals, Metals Park, Ohio, 1973), p. 47.

17. J. N. Mundy, J. W. Miller and S. J. Rothman, Phys. Rev. B10, 2275 (1974).

18. J. W. Miller, J. N. Mundy, L. C. Robinson and Ronald E. Loess, Phys. Rev. B8, 2411 (1973).

19. J. W. Miller and A. Edelstein, Phys. Rev. 188, 1081 (1969).

20. J. W. Miller, Phys. Rev. 188, 1074 (1969).

21. W. K. Warburton, Phys. Rev. B11, 4945 (1975).

22. B. M. Cohen, D. Turnbull and W. K. Warburton, Phys. Rev. B16, 2491 (1977).

23. F. Dworschack, C. Herzig and J. N. Mundy, J. Phys. F: Met. Phys. 10, 367 (1980).

24. E. Stracke and C. Herzig, Phys. Stat. Sol. (a) 66, 189 (1981).

25. T. Bolze, H. Metzger, J. Peisl and S. C. Moss, J. Phys. F: Met. Phys. 14, 1073 (1984).

26. T. Bolze, H. Metzger, J. Peisl and S. C. Moss, J. Phys. F: Met. Phys. 14, 1085 (1984).

27. K. Kusunoki, K. Tsumuraya and S. Nishikawa, Trans. Jap. Inst. Met. 22, 501 (1981).

28. J. W. Miller, D. S. Gemmell, R. E. Holland, J. C. Poizat, J. N. Worthington and R. E. Loess, Phys. Rev. 11, 990 (1975).

29. J. S. Carpenter and W. N. Cathey, Phys. Lett. 64A, 313 (1977).

30. T. J. Turner and C. H. Nielsen, Solid State Commun. 15, 243 (1974).

31. A. A. Sagues and A. S. Nowick, Solid State Commun. 15, 239 (1974).

32. P. N. Tomlinson and A. Howie, Phys. Lett. 27A, 491 (1968).

33. L. W. Barr, A. D. Le Claire and F. A. Smith, in Atom Transport in Solids and Liquids (Verlag der Zeitschrift fur Naturforschung, Tubingen, 1971), p. 336.

34. T. R. Anthony, Acta Met. 18, 877 (1970).

35. S. J. C. Rushbrook Williams and L. W. Barr, J. Nucl. Mater. 69 & 70, 556, (1978).

36. P. A. Flinn, U. Gonser, R. W. Grant and R. M. Houseley, Phys. Rev. 157, 530 (1967).

37. G. Vogl, W. Miekeley, A. Hiedemann and W. Petry, Phys. Rev. Lett. 53, 934 (1984).

38. W. N. Weins and O. N. Carlson, Met. Trans. 13A, 995 (1982).

SECTION I. AN INVESTIGATION OF A METASTABLE $ThCo_x$ PHASE AND THE SOLID SOLUBILITY OF COBALT IN THORIUM IN DILUTE THORIUM-COBALT ALLOYS

INTRODUCTION

Over 25 years ago Thomson (1) established a major portion of the equilibrium phase diagram for the Th-Co system. As seen from Fig. 1, obtained from (2), five different intermediate phases are present with the Th_7Co_3 phase forming an eutectic with thorium at 1373 K. Although the solid solubility of cobalt in thorium is indicated to be zero in the phase diagram, experimental data verifying the position of the solvus boundary were not reported.

Recently, cobalt has been observed to be a fast diffusing solute in thorium (3). The phenomenon of fast diffusion is associated with those metal-metal systems in which the diffusivity of the solute is much greater than the self diffusivity of the solvent and the activation energy for solute diffusion is markedly less than that for the self diffusion of the host metal. Several reviews have been written on this subject (4-7).

This study is part of a major investigation to characterize the fast transport behavior of cobalt in thorium. The overall investigation also includes a study of the thermotransport behavior of cobalt in thorium as well as a study of the nature of the defect associated with the fast diffusion process using internal friction. The initial goals of the present study were to determine the solvus boundary at the thorium rich end of the phase diagram and the maximum cobalt concentration at which a supersatured solid solution of cobalt in thorium could be retained upon quenching. The solid solubility data were required for the thermotransport study because of the need to perform experiments in both

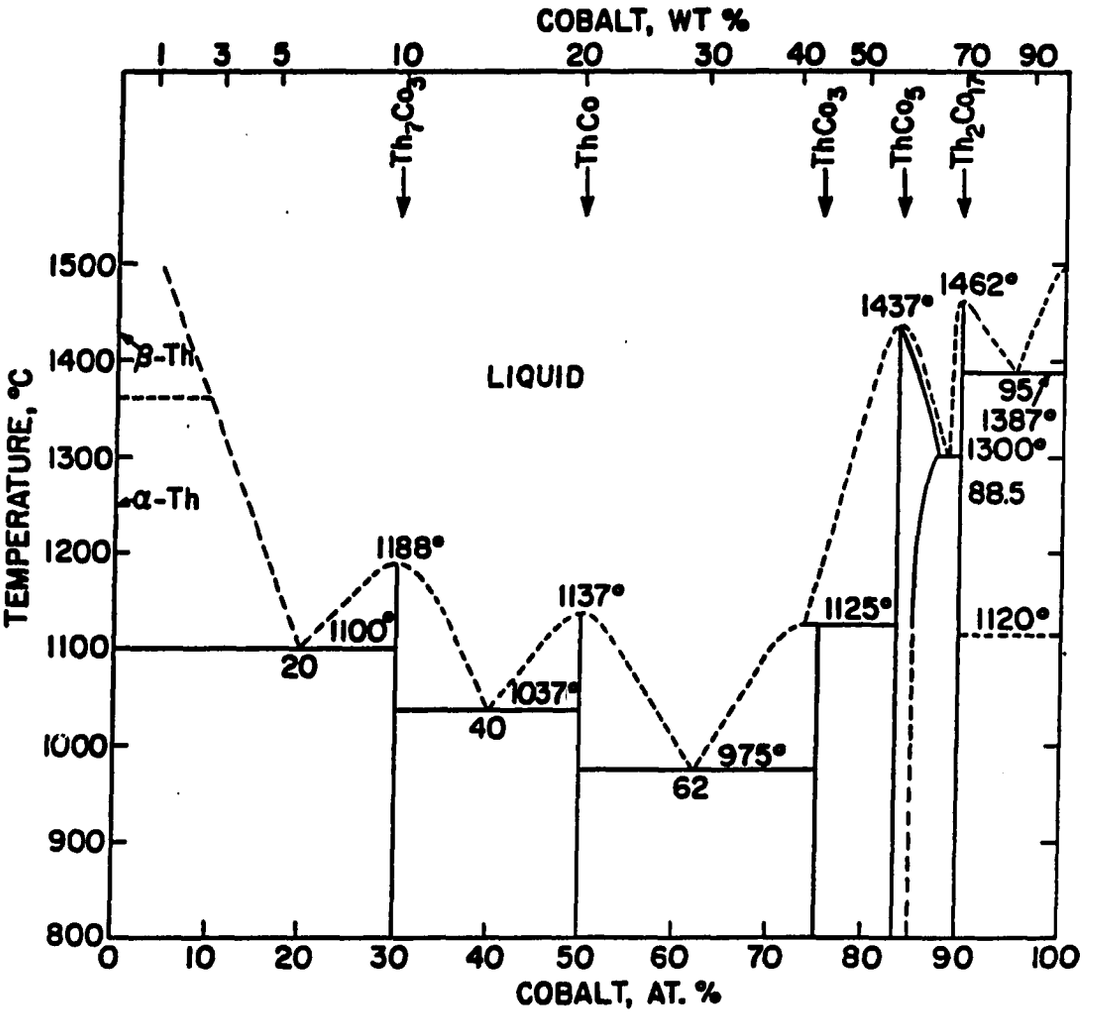

Figure 1. Th-Co phase diagram

the single- and two-phase fields. The knowledge of the maximum cobalt concentration that can be retained in a supersaturated solid solution upon quenching was important to the internal friction study because, due to the low solubility of cobalt in thorium at room temperature, the specimens had to be quenched from the single-phase field in order to obtain a supersatured solid solution.

During the study, another phase with a morphology unlike that associated with the Th_7Co_3 phase was observed in the higher cobalt concentrated alloys. As a result, the goals of the study were expanded to include a determination of the crystal structure, chemical composition, morphology and stability of this second phase.

EXPERIMENTAL PROCEDURES

The thorium used in this investigation was obtained from the Materials Preparation Center of the Ames Laboratory. Chemical analysis showed the major impurities to be 350 ppma O, 350 ppma C, 5 Ta, 7 Re, 4 W, 10 Si, 5 Mo and 0.04 Co. Master alloys containing 0.24 and 0.56 at.% were prepared by arc-melting small amounts of 99.9% pure Co with the thorium in a purified argon atmosphere. Alloys containing 0.004, 0.006, 0.016, 0.05, 0.14, and 0.40 at.% cobalt were prepared by adding portions of the master alloys to the pure thorium in subsequent arc-melting steps. The cobalt concentrations of the alloys were determined by atomic absorption.

A portion of the alloys containing 0.05, 0.14, 0.24, 0.4 and 0.56 at.% Co were swaged into 0.38-cm diameter rods and 0.28 cm thick discs were cut from these for use in the solvus determination. These were wrapped in tantalum foil, equilibrated at various temperatures between 1113 and 1573 K and quenched in oil. The quenched specimens were then electropolished for examination by optical and scanning electron microscopy.

The specimens used in the helium quenching and aging studies were prepared by swaging segments of the aformentioned alloy rods into 0.1 cm diameter wires and cutting them into 9-cm long sections. The sections were heated at 1573 K for 1 h under a pressure of less than 5×10^{-7} Torr by internal electrical resistance using a constant a.c. power supply. Quenching was achieved by terminating the power to the sample while simultaneously injecting liquid-nitrogen-cooled helium gas

into the chamber through an inlet system directed at the sample. It is estimated that a quench rate of $\sim 800^{\circ}C/s$ was attained.

Aging experiments were performed on the Th-0.14 at.% Co alloy wire specimen following helium quenching. The specimen was cut into 3-mm long segments which were wrapped individually in tantalum foil and heated in a furnace under a vacuum of 1×10^{-6} Torr. Different segments were aged for times ranging from 0.5 to 90 h between 773 and 1073 K. The aged specimens were examined by optical and scanning electron microscopy.

A one-cm length of the Th-0.14 at.% Co wire specimen that had been quenched from 1573 K was examined by X-ray diffraction using the Debye-Scherrer technique. The X-ray specimen was prepared by eletropolishing one end of the wire to a fine point, in a 94 % methanol - 6 % perchloric acid solution.

A portion of the Th-0.40 at.% Co alloy was rolled into a strip 0.25 mm thick. It was then heated by internal resistance at 1423 K for 4 h and quenched with liquid-nitrogen-cooled helium by a technique similar to that performed on the wire specimens. A section of the quenched foil was thinned by a combination of jet-polishing and ion milling for examination in a JEOL 100CX electron microscope.

RESULTS

Solid Solubility Studies

The results of the metallographic examination of the various quenched alloys are summarized in Fig. 2. The solubility of cobalt in thorium increases from 0.05 at 1120 K to 0.40 at.% at 1350 K The solvus line was determined by the quantitative metallographic analysis of specimens ranging in cobalt concentration from 0.05 to 0.56 at.% which were equilibrated and quenched from various temperatures in the two-phase region. The procedure which was followed was to determine the volume percent of the second phase (assumed to be Th_7Co_3) that was present in the quenched specimens and then, estimating the solute concentration, c_s, corresponding to a point on the solvus at the given temperature by use of the lever law. The equation that was used in these calculations is

$$c_s(\text{at.}\%) = \frac{\left[\left(V_{Th_7Co_3}\right)\left(X_{Th_7Co_3}\right)\right] - 100\ X_A}{V_{Th_7Co_3} - 100} \qquad (1)$$

where $V_{Th_7Co_3}$ is the volume percent of Th_7Co_3 phase, $X_{Th_7Co_3}$ is the at.% cobalt in Th_7Co_3 and X_A is the at.% cobalt in the alloy. The micrographs in Fig. 3 illustrate the difference between the microstructure of an alloy that was quenched from 1308 K in the one-phase region and one that was quenched from the same temperature in the two-phase region. Note that although a plate-like phase is observed in both micrographs, large spherical particles are also observed in the specimen quenched from the two-phase region (Fig. 3(b)). The identity of the plate-like phase

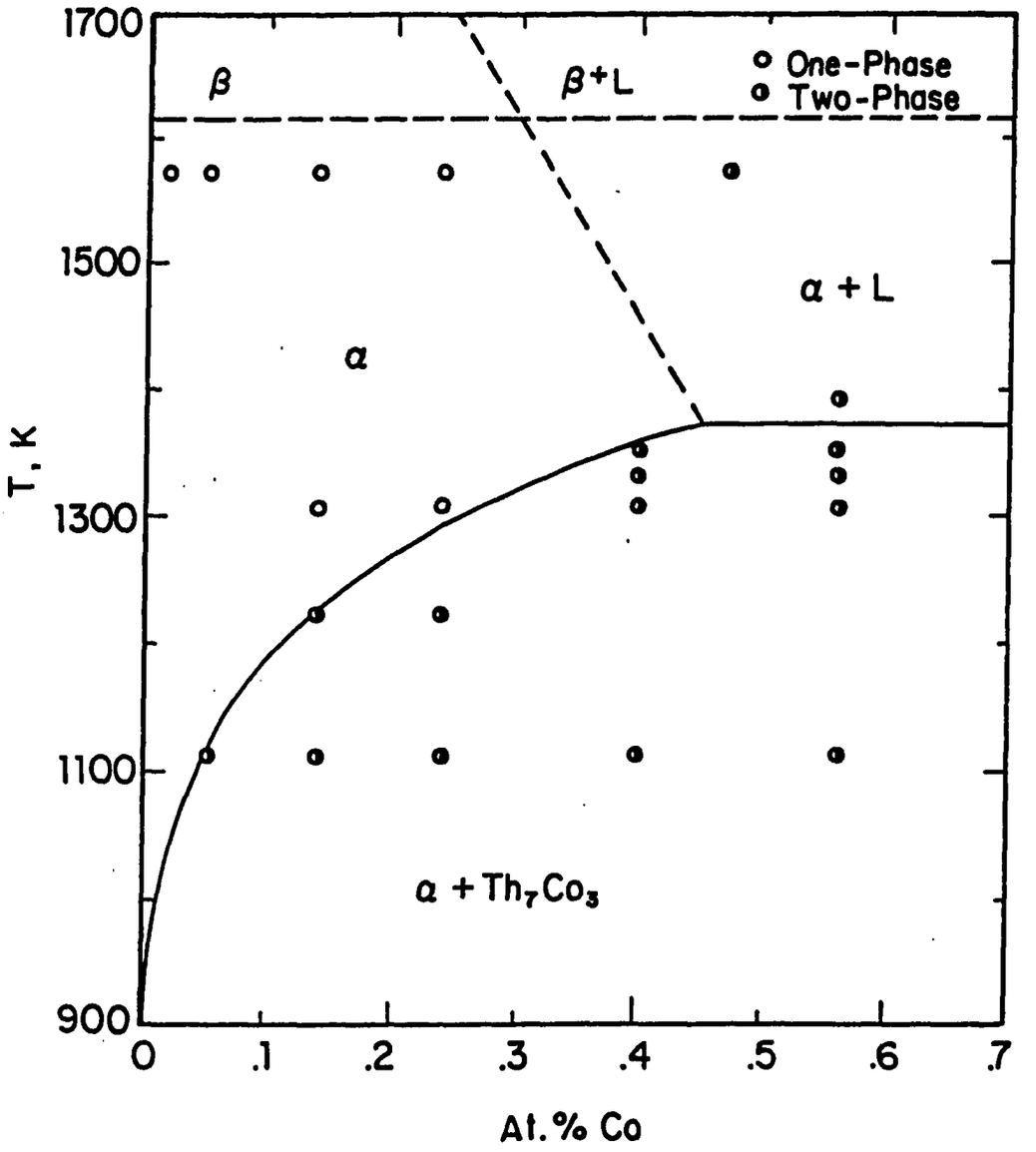

Figure 2. Thorium-rich end of the Th-Co phase diagram

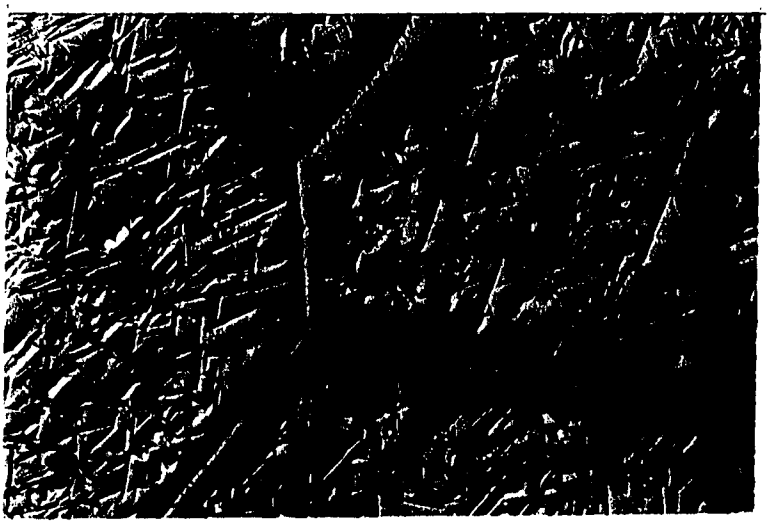

(a)

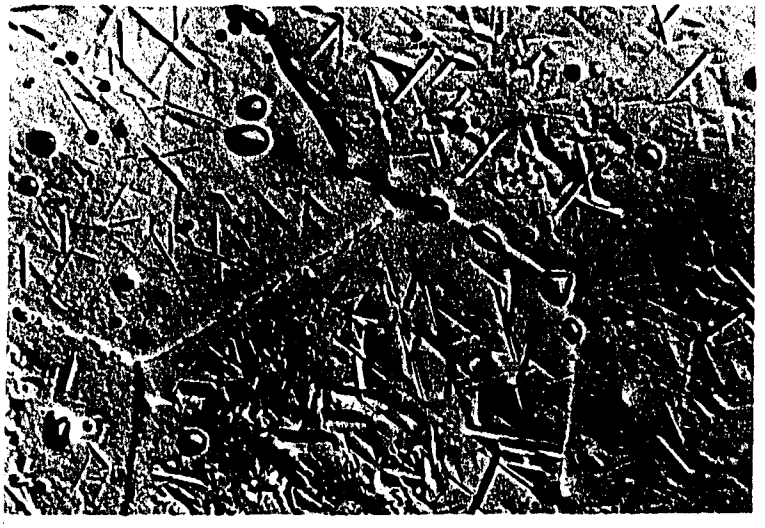

(b)

Figure 3. Optical micrographs of Th-Co alloys after heating at 1308 K for 3 h and quenching; (a) Th-24 at.% Co; single phase at temperature and (b) Th-0.56 at.% Co; Th_7Co_3 precipitates in thorium grains and grain boundaries at temperature. Electropolished, 1000X DIC

formed on quenching will be discussed later. The volume fraction of the spherical particles was determined since they were considered to be the only second phase present prior to quenching.

A summary of the solubility data obtained from the calculations employing the lever law are shown in Table 1. The solute concentration of the solvus, c_s, at 1308, 1333 and 1353 K is an average of the c_s values calculated from the Th-0.24 and Th-0.56 at.% Co specimens. At 1223 and 1113 K, the c_s value is that calculated from only the Th-0.14 at.% Co and Th-0.05 at.% Co specimens, respectively. The reason for the latter is that the Th-0.14 and Th-0.05 at.% Co specimens were quenched from temperatures very close to the solvus boundary, as indicated by the small volume fraction of Th_7Co_3 in the micrographs shown in Fig. 4, and therefore most likely provide the most reliable value for c_s. It will also be noted in the micrographs shown in Fig. 4 that only a small amount of the plate-like precipitates are present. This is apparently due to the low temperature of quenching as compared to those that were helium quenched. A plot of ln c_s versus reciprocal temperature for the data given in Table 1 is shown in Fig. 5. The equation which provides the best fit to the data as determined by a linear least squares analysis is

$$c_s(\text{at.\%}) = 7044 \exp(-110.5 \text{ kJ mol}^{-1}/RT) \qquad (2)$$

Extrapolation of this equation to the eutectic temperature of 1373 K gives a terminal solubility of 0.45 at.% Co.

Table 1. Volume percent of Th_7Co_3 phase and estimated solute concentration of solvus for alloys quenched from various temperatures in the two-phase field

Temperature (K)	At.% Co	% Th_7Co_3		c_s (At.%)
1353	0.40	0.08		0.368
"	0.56	0.60		0.381
"			Avg.	0.375
1333	0.40	0.14		0.351
"	0.56	0.70		0.352
"			Avg.	0.351
1308	0.40	0.42		0.266
"	0.56	0.90		0.294
"			Avg.	0.280
1223	0.14	0.04		0.124
1113	0.05	0.02		0.048

(a)

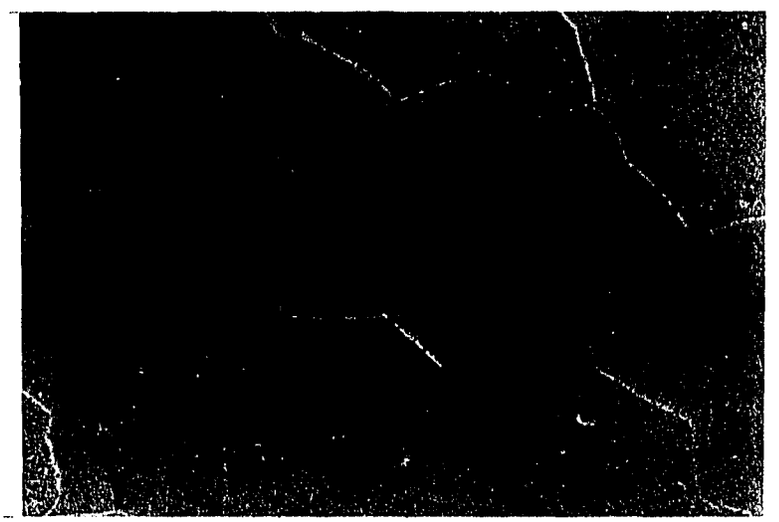

(b)

Figure 4. Optical micrographs of (a) Th-0.05 at.% Co alloy heated at 1113 K for 7 h and quenched and (b) Th-0.14 at.% Co alloy heated at 1223 K for 7 h and quenched. Very small amounts of Th_7Co_3 phase in thorium matrix at temperature. Electropolished, 250X

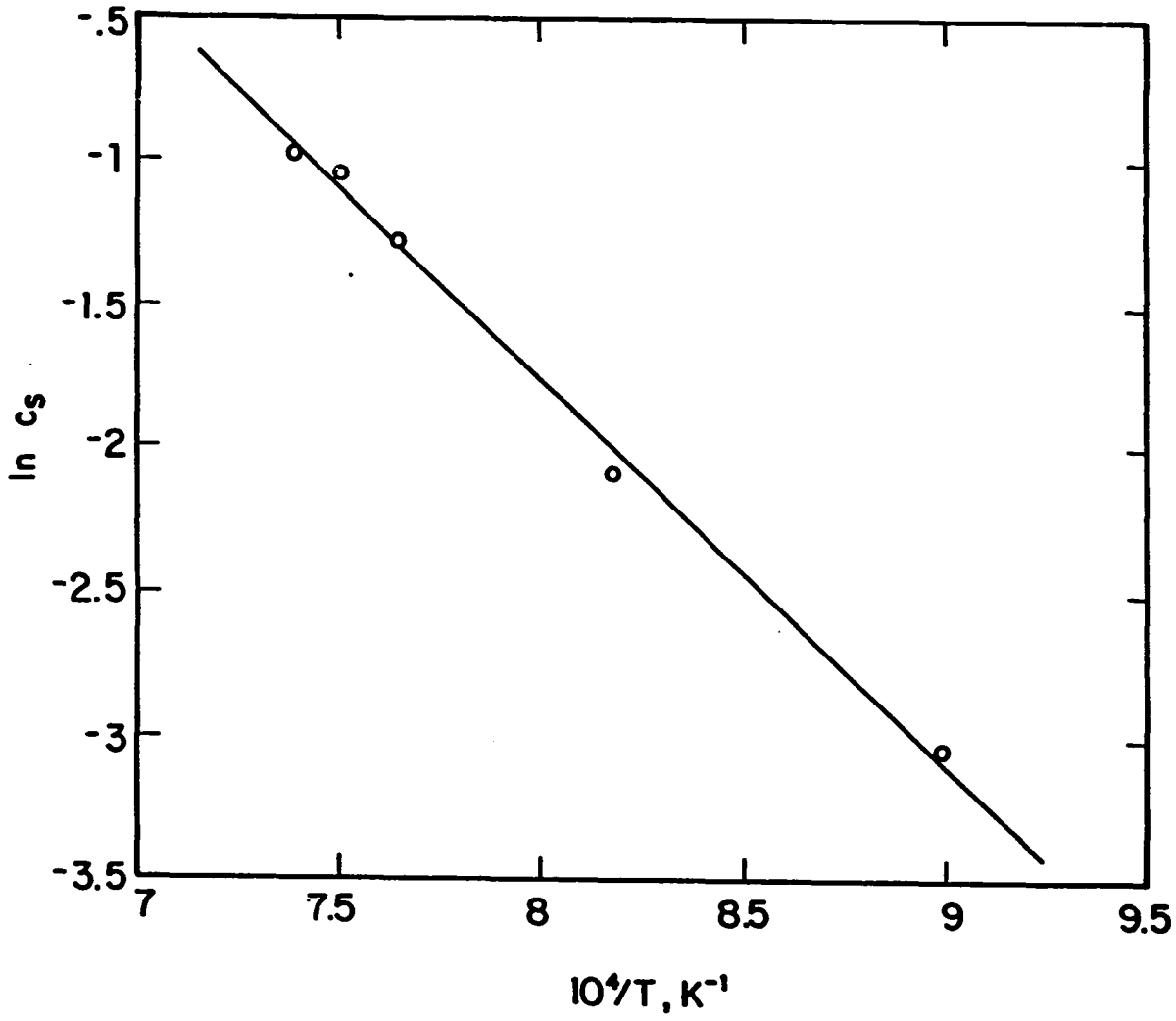

Figure 5. Plot of ln c_s versus reciprocal temperature for cobalt in thorium

Metastable Plate Phase

Quenching Studies

Optical micrographs of unalloyed thorium and alloys containing between 0.004 and 0.47 at.% Co which were equilibrated and helium quenched from 1573 K are shown in Figs. 6 and 7. In Fig. 6(a) the thorium phase appears to be free of inclusions or precipitates as is the alloy containing 0.004 at.% Co (Fig. 6(b)). However, alloys with cobalt concentrations greater than 0.004 at.% have an ever increasing amount of second phase particles. In the more dilute alloys (Figs. 6(c) and 6(d)) the amount of this precipitate is relatively small but as the cobalt concentration of the alloys increases to 0.05 at.% and higher there is a notable increase in the size and volume fraction of these particles (see Fig. 7) and the plate-like morphology of this phase is readily apparent. The plate-like shape of this phase is also evident in the SEM micrograph of the Th-0.14 at.% alloy which was equilibrated and helium quenched from 1573 K as shown in Fig. 8. The circular regions in the micrograph are the erosions that were produced by the electron beam during the microanalysis of the plate precipitate and the surrounding thorium matrix.

In an effort to determine the crystal structure and lattice parameter of the plate-like phase a Debye-Scherrer X-ray diffraction pattern of the helium-quenched Th-0.14 at.% Co alloy was indexed. As is seen from the data of Table 2 strong α-thorium lines are present together with weaker lines which may be due to an fcc phase with a lattice parameter of 5.63 Å, which is about 10% greater than that of thorium.

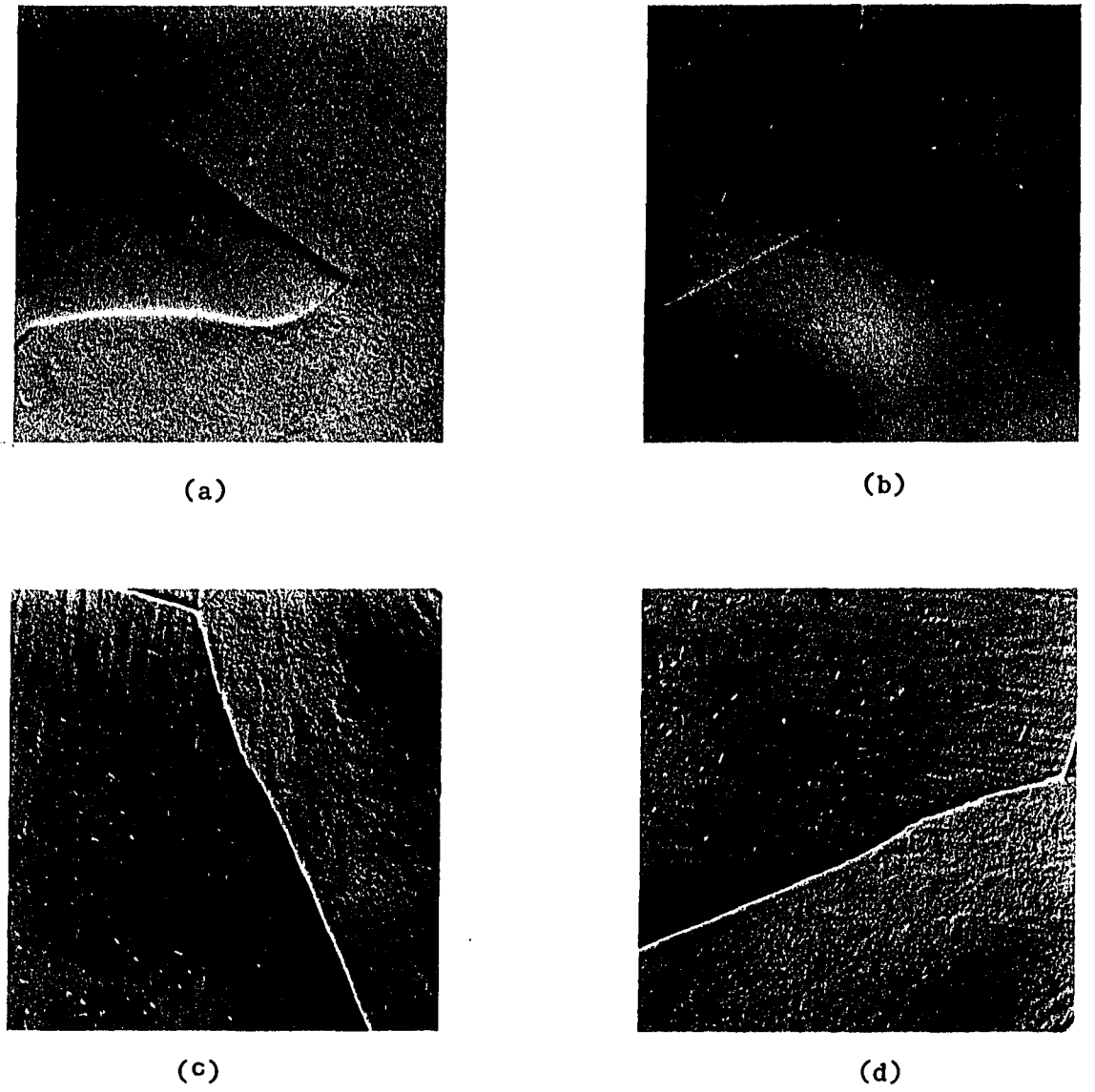

Figure 6. Optical micrographs of (a) Th, (b) Th-0.004 at.% Co alloy, (c) Th-0.006 at.% Co alloy and (d) Th-0.016 at.% Co alloy heated at 1573 K for 1 h and helium quenched. Single-phase structure in (a) and (b). Small amount of plate precipitates within thorium-rich matrix in (c) and (d). Electropolished, 1000X DIC

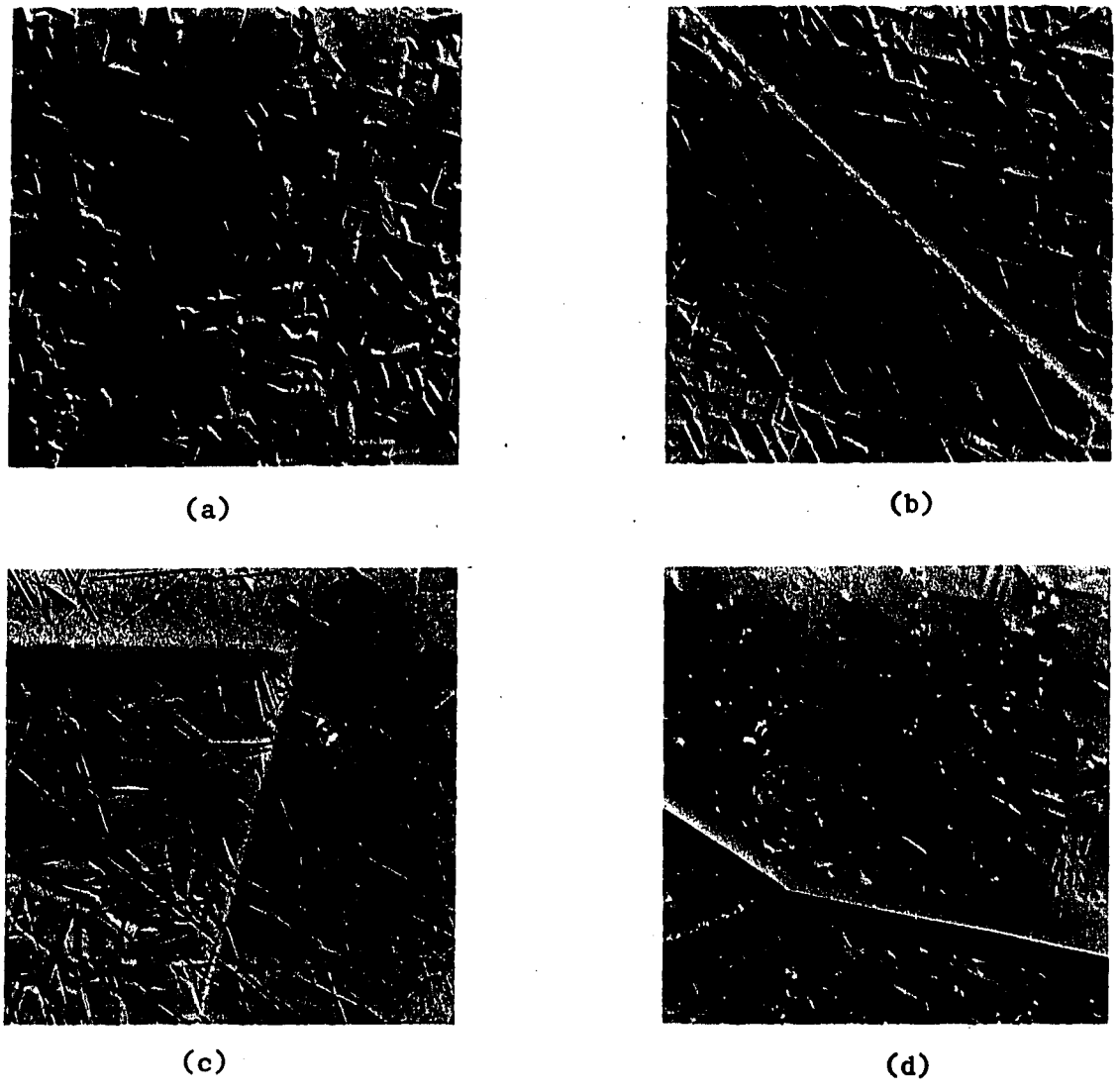

Figure 7. Optical micrographs of (a) Th-0.05 at.% Co alloy, (b) Th-0.14 at.% Co alloy, (c) Th-0.24 at.% Co alloy and (d) Th-0.47 at.% Co alloy heated at 1573 K for 1 h and helium quenched. Plate precipitates within thorium-rich matrix in (a), (b) and (c). Plate precipitates and quenched droplets of cobalt-rich liquid in thorium in (d). Electropolished, 1000X DIC

Figure 8. SEM micrograph of plate-like precipitate in Th-0.14 at.% Co alloy helium quenched from 1573 K

Table 2. X-ray data for Th-0.14 at.% Co heated at 1573 K for 1 h and helium quenched

Line	Relative Intensity I/I_o	Reflection Angle (2θ)	Plane Spacing d, Å	Phases	hkl
1	vvw	27.71	3.2189	P	111
2	s	30.69	2.9130	α	111
3	wvw	31.99	2.7975	P	200
4	vs	35.44	2.5326	α	200
5	vvw	45.77	1.9823	P	220
6	vs	50.83	1.7964	α	220
7	vvw	54.23	1.6915	P	311
8	vvw	56.72	1.6230	P	222
9	vs	60.48	1.5307	α	311
10	s	63.58	1.4633	α	222
11	vvw	66.58	1.4045	P	400
12	vvw	72.96	1.2966	P	331
13	vs	74.71	1.2705	α	400
14	vvw	75.61	1.2576	P	420
15	vs	82.87	1.1650	α	331
16	vs	85.52	1.1355	α + P	420 + 422
17	vvw	90.76	1.0831	P	511, 333
18	s	95.88	1.0375	α_1	422
19	vvw	101.56	0.9951	P	440
20	vs	103.89	0.9782	α_1	511, 333
21	vvw	108.26	0.9513	P	531
22	vvw	110.62	0.9376	P	600, 442
23	s	?	?	α_1	440
24	vvw	119.97	0.8903	P	620
25	vs	127.30	0.8596	α_1	531
26	vvw	127.95	0.8593	P	533
27	vs	130.68	0.8476	α_1	600, 442
28	vs	146.71	0.8040	α_1	620
29	vvw	155.69	0.7886	P	711,551
30	vvw	161.49	0.7804	P	640
31	vvw	163.07	0.7807	P	
32	s	166.64	0.7755	α_1	533

However, it is possible that these faint lines are thorium α lines. The X-ray data, therefore, are inconclusive.

The results of a TEM study of a Th-0.40 at.% Co alloy helium quenched from 1423 K seem to corroborate those of the X-ray diffraction study. A bright field micrograph of this alloy, containing the plate-like precipitates is shown in Fig. 9. The rectangular-shaped particles in the microstructure were not identified.

A selected area diffraction pattern from this region is seen in Fig. 10. It will be noted from the diffraction pattern that an extra spot, presumably due to the plate-like precipitates, is associated with each matrix reflection and lies just slightly closer to the transmitted spot. Assuming that the extra reflections are associated with a phase having an fcc structure, the corresponding lattice parameter would be about 5.6 Å. This is in good agreement with the X-ray diffraction results if it assumed that the faint X-ray lines are due to the same phase as that associated with the extra electron diffraction spot.

Three independent techniques were used in an attempt to determine the cobalt content of the plate-like precipitate. As is seen from Table 3, quantitative metallographic analyses of the 0.016, 0.05, 0.14 and 0.24 at.% Co alloys from optical metallographic data indicate that the cobalt concentration is about 0.6 at%. However, a similar analysis of a 0.4 at.% Co alloy from the TEM bright field image shown in Fig. 9 indicates that the cobalt concentration is about 8 at.% (Table 3). The difference in these values is due to the fact that the analyses of the optical data give high volume fractions of the plate phase. The reason

Figure 9. TEM micrograph of Th-0.40 at.% Co alloy heated at about 1423 K for 4 h and helium quenched. Plate and equiaxed precipitates in thorium matrix. 10,000X

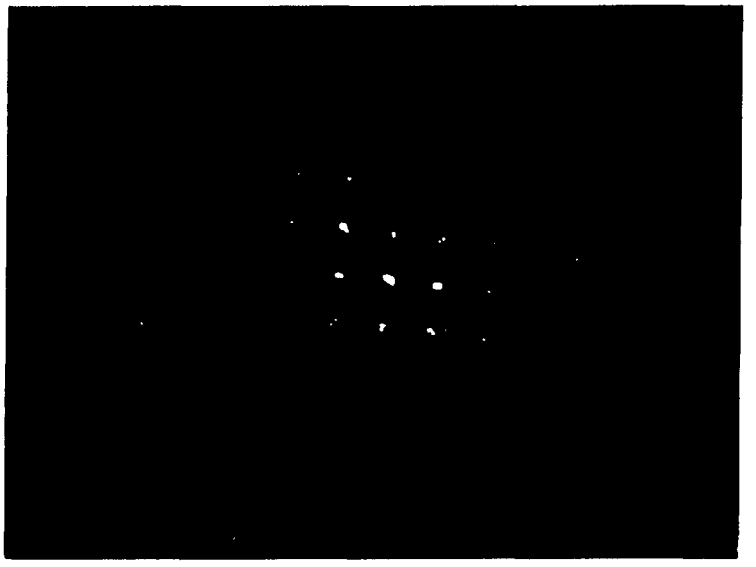

Figure 10. Selected area diffraction pattern of region shown in Figure 9. Zone axis = [001]

Table 3. Volume percent of plate precipitates and corresponding cobalt concentration as estimated for several alloys using the lever law

Specimen	Alloy At.% Co	% Plate Precipitates	At.% Co in Plate Precipitates
Optical	0.016	2	0.60
"	0.05	8	0.58
"	0.14	30	0.46
"	0.23	35	0.65
			Avg. = 0.57
TEM	0.40	5	8

for this is that, as a result of electropolishing, the apparent width of the plate precipitate projecting from the surface of the specimen is greater than the actual width. Since a projection of the precipitate is seen in the TEM image, the actual width is observed. Therefore, the TEM value should be the more accurate. According to the TEM results the stoichiometry of the plate phase is $ThCo_{0.08}$. The equation that was used to estimate the at.% cobalt content of the plate precipitates, X_P according to the lever law is

$$X_P = \frac{100\ X_A + ((0.004)\ (V_P - 100))}{V_P} \qquad (3)$$

where X_A is the cobalt concentration in the alloy in at.% and V_P is the volume percent of the plate phase. EDS X-ray and Auger microanalyses of this phase were also performed but no cobalt was detected. The reason why the EDS X-ray microanalysis is unable to detect any cobalt is most likely due to beam spreading, however, it is not understood why the Auger microanalysis doesn't detect any cobalt.

Aging Studies

In order to verify the metastable nature of the plate-like precipitates observed in the quenched specimens, a series of aging experiments was performed on the Th-0.14 at.% Co alloy. The results of these experiments are summarized in Fig. 11. As is seen from this figure, the plate-like precipitates transform to rod-like precipitates during aging. The rod-like nature of this new phase is readily apparent from the SEM micrograph of the Th-0.14 at.% Co alloy in Fig. 12. A

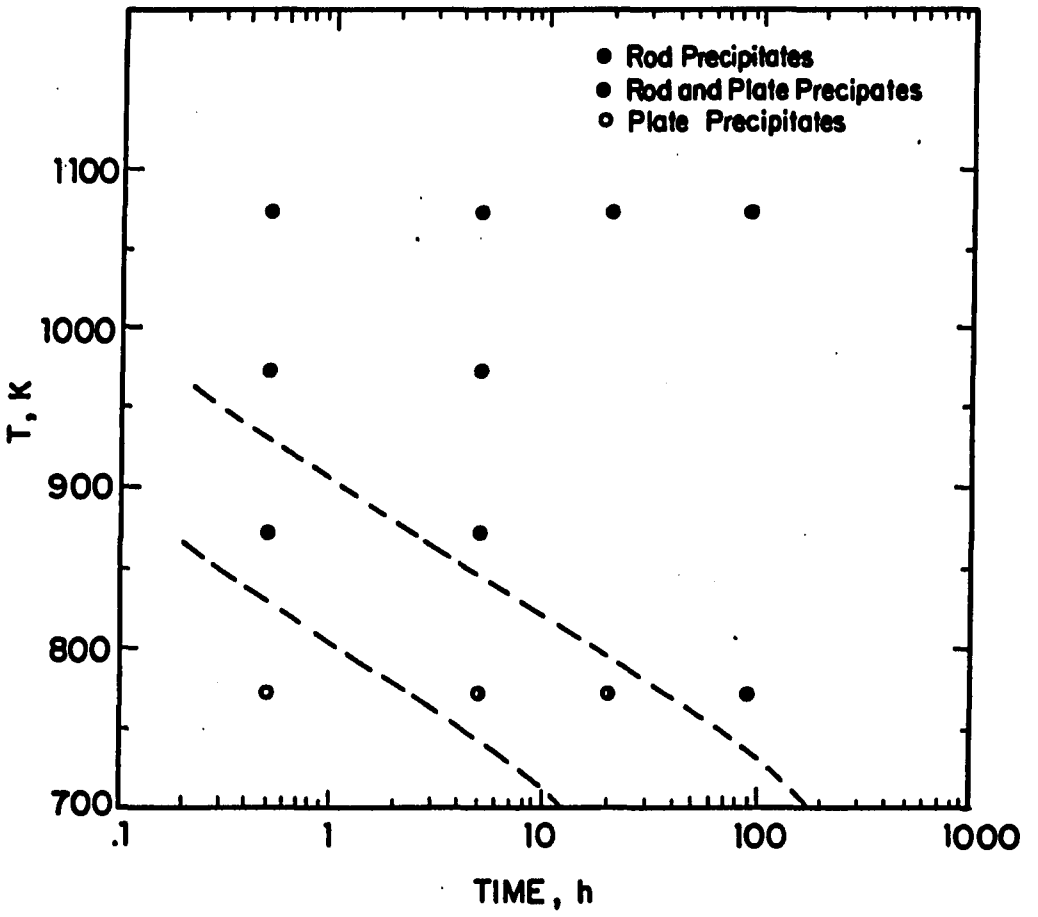

Figure 11. Isothermal transformation diagram for transformation of plate precipitates to rod precipitates

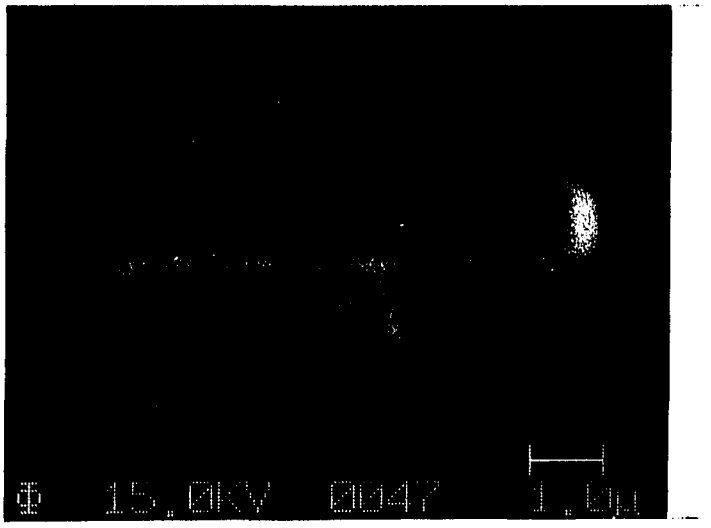

Figure 12. SEM micrograph of rod-like particle in Th-0.14 at.% Co alloy heated at 1573 K for 1 h, helium quenched, aged at 973 K for 0.5 h and furnace cooled.

series of optical micrographs showing various stages of this transformation are shown in Figs. 13-15. In Fig. 13 it is seen that no transformation to rod-like precipitates has occurred after aging at 773 K for 0.5 h but, as is seen in Fig. 14, after 0.5 h at 873 K the transformation is partially complete. After aging at 973 K for 0.5 h the transformation is complete as is seen from Fig. 15. It will be noted that the volume fraction occupied by the rod-like precipitates is considerably less than that occupied by the plate-like precipitates.

An inspection of Fig. 11 indicates that the rod-like precipitates are stable after aging at 1073 K for 90 h. This suggests that these precipitates are the equilibrium second phase Th_7Co_3. In order to confirm this, an EDS X-ray microanalysis of these precipitates was performed. The results of this analysis, shown in Fig. 16, indicate that the cobalt concentration is approximately 30 at.%, corresponding to that of Th_7Co_3.

In addition to the plate-like precipitates, spherical particles are visible along the grain boundary in Fig. 13. These are most likely the equilibrium Th_7Co_3 phase. The small spherical particles within the thorium grains in Fig. 15 are probably ThO_2, as they are also present in the furnace-cooled thorium metal.

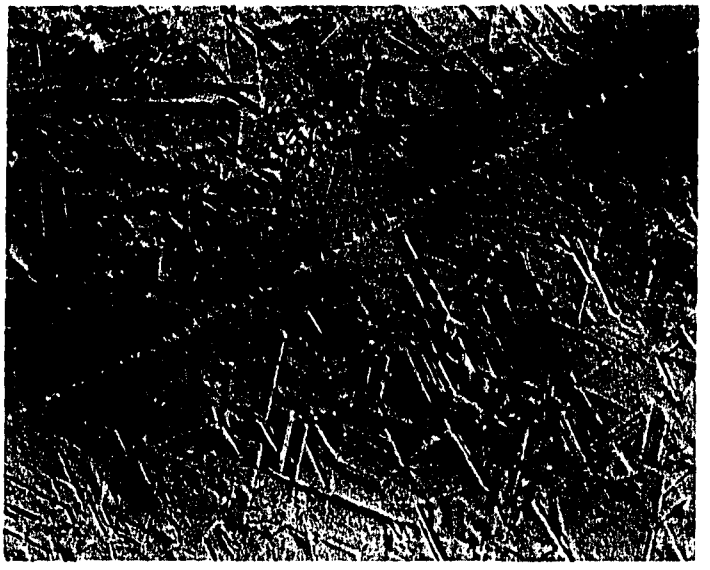

Figure 13. Optical micrograph of Th-0.14 at.% Co alloy heated at 1573 K for 1 h, helium quenched, aged at 773 K for 0.5 h and furnace cooled. Plate precipitates within thorium grains and Th_7Co_3 at grain boundary. Electropolished, 1000X DIC

Figure 14. Optical micrograph of Th-0.14 at.% Co alloy heated at 1573 K for 1 h, helium quenched, aged at 873 K for 0.5 h and furnace cooled. Plate and Th_7Co_3 rod precipitates in thorium matrix. Electropolished, 1000X DIC.

Figure 15. Optical micrograph of Th-0.14 at.% Co alloy heated at 1573 K for 1 h, helium quenched, aged at 973 K for 0.5 h and furnace cooled. Rod-like Th_7Co_3 precipitates and small ThO_2 particles in thorium matrix. Electropolished, 1000X DIC

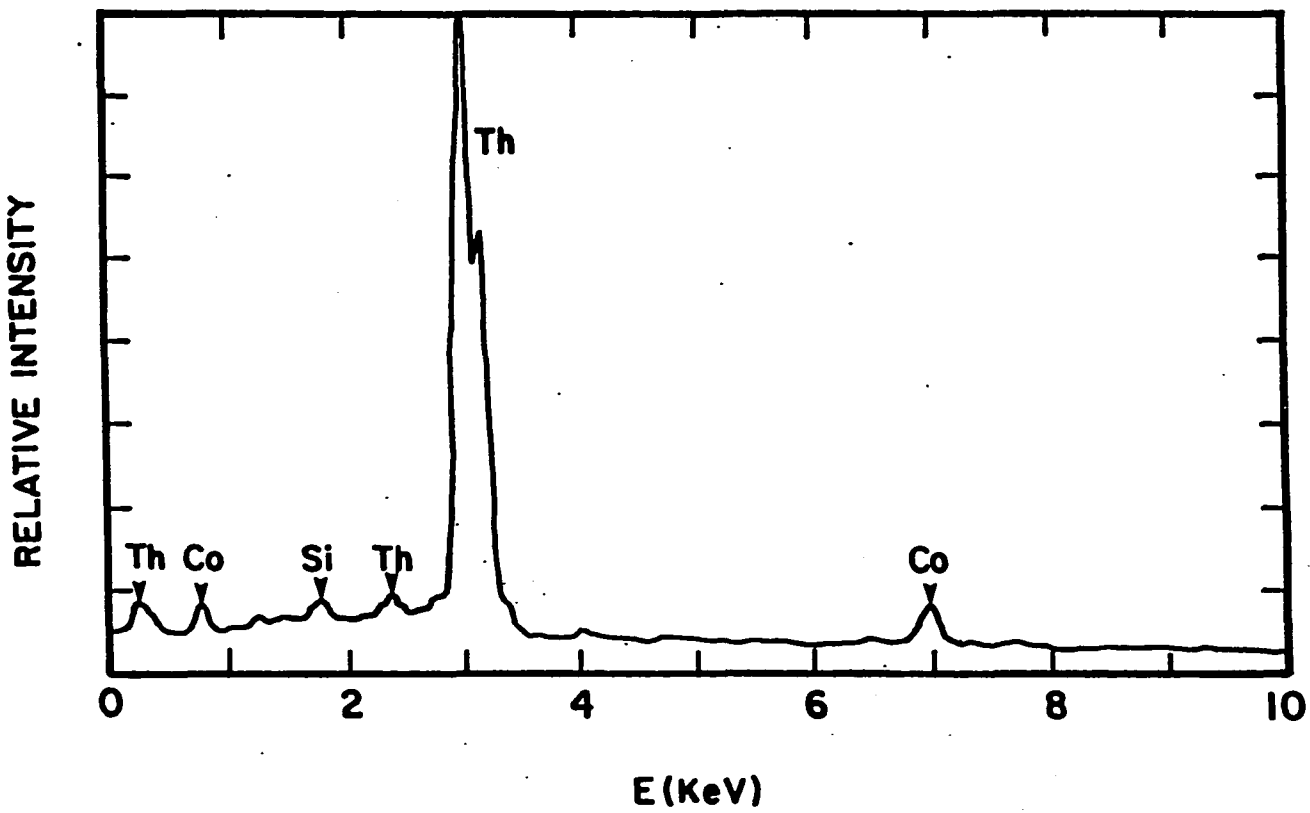

Figure 16. EDS X-ray spectrum of rod-like particle in Th-0.14 at.% Co alloy heated at 1573 K for 1 h, helium quenched, aged at 973 K for 0.5 h and furnace cooled

DISCUSSION

The results of this investigation strongly suggest that the formation of the metastable phase involves long-range diffusion of cobalt atoms. The precipitate-free zone (PFZ) at the grain boundaries of the quenched specimens of Figs. 3 and 7, as well as the presence of precipitates at the grain boundaries in the quenched specimens of Figs. 7(a) and 7(b), indicate that during helium quenching there is sufficient time for the cobalt atoms to diffuse to the boundaries. It will be noted from Figs. 3 and 7 that the width of the PFZ is about the same as the spacing between the plate precipitates. This would indicate that even during the rapid helium quench the cobalt atoms are able to diffuse over a distance that is consistent with formation of the plate phase. The presence of a PFZ at the grain boundaries also suggests that a critical cobalt supersaturation exists below which the formation of the plate phase does not occur.

Further evidence for a diffusional transformation has been obtained from an internal friction study of quenched dilute Th-Co alloys as described in the following section of this thesis. This study indicates that, in those alloys in which the plate phase is observed, the cobalt concentration of the matrix is about 0.004 at%. The plate phase, therefore, must be enriched in cobalt with respect to the matrix, which could only occur if the diffusion of cobalt atoms was associated with the formation of this phase. The fact that relatively large precipitates form during quenching appears to be a reflection of the fast diffusion behavior of cobalt in thorium.

On the basis of the experimental results and a knowledge of the fast diffusion behavior of cobalt in thorium it is concluded that the metastable phase forms by a nucleation and growth process. The fact that this phase forms during quenching rather than the equilibrium phase would seem to indicate that the nucleation barrier for the plate phase is less than that for the equilibrium phase. The similarity between the crystal structures and lattice parameters of the plate phase and the thorium matrix supports this conclusion since these conditions would favor the formation of low energy semicoherent boundaries between the plate precipitates and the thorium matrix. The plate morphology of the precipitate appears to be evidence that a semicoherent boundary exists between the two phases, i.e., at the broad faces of the plates.

A careful examination of the microstructures of the aged specimens suggests that the transformation of the plate precipitates to the rod precipitates occurs by a nucleation and growth process, where nucleation occurs heterogeneously at the plate precipitates. It will be noted in Fig. 11 that a "nose" is not present in the isothermal transformation curve over the range of times of the experiments. This is most likely due to the relatively high nucleation rate of the rod precipitates caused by the heterogeneous nucleation process.

CONCLUSIONS

1. The solid solubility of cobalt in thorium increases from 0.05 at.% at 1120 K to 0.40 at.% at 1350 K according to the relation $c = 7044 \exp(-110.5 \text{ kJ mol}^{-1}/RT)$. The terminal solid solubility at the eutectic temperature 1373 K is 0.45 at.%.
2. A metastable phase having a plate morphology and a stoichiometry of $ThCo_{0.08}$ forms in dilute Th-Co alloys containing greater than 0.004 at.% Co that have been quenched from the single-phase field.
3. The metastable plate phase transforms to rod-like equilibrium Th_7Co_3 upon aging between 773 and 1073 K.

REFERENCES CITED

1. J. R. Thomson, J. Less-Common Metals 10, 432 (1966).

2. J. F. Smith, O. N. Carlson, D. T. Peterson and T. E. Scott, Thorium: Preparation and Properties (Iowa State University Press, Ames, Iowa, 1975), p. 270.

3. W. N. Weins and O. N. Carlson, J. Less-Common Metals 66, 99 (1979).

4. W. K. Warburton and D. Turnbull, in Diffusion in Solids: Recent Developments, edited by A. S. Nowick and J. J. Burton (Academic Press, New York, NY, 1974), p. 171.

5. A. D. Le Claire, J. Nuc. Mater. 69 & 70, 70 (1978).

6. C. Herzig, in DIMETA-82. Diffusion in Metals and Alloys, edited by F. J. Kedves and D. L. Beke (Trans Tech Publications, Switzerland, 1983) p. 23.

7. T. R. Anthony, in Vacancies and Interstitials in Metals, edited by A. Seeger (North-Holland, Amsterdam, 1970), p. 935.

SECTION II. A STUDY OF THE MECHANISM OF FAST DIFFUSION OF COBALT IN THORIUM USING DIFFUSION AND INTERNAL FRICTION EXPERIMENTS

INTRODUCTION

Ever since it was discovered that gold diffuses rapidly in lead (1), there has been considerable interest in the mechanism responsible for fast diffusion in metal-metal systems (2-7). Fast diffusion is associated with those systems in which the solute diffuses at least an order of magnitude faster than the solvent and the activation energy for diffusion of the solute is markedly less than that for self diffusion of the solvent. Measurements of the solute diffusivity in a number of metal systems (5), as well as of the small enhancement of the self-diffusivity of lead due to additions of copper, silver and gold (8,9), seemed to indicate that fast diffusion proceeds by an interstitial mechanism. Frank and Turnbull introduced the dissociative model in which it is assumed that the solute occupies both substitutional and interstitial sites with solute migration being dominated by an interstitial mechanism (10). The relatively large enhancement of the self-diffusivity of lead due to additions of cadmium and mercury (11,7), as well as a small isotope effect of cadmium, silver and copper in lead (12-14) suggested that mechanisms more complex than that for interstitial diffusion may be involved. Extensions of the dissociative model to include host-solute diplon and interstitial-vacancy pair mechanisms were made to explain these results (2,6,7).

Attempts have been made to characterize the solute defects present in several fast diffusing systems although no conclusive evidence as to the nature of the defects responsible for fast diffusion has been obtained. X-ray and neutron diffraction experiments performed by Bolze

et al. (15,16) on dilute solutions of gold in lead indicate that the gold atoms exist primarily as substitutional defects. No direct evidence for the type of defect responsible for fast diffusion was reported, but it was stated that the concentration of such defects in this system must be very small. On the basis of channeling experiments, Miller et al. indicate that gold atoms occupy primarily substitutional sites in tin (17). Although no evidence for the defect associated with fast diffusion was reported, it was indicated that the concentration of such defects must be below the limits of detection for their measurement technique.

Carpenter and Cathey (18) used Mössbauer measurements to study the diffusion of iron in yttrium. Their results indicate that the majority of the iron atoms migrate in yttrium at a rate much slower than that given by bulk diffusion experiments suggesting that at least two different mechanisms are operating. However, the nature of the defect associated with the fast diffusion mechanism could not be identified. Vogl et al. (19) studied the diffusion of cobalt in zirconium using quasielastic neutron scattering. Their results indicate that a fraction of the cobalt atoms diffuse several hundred times faster than zirconium while the remainder diffuse only 25 times faster. Although this may appear to be supportive of a dissociative mechanism, the authors have stated quite emphatically that they must reject any model where only a small fraction of all atoms participates in fast diffusion. It should be pointed out, however, that the identity of the defects associated with the fast diffusion of cobalt was not indicated.

Weins and Carlson determined the chemical diffusivities of iron and nickel in thorium (20) and observed similarities between the activation energies for diffusion and for anelastic relaxation as determined from internal friction measurements (21). They concluded that the diplon model provides a plausible explanation for the iron and nickel data, although they could not rule out the possibility of interstitial-vacancy pair and Jahn-Teller desymmetrized interstitial defects. They obtained quite dissimilar values for the activation energies for diffusion and for relaxation for cobalt in thorium, however, which provided the major stimulus for the present investigation.

Anelastic relaxation data may be used to characterize the solute defects present in a fast diffusing system. Internal friction peaks occur due to the presence of defects whose symmetry are lower than that of the lattice (22). Simple defects that produce this effect in close-packed fcc crystals include desymetrized interstitials and point defect combinations such as solute-solute, host-solute, solute-vacancy or vacancy-vacancy pairs. Since the defect symmetry associated with a solute atom located at a substitutional or interstitial site of an fcc lattice is cubic, such defects will not produce internal friction peaks. Therefore, the appearance of an internal friction peak in a fast diffusing system would indicate that at least some of the solute atoms are not present as single point defects, i.e., on an interstitial or substitutional site.

For an anelastic solid, the internal friction Q^{-1} is given by the Debye equation

$$Q^{-1} = \Delta_E \frac{\omega\tau_r}{1 + (\omega\tau_r)^2} \quad (1)$$

where Δ_E is the relaxation strength, τ_r is the relaxation time and ω is the circular frequency. If the rate limiting step for the anelastic relaxation process is that of movement over an energy barrier then τ_r is given by the Arrhenius relationship

$$\tau_r = \tau_{ro} \exp (Q_R/RT) \quad (2)$$

where τ_{ro} is the time constant and Q_R is the activation energy for relaxation. If the defect producing an internal friction peak is associated with diffusion, proposed diffusion models can be evaluated by comparing Q_R to the activation energy for diffusion Q_D. Depending upon the actual mechanism, Q_R may be greater than, less than or equal to Q_D. For example, for interstitial solutes producing Snoek peaks in bcc crystals, Q_R and Q_D are equal. This is because diffusion and anelastic relaxation proceed by the same atom jump process.

The primary purpose of this investigation was to determine the activation energy for diffusion of cobalt in thorium and the activation energy for relaxation for the internal friction peak associated with cobalt in thorium with higher precision than the Weins and Carlson studies (19,20). Furthermore, the effect of cobalt concentration on the

magnitude of the internal friction peak was determined and a characterization of a lower temperature peak observed in the earlier study was attempted. From these data a critical evaluation of the atomistic models for fast diffusion will be made.

EXPERIMENTAL PROCEDURES

Materials and Sample Preparation

The thorium metal used in this investigation was obtained from the Materials Preparation Center of the Ames Laboratory. Chemical analysis showed the major impurities to be 350 ppma O, 30 N, 350 C, 5 Ta, 7 Re, 4 W, 10 Si, 5 Mo and 0.04 Co. Master alloys containing 0.24 and 0.56 at.% cobalt were prepared by arc-melting small amounts of high-purity cobalt with the thorium in a purified argon atmosphere. Alloys containing 0.004, 0.006, 0.016, 0.05 and 0.14 at.% cobalt were prepared by combining portions of the master alloys with pure thorium in subsequent arc-melting steps. The cobalt concentrations of these alloys were determined by atomic absorption.

Portions of the Th-0.05 at.% Co alloy and an unalloyed thorium ingot were swaged into 0.25-cm diameter rods for the diffusion experiments. Diffusion couples were prepared by butt-welding a 2.25-cm segment of the alloy rod to a 2.5-cm segment of the unalloyed thorium.

Internal friction specimens were prepared from the arc-melted ingots by swaging into 0.12-cm diameter wires. These were then cut into 9-cm long segments. Due to the low solubility of cobalt in thorium at room temperature, the specimens were heated at about 1300°C for 1 hour and quenched in order to retain the cobalt in a supersaturated solid solution. The specimens were heated under a pressure of less than 5×10^{-7} Torr by internal electrical resistance using an alternating current provided by a constant current power supply. Special tantalum foil adapters were used to maintain a constant temperature along the

within ±5°C. The solutionizing temperature of 1300°C, which is slightly below the phase transition temperature of thorium, was chosen in order to be consistent with that of previous work on this system (20). Quenching was achieved by terminating the power to the sample while simultaneously injecting liquid-nitrogen-cooled helium gas into the chamber through an inlet system directed at the sample. It was estimated that a quench rate of about 800°C/s was attained.

Method

Diffusion

The diffusion experiments were performed by heating the diffusion couples at various temperatures for different times and determining the cobalt concentration profile. A solution to Fick's second law of diffusion for two semi-infinite solids is given by

$$c_x = c_o + (c_H - c_o)\ \mathrm{erf}\left[\frac{-x}{\sqrt{4Dt}}\right] \tag{3}$$

where c_x is the cobalt concentration at a distance x from the diffusion interface at time t, c_H is the concentration of the solute in the doped segment and c_o is the mean concentration of the solute between the doped and undoped segments. Equation (3) can be rewritten as

$$\mathrm{erf}^{-1}\left[\frac{c_x - c_o}{c_H - c_o}\right] = \frac{-x}{\sqrt{4Dt}} \tag{4}$$

This indicates that a linear relationship exists between the inverse error function and the distance from the weld interface in the diffusion

region with a slope of $-1/\sqrt{4Dt}$. The diffusion coefficient can, therefore, be obtained from the slope of a plot of the inverse error function versus distance. The activation energy for diffusion, Q_D, and the diffusion constant, D_o, can be obtained from a plot of ln D versus reciprocal temperature according to the Arrhenius relation

$$D = D_o \exp(-Q_D/RT) \tag{5}$$

The diffusion couples were heated under an atmosphere of purified helium by internal electrical resistance using an alternating current. Specially designed tantalum adapters were used to maintain the temperature along the sample in the diffusion region to $\pm 10^{o}C$. A calibrated optical pyrometer was used to measure the temperature of the sample at regular intervals along the heated rod. The cobalt concentration profiles were determined by scanning laser mass spectrometry (SLMS) which uses a focussed laser to vaporize and ionize a small portion of the sample at desired postions along the rod (23).

Internal friction

The internal friction measurements were performed on a low-frequency inverted torsion pendulum machine by ascertaining the extent of the strain decay of a freely oscillating specimen. A schematic drawing of the internal friction machine is shown in Figure 1. The relation between internal friction and the strain decay or "log decrement", δ, is given by

$$Q^{-1} = \frac{\delta}{\pi} = \frac{\ln [A_o/A_n]}{n\pi} \tag{6}$$

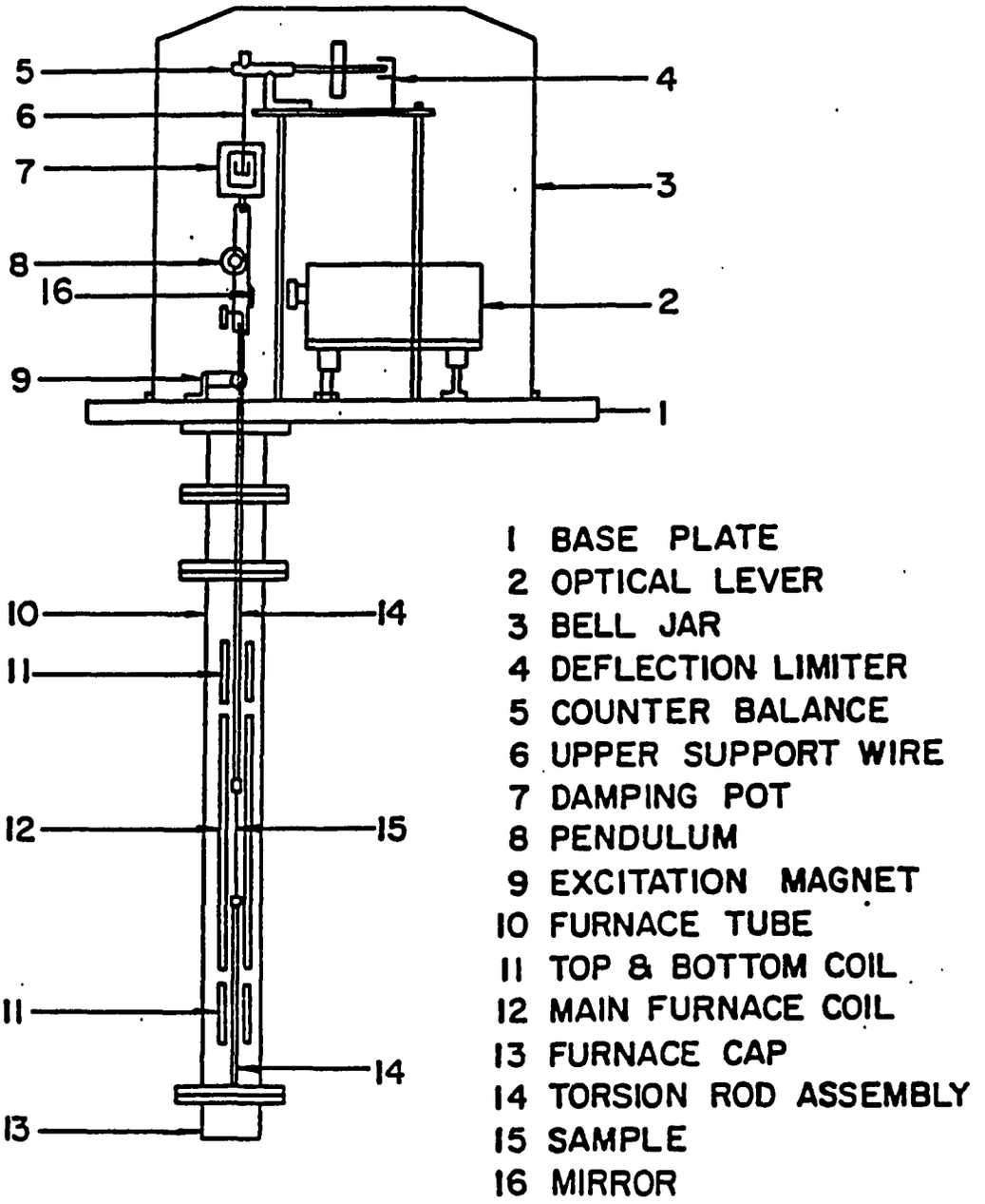

Figure 1. Schematic diagram of the inverted torsion pendulum internal friction machine used in this study

where A_o is the initial amplitude, A_n is the amplitude of the nth cycle and n is the number of cycles. The initial amplitude was 3×10^{-6}.

The experiments were carried out by varying the specimen temperature while maintaining a constant frequency. A series of internal friction measurements were made on the unalloyed Th and all but the 0.56 at.% Co alloy at temperatures lying between -199 and 348°C at frequencies within the range of 1.30 to 1.76 Hz. In addition, internal friction measurements were made on the Th-0.24 at.% Co alloy at temperatures between 0 to 100°C at frequencies ranging from 0.19 to 6.76 Hz.

The activation energy for relaxation was determined from an analysis of the shift of the peak temperature with frequency. At the peak temperature T_p, the relaxation time is the inverse of the circular frequency, i.e., $\tau_r = 1/\omega$ where $\omega = 2\pi f$. Substituting $1/\omega$ for τ_r in equation (2) and taking the log of both sides gives

$$\ln (1/\omega) = \ln (\tau_{ro}) + Q_R/RT_P \qquad (7)$$

Thus it can be seen that Q_R and τ_{ro} can be obtained from a plot of $\ln(1/\omega)$ versus the reciprocal of the peak temperature.

RESULTS

Diffusion Studies

Typical plots of the concentration profile and of the inverse error function versus distance for cobalt in α thorium after 2 h at 1332°C are shown in Figs. 2 and 3. The diffusion coefficients were determined for cobalt in α thorium over the temperature ranges 900 to 1315°C. As is seen from Table 1 the value of D range from 10^{-9} to 10^{-10} m^2/s over this temperature regime. A linear least squares fit of diffusivity versus 1/T (Fig. 4) yielded an activation energy for diffusion of 83.7 ± 4 kJ/mole and a diffusion constant of 7.4×10^{-7} m^2/s where the reported error is the standard deviation. This value for Q_D is significantly greater than Weins and Carlson's value of 58.2 ± 5.8 kJ/mol (20) but it is believed that the value reported here is the more reliable of the two investigations since a larger number of data points were obtained in the present investigation.

Internal Friction Studies

Plots of internal friction versus reciprocal temperature for an unalloyed thorium metal specimen and alloy specimens containing 0.004, 0.006 and 0.016 at.% cobalt are shown in Fig. 5. The frequencies used in these analyses lie in the range of 1.30 to 1.44 Hz. It is seen from the figure and also from Table 2 that a small internal friction peak, referred to as P1, occurs in the unalloyed thorium specimen at 94°C. This peak is attributed to an unknown impurity solute other than cobalt. However, at lower temperatures there are no peaks present. For the 0.004

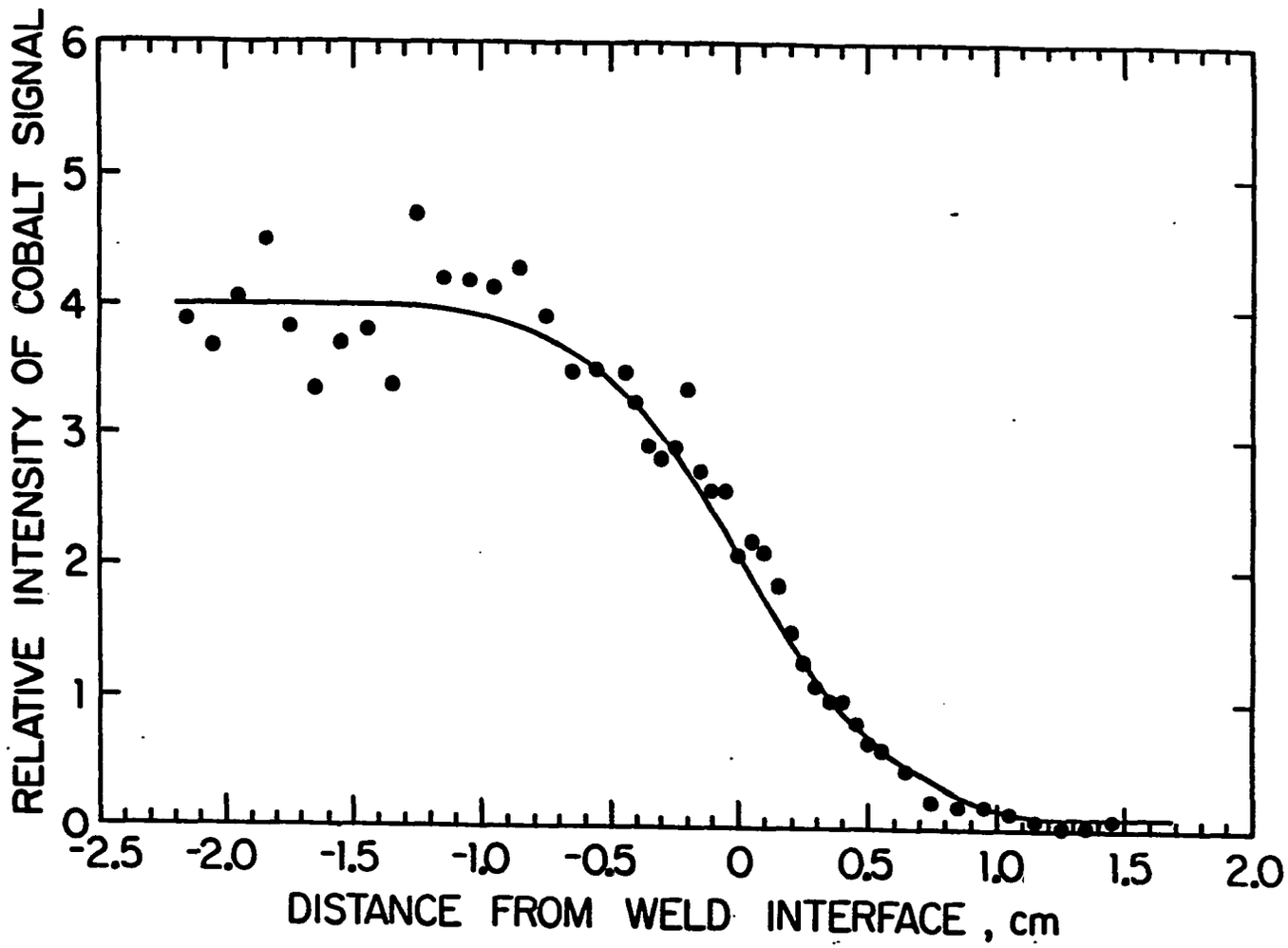

Figure 2. Concentration profile for cobalt in thorium after two hours at 1332°C

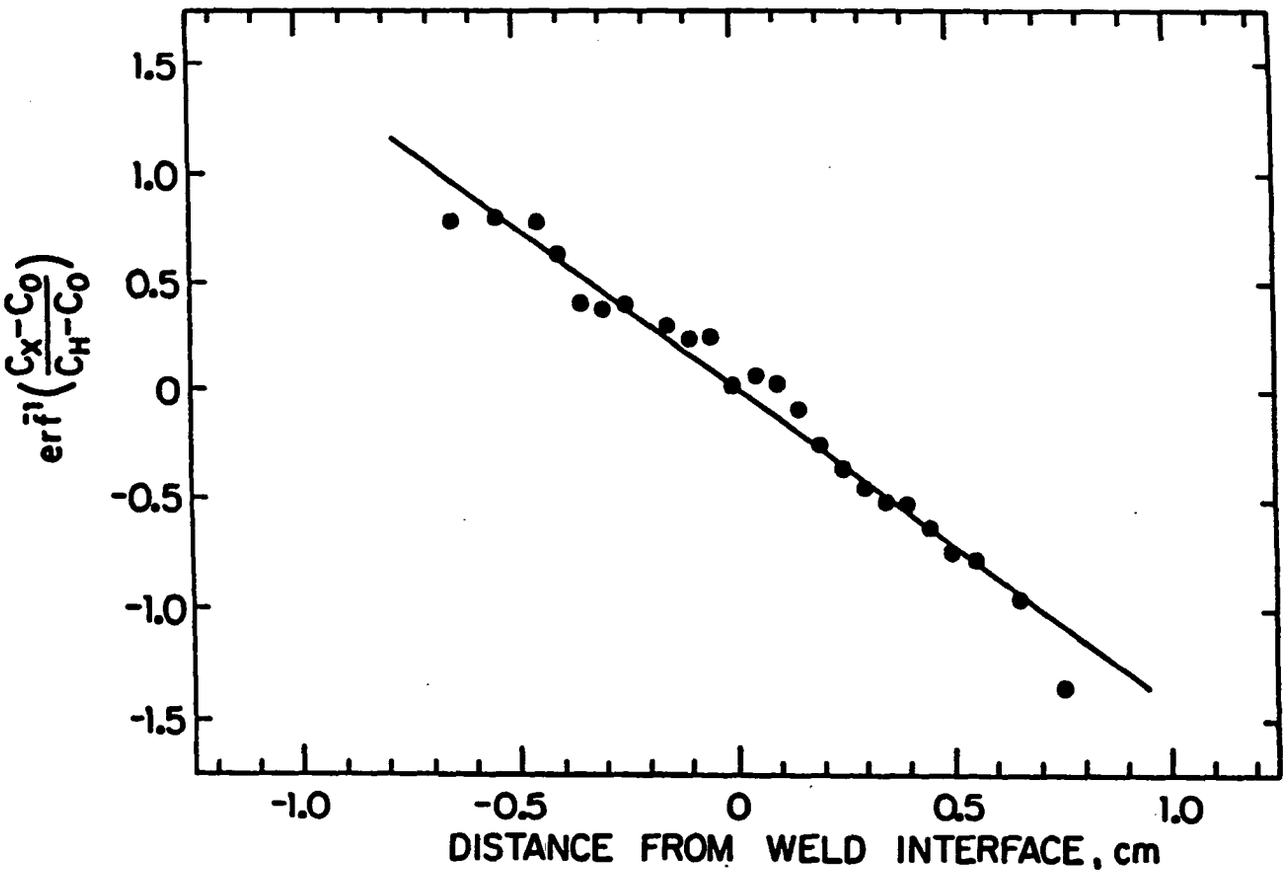

Figure 3. Plot of the inverse error function vs. distance for cobalt in thorium after two hours at 1332°C

Table 1. Diffusivities for Co in α-Th

Temperature (°C)	Time (h)	Diffusivity, D (x 10^{-10} m^2s^{-1})
1332	2.0	16.0
1270	4.7	9.8
1188	4.0	7.1
1164	8.8	6.5
1112	7.0	5.3
1100	6.5	4.5
1002	8.0	2.4
977	26.0	1.9
900	22.5	1.7

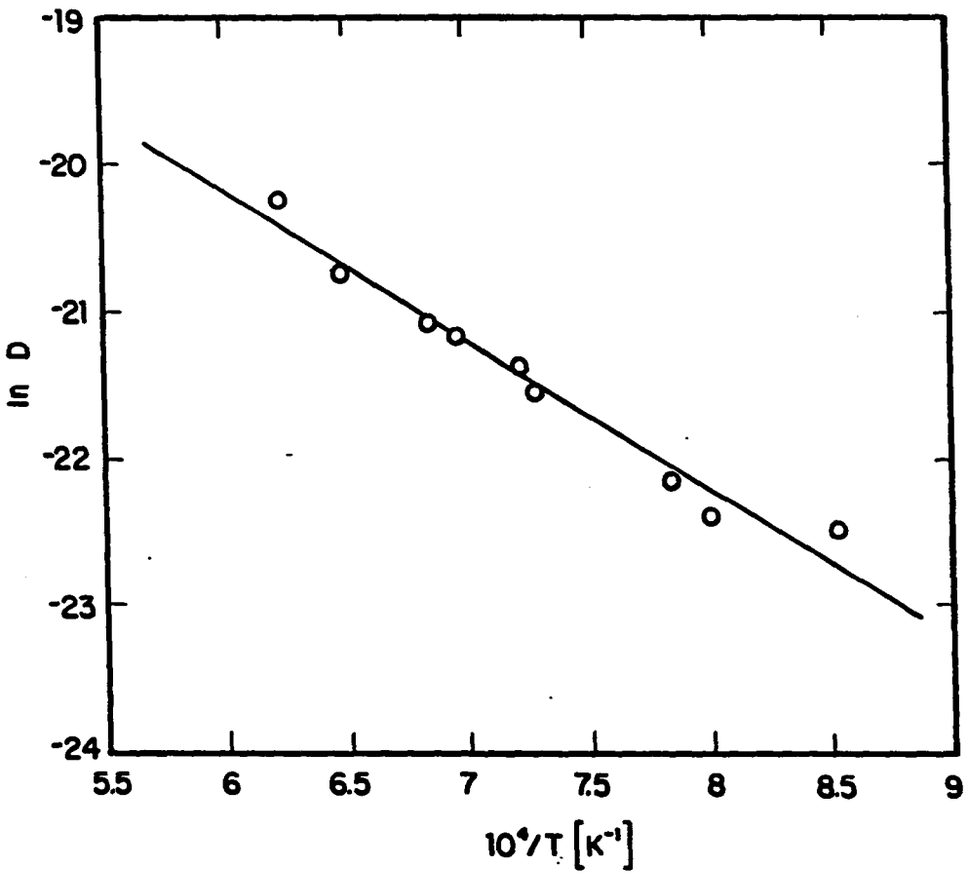

Figure 4. Plot of ln D vs. 1/T for cobalt in α thorium

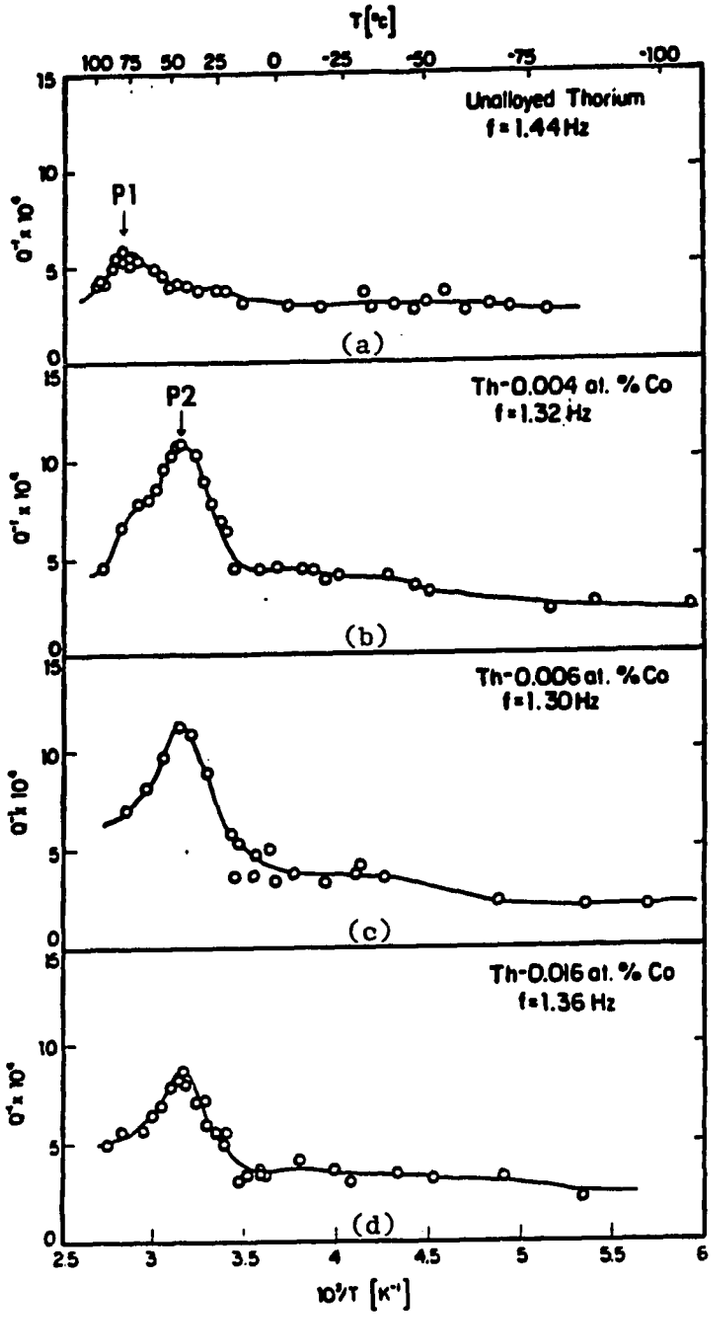

Figure 5. Plots of internal friction vs. reciprocal temperature for (a) an unalloyed thorium metal specimen and alloy specimens containing (b) 0.004, (c) 0.006 and (d) 0.016 at.% Co

Table 2. Internal Friction Results for As-quenched Unalloyed Thorium and Alloys Containing Different Cobalt Concentrations

At.% Co	f (Hz)	T_{P1} (^{o}C)	$Q^{-1}_{MAX(P1)}$ (x 10^4)	T_{P2} (^{o}C)	$Q^{-1}_{MAX(P2)}$ (x 10^4)	T_{P3} (^{o}C)	$Q^{-1}_{MAX(P3)}$ (x 10^4)
0.000	1.44	94	6	-	-	-	-
0.004	1.32	-	-	45	11	-	-
0.006	1.30	-	-	45	11	-	-
0.016	1.36	-	-	45	9	-	-
0.05	1.76	-	-	48	10	-	-
0.14	1.63	-	-	47	12	-	-
0.24	1.64	-	-	47	13	-35	8

at.% Co specimen a peak, referred to herein as P2, was observed at about 45 C with $Q^{-1}_{MAX} = 11 \times 10^{-4}$. This peak temperature corresponds to that of the higher temperature cobalt peak observed by Weins and Carlson (20). For the alloy specimens containing 0.006 and 0.016 at.% Co the height of P2 is essentially the same as that for the 0.004 at.% Co alloy specimen; Q^{-1}_{MAX} lies in the range of 9 to 11 x 10^{-4}. The appearance of a shoulder on the cobalt peak for the 0.004 at.% Co alloy occurs at approximately the same temperature as P1 in the unalloyed thorium (94^{o}C). Optical microscopy analyses of these specimens (24) have indicated that the as-quenched 0.004 at.% Co specimen is in a one-phase condition whereas a plate-like precipitate is present in the alloys containing 0.006 and 0.016 at.% Co. This, along with the internal friction results, suggests that the supersaturation limit for cobalt, for a quench rate of $\sim 800^{o}$C/s, is about 0.004 at.%.

Plots of internal friction as a function of reciprocal temperature for quenched alloy specimens containing 0.05, 0.14 and 0.24 at.% Co are shown in Fig. 6. The frequencies used in these analyses lie in the range of 1.63 to 1.76 Hz. As is evident from the figure and from Table 2 the P2 peak was also observed in these alloy specimens and found to have the same height. It will be noted that there is no shoulder on the higher temperature side of this peak as observed in the Th-0.004 at.% Co specimen. Optical microscopy analyses of the specimens revealed the presence of the plate-like precipitate consistent with the lower cobalt alloys (22).

Weins and Carlson (20) observed a second peak in the Th-0.2 at.% Co

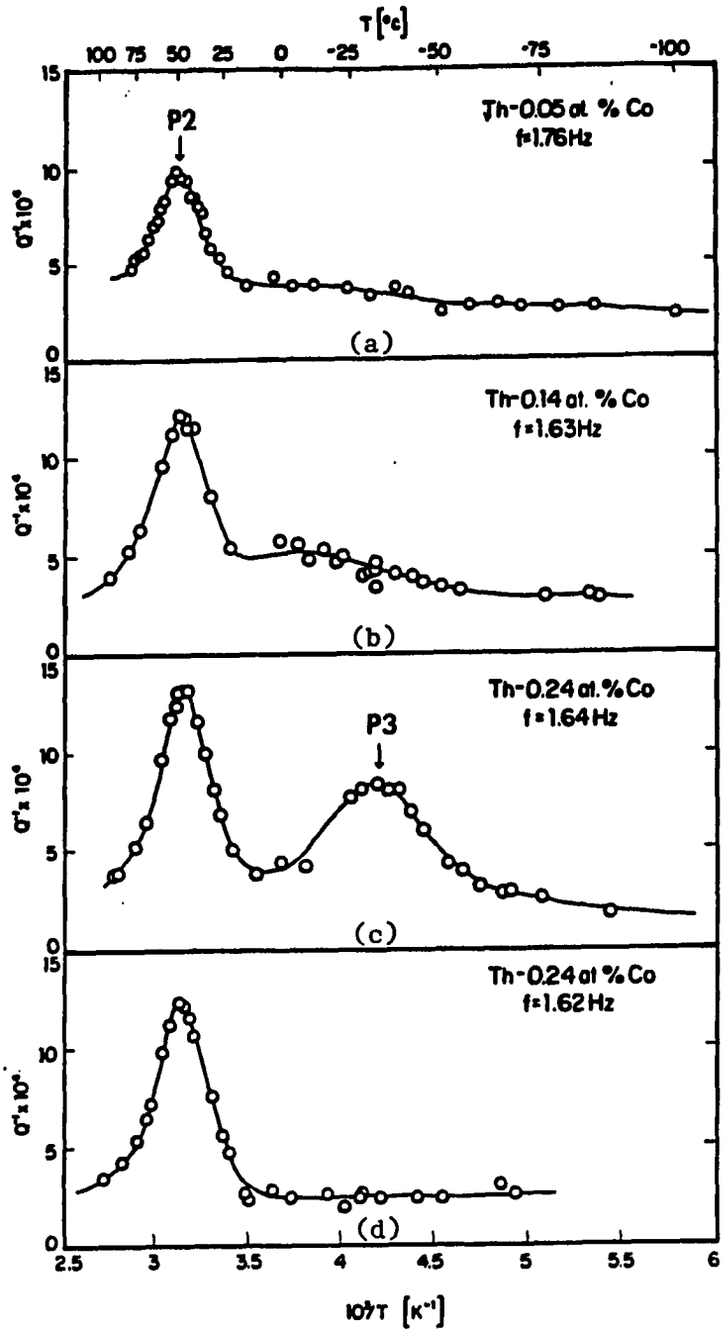

Figure 6. Plots of internal friction vs. reciprocal temperature for alloy specimens containing (a) 0.05, (b) 0.14 and 0.24 at.% Co (c) as quenched and (d) after room temperature aging

specimen at approximately -55°C at f = 1.35 Hz. Likewise, in this investigation a second peak referred to as P3 was observed in the 0.24 at.% Co specimen, although the temperature at which this peak occurs is about 20°C higher than that observed in the previous study. After aging at room temperature for a period of 10 months, the P3 peak disappeared (Fig. 6(d)). Although the peak appears to be cobalt related, its nature and origin were not determined. Since this peak is not observed in the more dilute alloy specimens, it does not appear that the defect producing this effect is associated with the fast diffusion process.

The activation energy for relaxation, Q_R, and the time constant, τ_{ro}, associated with the peak near 45°C was obtained from a study of the frequency dependence of the peak temperature in the Th-0.24 at.% cobalt alloy specimen. Plots of normalized internal friction, Q_N^{-1}, versus reciprocal temperature for eight frequencies are shown in Fig. 7. Normalized internal friction is defined as the ratio of Q^{-1} at the measured temperature to that at the peak temperature. It should be pointed that these peaks are single relaxation peaks. A list of the frequencies and corresponding peak temperatures is shown in Table 3. From a linear least squares analysis of a plot of ln $(1/\omega)$ versus reciprocal peak temperature (Fig. 8) an activation energy for relaxation of 78.0 ± 1.5 kJ/mole and a time constant of 1.77×10^{-14} s was determined. This value for Q_R is slightly smaller than the value of 83.7 ± 6 kJ/mol reported by Weins and Carlson (20) for a 0.2 at.% Co alloy.

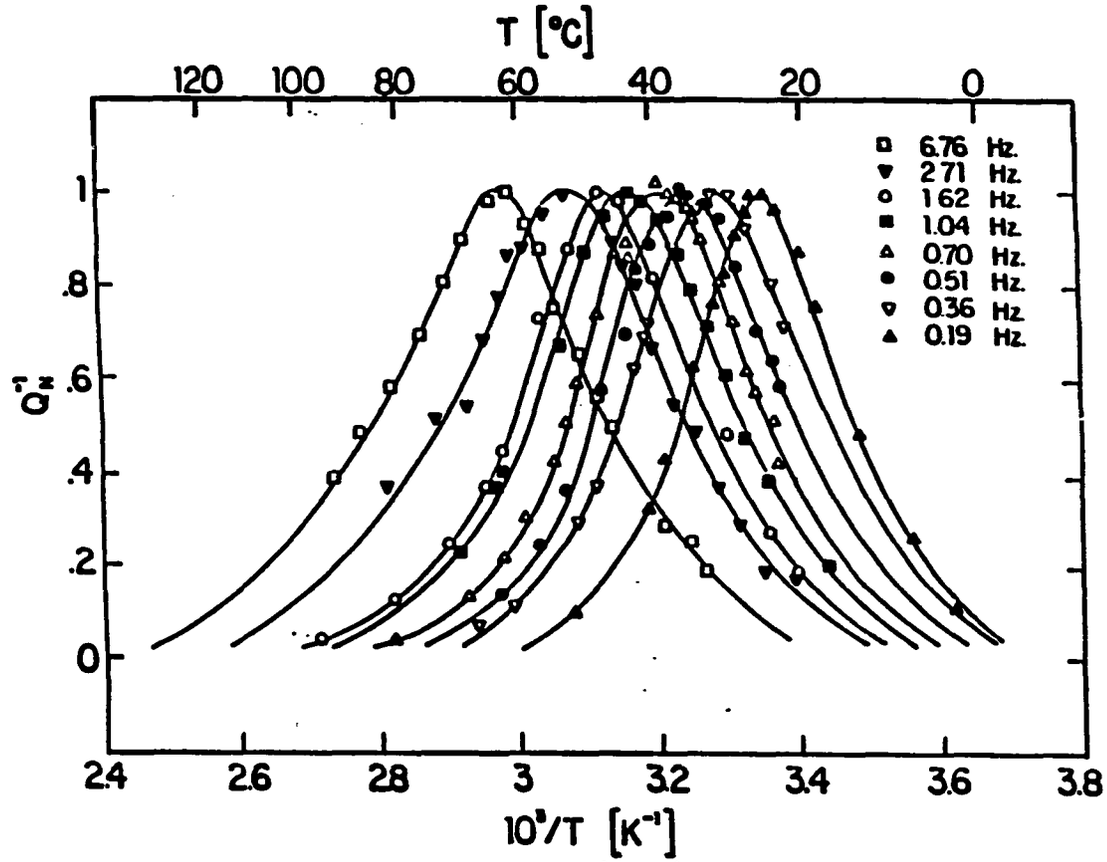

Figure 7. Plots of normalized internal friction vs. reciprocal temperature for the cobalt peak of the Th-0.24 at.% Co alloy for eight different frequencies

Table 3. Internal Friction Results for the Th-0.24 at.% Co Alloy

f (Hz)	T_P (^oC)	Q_R (kJ/mol)	τ_{ro} (x 10^{-14} s)
6.76	63		
2.71	52		
1.65	46		
1.04	43		
0.70	38	78.0 ± 1.5	1.77
0.51	35		
0.36	31		
0.19	25		

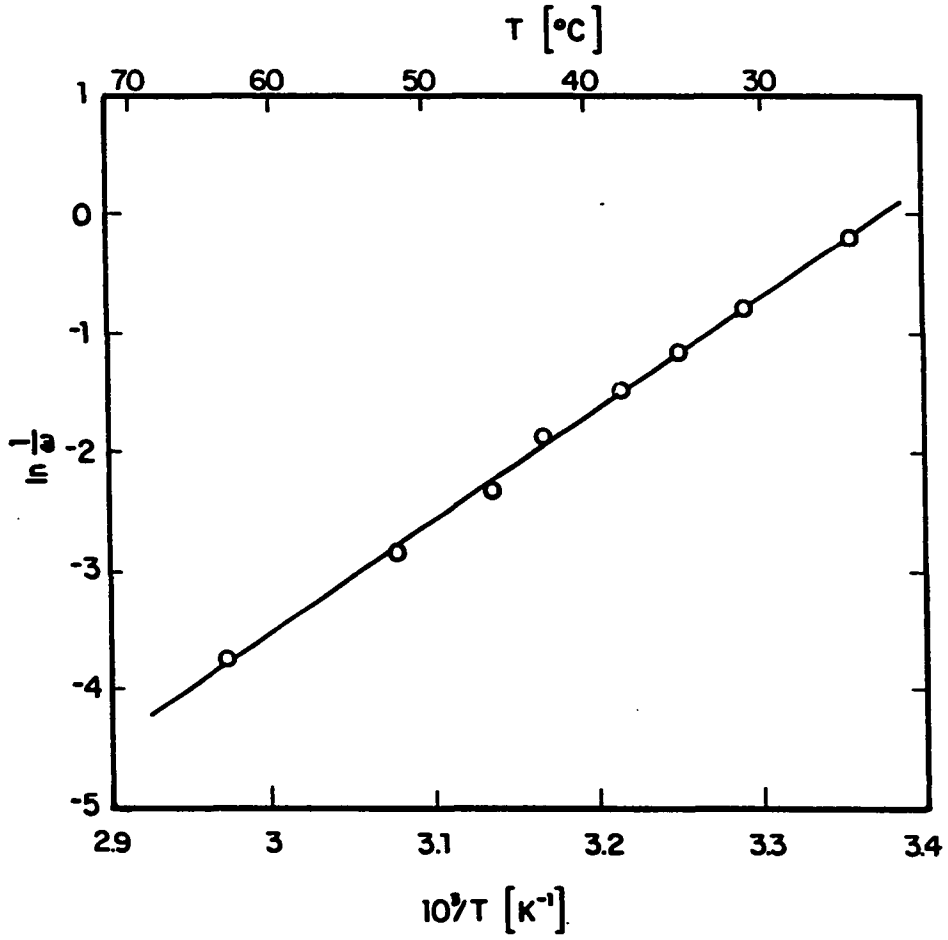

Figure 8. Plot of ln (1/ω) vs. reciprocal peak temperature for the data obtained from Figure 7

DISCUSSION

The occurrence of the cobalt internal friction peak indicates that at least some of the cobalt atoms in solution are associated with a defect that can be characterized as an elastic dipole. Since α thorium has a close-packed fcc structure, this defect may be a solute-vacancy, host-solute or solute-solute pair. If only a fraction of the cobalt atoms are associated with this type of defect, then it is possible that the remainder are present as interstitial or substitutional point defects. The activation energy for relaxation, Q_R, for the cobalt peak is only slightly smaller than that for diffusion, Q_D. This is consistent with the earlier findings of Weins and Carlson for nickel but they obtained nearly identical values of Q_R and Q_D for iron in thorium. The overall results of these studies, however, indicate the same type of defect is responsible for the motion of all three solutes in close-packed thorium. Of the three mechanisms proposed for fast diffusion, i.e., the interstitial, host-solute diplon and interstitial-vacancy mechanisms, only the latter two involve defects that can produce internal friction peaks in a close-packed structure. This would appear to eliminate the interstitial jump process as the dominant diffusion mechanism. If, however, the internal friction peak is due to substitutional-interstitial solute pairs, as observed by Mah and Wert (25) for O and N in Yb containing Ta or other metallic imppurities, an interstitial mechanism could be considered. The host-solute diplon and interstitial-vacancy pair mechanisms are consistent with the presence of an internal friction peak and, therefore, these mechanisms will be considered more closely.

The defect associated with the host-solute diplon mechanism consists of a host atom and a solute atom which form a close-pair on a lattice site. Fast diffusion is the result of two atom motions, as shown in Fig. 9, which include 1) the rotation of the defect pair about the lattice site (Fig. 9(a)) and 2) the translation of the solute atom from one host atom to another one (Fig. 9(b)) (2). Each of these two atom motions can affect a reorientation of the defect pair and can, therefore, be associated with an anelastic relaxation effect. If the activation energies for these two atom motions are not the same, however, anelastic relaxation will proceed primarily by the atom motion with the lower activation energy. Since both atom motions are required for long-range solute diffusion, the rate-controlling step will be the motion with the higher activation energy. Thus, if solute diffusion is dominated by the host-solute diplon mechanism, it is expected that the activation energy for relaxation would be less than that for diffusion; the internal friction being sensitive to the low energy step and the diffusion being sensitive to the high energy step (2). If the measured activation energy for relaxation is interpreted as being slightly smaller than that for diffusion, then the experimental results of this investigation are consistent with this model if the difference between the energies of these two motions are small. Warburton and Turnbull have indicated that if the activation energy for diffusion and for relaxation are equal then either there is an unlikely coincidence or a single motion which produces the effects of both translation and rotation exists (2).

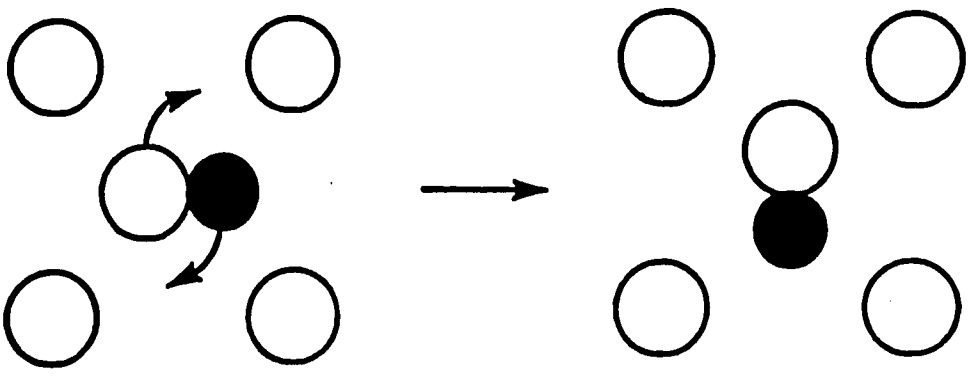

(a)

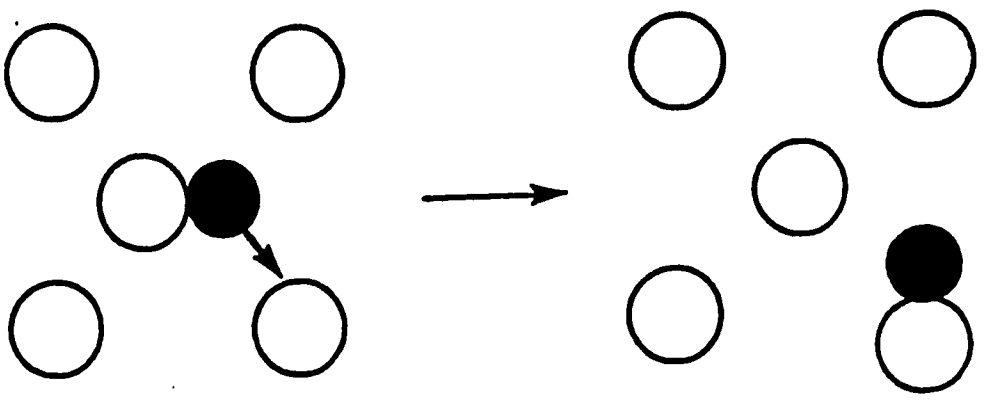

(b)

Figure 9. Schematic drawing of proposed host-solute diplon model showing the possible diplon motions of (a) rotation and (b) translation

The interstitial-vacancy pair consists of an interstitial solute atom and a vacancy which is located on a nearby lattice site. The two atom motions associated with the migration of this defect pair, as proposed by Miller (6), are illustrated in Fig. 10 and include 1) interstitial jumps around the vacancy with the frequency k_2 (solid arow in Fig. 10(a)) and 2) solvent jumps into the vacancy with frequency w_2 (Fig. 10(b)). Both motions are required for long-range solute diffusion, with the higher energy one being the rate-controlling step. Since the defect pair can reorient by either jump process, anelastic relaxation should proceed by the lower energy motion. Miller assumed that the frequency of the interstitial atom jumps is much greater than that of the solvent jumps, i.e., $k_2 \gg w_2$ implying that the activation energy for the former is less than that for the latter. Therefore, anelastic relaxation would be controlled by the k_2 jumps and diffusion by the w_2 jumps. This implies that the activation energy for diffusion should be much greater than that for anelastic relaxation. This, however, is not in agreement with the experimental results of this investigation.

Warburton (7) later modified Miller's model suggesting that, for geometrical reasons, the interstitial jumps (solid arrow in Fig. 10(a)) will not occur. Instead, the solute atom would be mobile only through pair annihilation jumps (v_2 in Fig. 10(a)) and pair formation jumps (v_1 in Fig. 10(a)). It was further assumed that the frequency of the w_2 jumps would be much greater than that of the v_2 jumps. Thus, anelastic relaxation would be controlled by the w_2 jumps, whereas diffusion by the

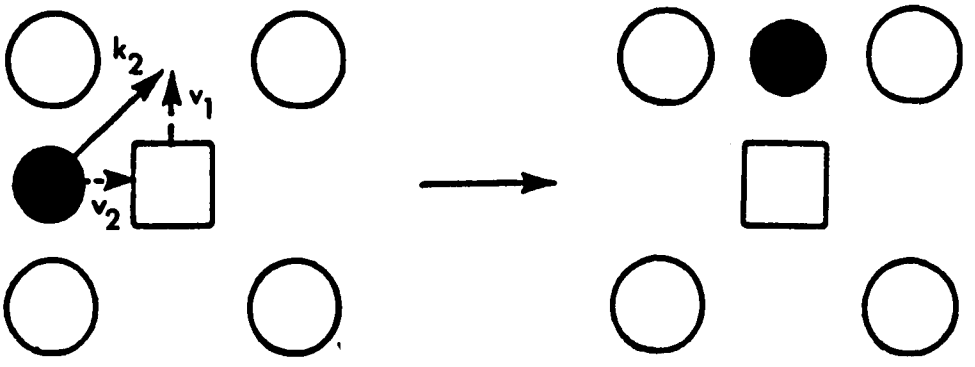

(a)

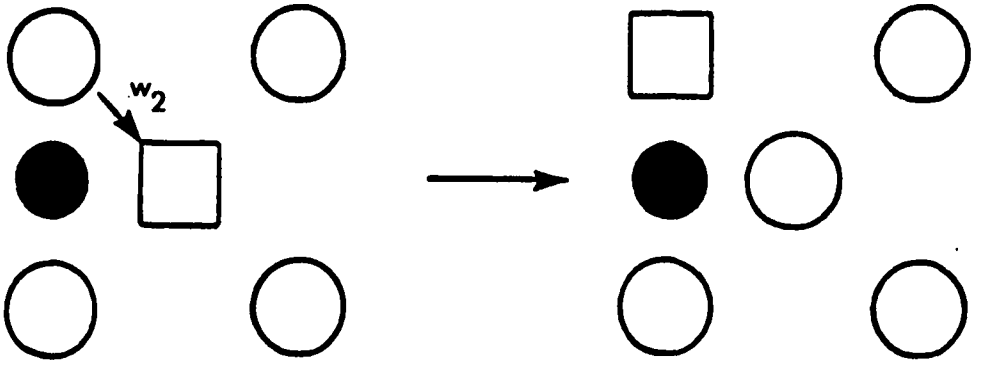

(b)

Figure 10. Schematic drawing of proposed interstitial-vacancy pair models showing the possible (a) solute jumps and (b) solvent jump

v_2 jumps. As in the case of Miller's model, the activation energy for diffusion should be much greater than that for relaxation.

Substitutional-interstitial Pairs

Although the concentration of metallic impurities in the starting material is considered to be low, the possiblity of an interaction between a substitutional impurity and interstitially-sited cobalt atoms can not be ruled out. The presence of S-I pairs could be responsible for the observed internal friction peak. Mah and Wert (25) observed internal friction peaks due to oxygen and nitrogen in ytterbium, a face-centered cubic metal. They concluded that the relaxation peaks are probably caused by substitutional-interstitial pairs. The model for relaxation of these defect pairs is shown in Fig. 11 (26). The defect pair consists of a substitutional impurity and an interstitial atom which are located on adjacent sites. As the result of an applied stress, an anelastic strain may be produced by the interstitial atom jumping to one of the other interstitial sites adjacent to the substitutional impurity. It has been observed that the activation energy for relaxation associated with the peak which is produced by this defect pair is nearly equal to that of the activation energy for interstitial diffusion (27). This is consistent with the present experimental results.

Turner and Nielsen (28) observed internal friction peaks for the fast diffusing elements gold, copper and silver in lead containing 300 ppm bismuth. Two sets of peaks were observed in each alloy; For one set the activation energy was equal to that for diffusion and for the other approximately 10% less. Inasmuch as the peaks were not present in

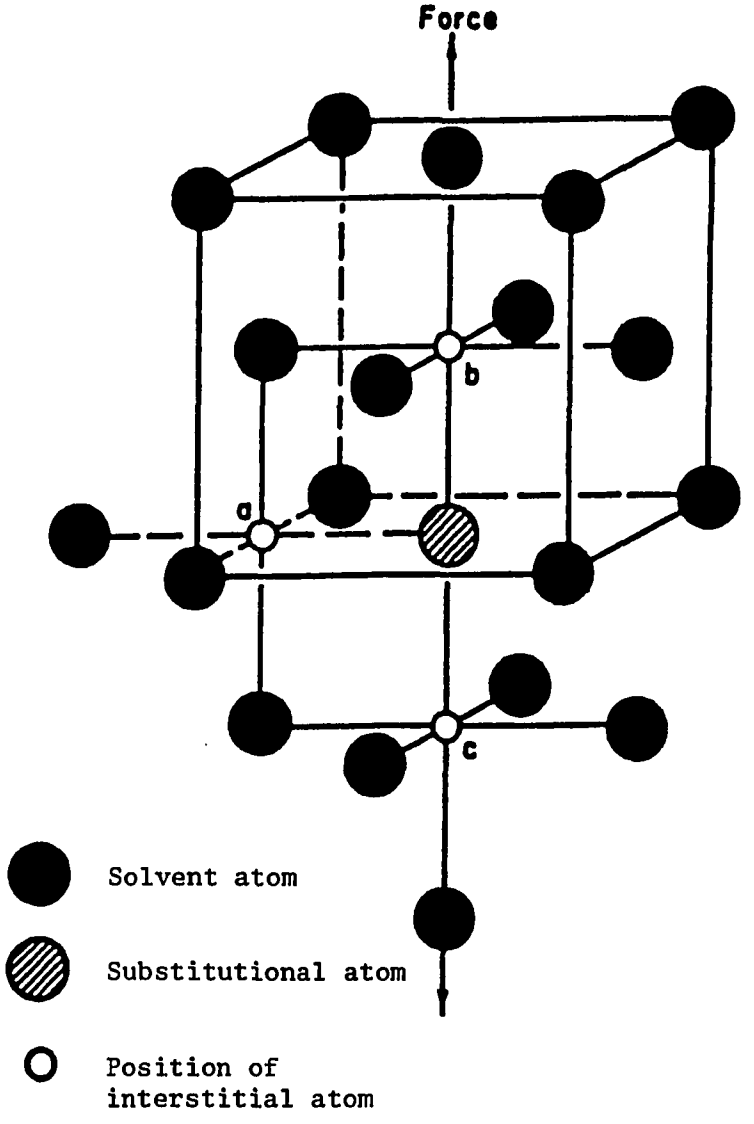

Figure 11. Model for relaxation of substitutional-interstitial pairs in an fcc crystal (reproduced from reference (26))

bismuth-free lead, they were ascribed to a solute-bismuth interaction. Sagues and Nowick (29), however, failed to confirm the presence of these peaks in Pb-Au alloys to which bismuth was deliberately added and suggested that their occurrence may be due to some other impurity.

Weins and Carlson (21) noted a decrease in the magnitude of the major internal friction peak for iron in thorium as the purity of the base metal was increased from 99.95+ to 99.995%. A possible explanation was that this decrease in magnitude was related to the increase in purity of the thorium.

Further evidence for substitutional-interstitial pairs in the Th-Co system might be gained from the diffusion and internal friction data. According to Wert (26) the relationship between the diffusivity, D, and the anelastic relaxation time, τ_r, for those relaxations involving atomic diffusion is

$$D = d^2/6\alpha\tau_r \qquad (7)$$

where d is the jump distance of the diffusing atom and α is a constant relating τ_r to τ, which is the mean time of stay of the diffusing atom on a given site. If D is assumed to be described by equation (5) and τ_{ro} by equation (2), then assuming that $Q_R = Q_D$, D_o can be expressed as

$$D_o = d^2/6\alpha\tau_{ro} \qquad (8)$$

where D_o and τ_{ro} are constants. For an interstitial atom jumping between octahedral sites immediately adjacent to a substitutional impurity in a

close-packed fcc crystal, α has the value of 1.5 (26). The value for α, assuming that the cobalt internal friction peak is due to substitutional-interstitial pairs, may be calculated from the experimentally determined values for D_o and τ_{ro}. For an fcc lattice, the distance, d, between octahedral sites is $d = a_o\sqrt{2}/2$ where a_o is the lattice parameter of the host structure. Making this substitution into equation (9) and rearranging the terms gives

$$\alpha = \frac{a_o^2}{12 D_o \tau_{ro}} \qquad (9)$$

Using the experimentally determined values for D_o and τ_{ro}, equation (9) yields a value for α of 1.7. Considering the experimental error in determining D_o and τ_{ro} this value is in good agreement with that expected by the substitutional-interstitial pair model. Using a value for α of 1.7, D values were calculated from the anelastic relaxation data. From a plot of log D versus 1/T these values are compared with those determined by chemical diffusion in Fig. 12. The solid line is a linear least squares fit to the internal friction data and extrapolated through the chemical diffusion data surprisingly well.

Both the host-solute diplon and the substitutional-interstitial pair models provide possible explanations for the appearance of the internal friction peak in the Th-Co system. The host-solute diplon model would be consistent with the experimental results if Q_R is interpreted as being slightly less than Q_D. On the other hand, if Q_R and Q_D are taken to be equal, the results would be more in line with the substitutional-

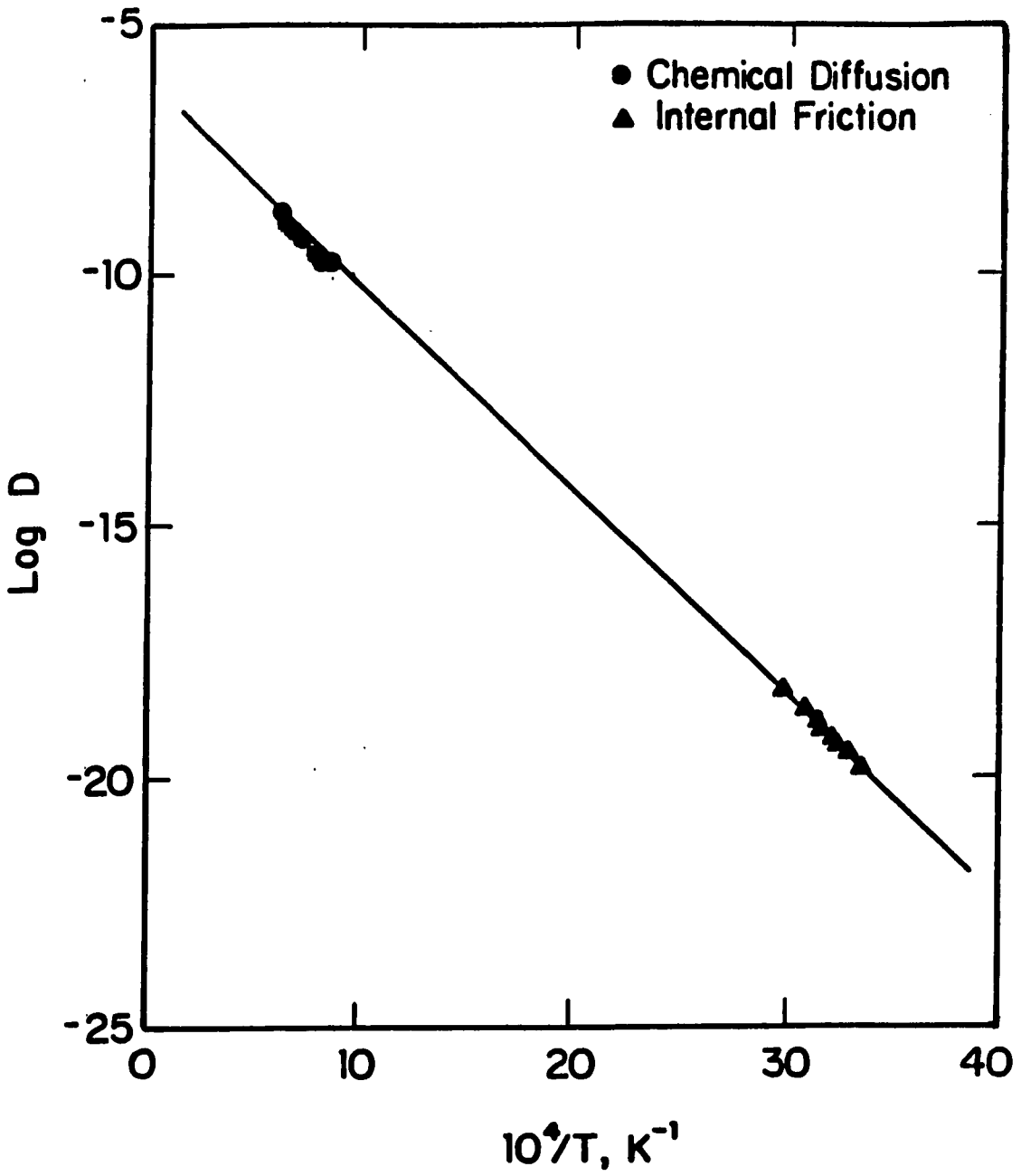

Figure 12. Plot of log D vs. reciprocal temperature for diffusion and internal friction data

interstitial pair model. Because of the excellent agreement of the log D versus 1/T plot, which would indicate that diffusion and anelastic relaxation are proceeding by the same jump process, the substitutional-interstitial model is preferred.

This interpretation, however, leaves the question open as to which impurity is the interacting element. The substitutional impurities in the thorium material used in this investigation are 7 ppma Re, 4 W and 5 Mo. Tungsten and molybdenum were present in the thorium used by Weins and Carlson, but at higher concentrations (5 ppma W and 48 ppma Mo). Since the magnitude of the internal friction peak observed by those authors was somewhat greater than that observed in the present investigation, tungsten and molybdenum are considered to be the most likely suspects.

CONCLUSIONS

1. The activation energy for diffusion of cobalt in α thorium was determined to be 83.7 ± 4 kJ/mol whereas that associated with the anelastic relaxation process at ~45°C for cobalt in thorium is 78.0 ± 1.5 kJ/mol.
2. The results can be interpreted as supporting either the host-solute diplon mechanism or the interstitial mechanism for fast diffusion.
3. Although the concentration of substitutional impurities is relatively low, a substitutional-interstitial pair is considered to be the more likely explanation for the internal friction peak observed at 45°C.
4. A second internal friction peak at -35°C was observed in the higher concentration alloy but does not appear to associated with the fast diffusion process.

REFERENCES CITED

1. W. C. Roberts-Austen, Proc. Roy. Soc. 59, 281 (1986); Phil. Trans. Roy. Soc. 187, 404 (1896).

2. W. K. Warburton and D. Turnbull, in Diffusion in Solids: Recent Developments, edited by A. S. Nowick and J. J. Burton (Academic Press, New York, NY, 1974), p. 171.

3. A. D. Le Claire, J. Nuc. Mater. 69 & 70, 70 (1978).

4. C. Herzig, in DIMETA-82. Diffusion in Metals and Alloys, edited by F. J. Kedves and D. L. Beke (Trans Tech Publications, Switzerland, 1983) p. 23.

5. T. R. Anthony, in Vacancies and Interstitials in Metals, edited by A. Seeger (North-Holland, Amsterdam, 1970), p. 935.

6. J. W. Miller, Phys. Rev. 188, 1074 (1969).

7. W. K. Warburton, Phys. Rev. 7, 1330 (1973).

8. J. W. Miller, Phys. Rev. 2, 1624 (1970).

9. B. F. Dyson, T. R. Anthony and D. Turnbull, J. Appl. Phys. 37, 2370 (1966).

10. F. C. Frank and D. Turnbull, Phys. Rev. 104, 617 (1956).

11. J. W. Miller, Phys. Rev. 181, 1095 (1969).

12. J. N. Mundy, J. W. Miller and S. J. Rothman, Phys. Rev. B10, 2275 (1974).

13. J. W. Miller, J. N. Mundy, L. C. Robinson and Ronald E. Loess, Phys. Rev. B8, 2411 (1973).

14. J. W. Miller, A. Edelstein, Phys. Rev. 188, 1081 (1969).

15. T. Bolze, H. Metzger, J. Peisl and S. C. Moss, J. Phys. F: Met. Phys. 14, 1073 (1984).

16. T. Bolze, H. Metzger, J. Peisl and S. C. Moss, J. Phys. F: Met. Phys. 14, 1085 (1984).

17. J. W. Miller, D. S. Gemmell, R. E. Holland, J. C. Poizat, J. N. Worthington and R. E. Loess, Phys. Rev. 11, 990 (1975).

18. J. S. Carpenter and W. N. Cathey, Phys. Lett. 64A, 313 (1977).

19. G. Vogl, W. Miekeley, A. Heidemann and W. Petry, Phys. Rev. Lett. 53, 934 (1984).

20. W. N. Weins and O. N. Carlson, J. Less-Common Metals 66, 99 (1979).

21. W. N. Weins and O. N. Carlson, Met. Trans. 13A, 995 (1982).

22. A. S. Nowick and B. S. Berry, Anelastic Relaxation in Crystalline Solids (Academic Press, New York, 1972) p. 185.

23. R. J. Conzemius, F. A. Schmidt and H. J. Svec, Anal. Chem. 53, 1899 (1981).

24. S. C. Axtell and O. N. Carlson, Department of Materials Science and Engineering, Iowa State University, and Ames Laboratory, Ames, Iowa and A. J. Bevolo, Ames Laboratory, Ames, Iowa, 1988 (Section I in this thesis).

25. G. Mah and C. Wert, Trans. TMS-AIME 230, 16 (1964).

26. C. Wert, in Physical Acoustics, edited by W. P. Mason (Academic Press, New York, 1966), Vol III, Part A, p. 43.

27. R. Gibala and C. Wert, in Diffusion in Body-Centered Cubic Metals, (American Society for Metals, Metals Park, Ohio, 1965) p. 131.

28. T. J. Turner and C. H. Nielsen, Solid State Commun. 15, 243 (1974).

29. A. A. Sagues and A. S. Nowick, Solid State Commun. 15, 239 (1974).

SECTION III. A STUDY OF THE THERMOTRANSPORT BEHAVIOR OF COBALT IN THORIUM

INTRODUCTION

When a temperature gradient is applied to an initially homogeneous material a redistribution of the components of the system may occur. This mass transport phenomenon is referred to as thermotransport or thermomigration. Thermotransport of solutes in metals is of practical interest because a redistribution of the solute atoms may have an undesirable effect on the properties of an alloy. However, this phenomenon is not very well understood at the present time. Critical experiments, such as the measurement of the effect of temperature on the magnitude and direction of thermotransport, are desirable in developing a better understanding of this phenomenon (1). Such experiments involve a determination of the heat of transport, Q*, which is a phenomenological parameter indicating the direction and magnitude of thermotransport.

In the past, thermotransport studies on solutes in metals have been primarily confined to systems involving substitutional or common interstitial elements, i.e., carbon, oxygen, nitrogen and hydrogen. Although many of these studies have been carried out on single-phase alloys, several have been performed on two-phase alloys as well (2-7). Shewmon (2) developed a model for the thermotransport of interstitial solutes in two-phase alloys which successfully explained the observed direction of thermotransport of carbon in two-phase iron-carbon alloys. Later, Marino (8), Okafor *et al.* (3) and Uz *et al.* (7) employed this model in numerical calculations of solute concentration profiles for two-phase zirconium-hydrogen, iron-nickel-carbon, vanadium-carbon, and niobium-carbon alloys exposed to temperature gradients. The excellent

agreement between the computer-calculated and experimental concentration profiles demonstrates the validity of Shewmon's model.

One class of alloys in which only a few studies of thermomigration have been performed are the fast diffusing metal systems. Two characteristics of these types of systems are 1) the solute diffusivity is at least one order of magnitude greater that the self-diffusivity of the host metal and 2) the activation energy for solute diffusion is markedly less than that for self diffusion of the solvent. According to current theory (9-11), fast diffusing solutes are present as substitutional and interstitial-type defects in the host metal with diffusion being dominated by the migration of the interstitial-type defects. Interstitial-type defects may be single interstitial atoms, interstitial-vacancy pairs, or host-solute diplons. Thermotransport studies have been performed on a few fast diffusing systems such as copper, gold, and silver in lead (12-15). Sullivan et al. (12) indicate that there is no significant temperature dependence of Q* for silver and gold in lead, but Stracke and Herzig (12) report that Q* for gold in lead decreases monotonically with increasing temperature. The effect of temperature on Q* was not determined for copper in lead (12,15).

In an earlier study, cobalt was found to be a fast diffusing element in thorium (16). The thermotransport behavior of cobalt in thorium has not been studied, however. Since the knowledge of a temperature dependence of Q* would be valuable in establishing an atomistic interpretation of thermotransport, this investigation was undertaken to determine Q* for cobalt in thorium and to determine whether or not Q* is

temperature dependent. Two techniques were used to determine Q* over a temperature range of 1125 to 1458 K. These include a steady-state technique and a method in which solute concentration profiles from two-phase experiments are compared to computer-calculated curves.

THEORY

For those metal-solute systems in which the mobility of the solute is much greater than that of the host metal, the solute flux, J, in the X direction of a single-phase alloy, due to the presence of a concentration gradient and a temperature gradient, is given by

$$J = - D \frac{dc}{dX} - \frac{Q^* c D}{RT^2} \frac{dT}{dX} \qquad (1)$$

where D and c are the diffusivity and concentration of the solute, R is the gas constant, T is the absolute temperature and Q^* is the heat of transport. The first term of equation (1) describes the diffusion flux while the second term describes the thermomigration flux. For the steady-state condition, i.e., J = 0, in which the thermomigration flux is balanced by the diffusion flux, equation (1) reduces to

$$d \ln c = \frac{Q^*}{R} d \left(\frac{1}{T}\right). \qquad (2)$$

This relation indicates that from a one-phase steady-state experiment, Q^* may be obtained from the slope of a plot of ln c versus 1/T. The sign and magnitude of Q^* indicate the direction and magnitude of the thermomigration flux of the solute where a positive value for this quantity represents a flux towards the cold end of the specimen.

An equation for the solute flux in a two-phase alloy under a temperature gradient may be obtained from equation (1) if several assumptions are made. This situation was first analyzed by Shewmon (2)

who assumed that only the solute migrates in the alloy and that local thermodynamic equilibrium between the solute in solution and in the second-phase particles is obtained in those regions where the solubility limit is exceeded. Shewmon has shown that under these assumptions equation (1) may be written as

$$J = - \frac{Dc}{RT^2} (\Delta\overline{H} + Q^*) \frac{dT}{dX} \qquad (3)$$

where H is the partial molar enthalpy of solution for the solute. This relation shows that in the two-phase region, the direction and magnitude of the net solute flux is indicated by the sign and magnitude of the quantity $(\Delta\overline{H} + Q^*)$. Later, Okafor et al. (3) introduced a factor, "a", defined as the fraction of the cross-sectional area of the specimen occupied by the matrix phase, as determined by the lever rule. It was suggest by these authors that if the mobility of the solute atoms in the second-phase particles is negligible compared to that in the matrix phase, then an increase in the fraction of the cross-sectional area occupied by these particles should be accompanied by a lower net solute flow through a given region. Taking this factor into account, they modified equation (3) to give

$$J = \frac{Dca}{RT^2} (\Delta\overline{H} + Q^*) \frac{dT}{dX} \qquad (4)$$

where "a" is determined by the lever law.

EXPERIMENTAL PROCEDURES

Materials and Sample Preparation

The thorium used in this investigation was obtained from the Materials Preparation Center of the Ames Laboratory. The concentrations of the major impurities were 350 ppma O, 30 N, 350 C, 5 Ta, 7 Re, 4 W, 10 Si, 5 Mo and 0.04 Co. The cobalt was obtained from the Materials Research Corporation and had a purity of greater than 99.9%. A master alloy containing 0.56 at.% cobalt was prepared by arc-melting a small amount of cobalt with thorium under an atmosphere of purified argon. Alloys containing 0.016, 0.05 and 0.24 at.% cobalt were prepared by adding unalloyed thorium to portions of the master alloy in subsequent arc-melting steps. The cobalt content of each of the alloys was determined by atomic absorption. Portions of the arc-melted ingots were swaged into 0.25-cm diameter rods. Specimens were prepared by cutting the rods into segments varying between 2.5 and 3 cm in length.

Mass Transport Studies

In this investigation one-phase steady-state experiments and two-phase nonsteady-state experiments were performed. The one-phase experiments involved heating the specimen entirely in the α thorium region until a near steady-state condition was achieved. In the two-phase experiments the specimens were heated partially or completely in the two-phase region (α + Th_7Co_3) for a predetermined length of time.

The apparatus used in this investigation consists of a stainless steel vacuum chamber equipped with two water-cooled copper electrodes and

a sight glass for optical pyrometer measurements. In the one-phase experiments the specimens were supported between two tapered tungsten adapters which were screwed into the copper electrodes as shown in Fig. 1(a). In the two-phase experiments, the specimens were inserted directly into the copper electrodes and secured with stainless steel set screws as shown in Fig. 1(b).

All of the specimens were heated under a pressure of less than 5×10^{-7} Torr by internal electrical resistance using a constant a.c. power source. Due to the cold adapters, an approximately parabolic temperature profile was produced along the specimens with the hottest portion being near the center of the rods (see Fig. 1). An optical pyrometer was used to measure the temperatures at fiducial marks which were engraved at regular intervals along the rod. Each of these measurement was corrected for emmisivity and sight glass absorption.

The degree of steady state, R_{ss} achieved in the one-phase experiments as a function of time is given by (17)

$$R_{ss} = 1 - \exp(-t/\theta) \tag{5}$$

where t is the experimental time and θ is the relaxation time which is given by

$$\theta = \frac{L^2}{\pi^2 D} \tag{6}$$

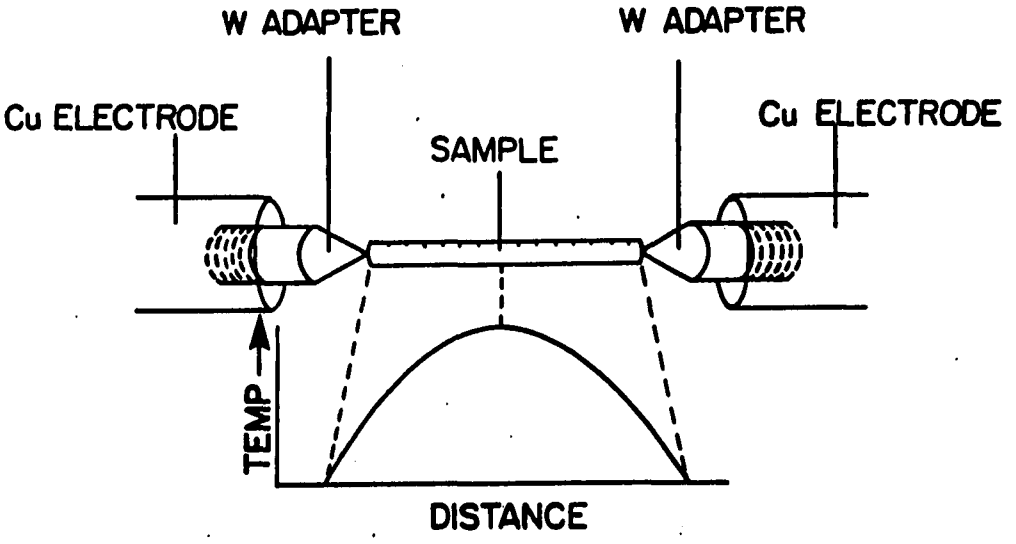

(a)

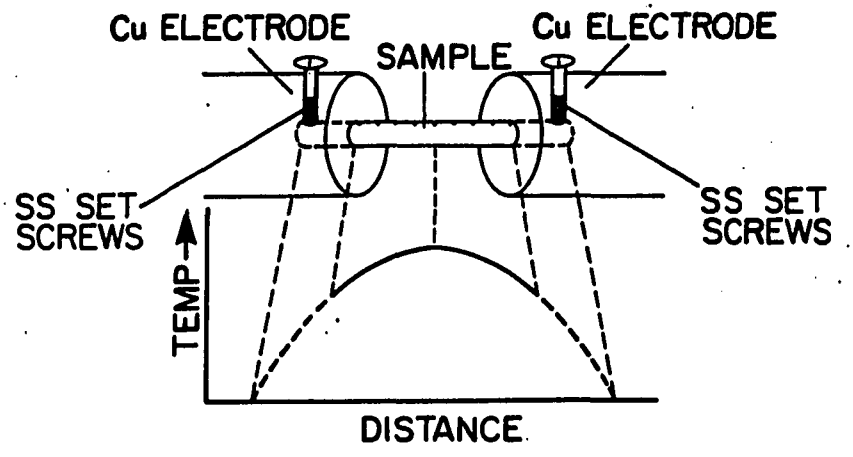

(b)

Figure 1. Experimental arrangement and typical temperature profiles for (a) one-phase experiments and (b) two-phase experiments

In this equation L is the length of the specimen over which a continuous temperature gradient exists and D is the solute diffusivity at the mean temperature of the specimen over that length. The time estimated for the one-phase experiments was 5θ which corresponds to 99.3% of steady state. Each of the one-phase specimens was heated for a long enough time to achieve at least 97% of steady state.

At the conclusion of each experiment, the cobalt concentration profile of each specimen was determined by scanning laser mass spectrometry (SLMS) (18). In this chemical analysis technique, a focused laser is used to vaporize and ionize a small portion of the sample at desired positions along the rod. The vaporized and ionized material is then collected and analyzed for the trace solute by a mass spectrometer. In this investigation, the cobalt concentrations were determined at 0.5 mm intervals along the rod.

In the one-phase steady-state technique the heat of transport was determined by analyzing the temperature and concentration profile data from the one-phase experiments. Each measured concentration and corresponding temperature were used to construct a plot of ln c versus 1/T. The heat of transport was then determined from the slope of this plot. The technique which was used to determine Q^* employing two-phase experiments will be discussed later.

In order to determine the effect of temperature on Q^* the one-phase and two-phase experiments were performed over different temperature ranges. The heat of transport was evaluated for each experiment and correlated with the mean temperature over the portion of the specimen in

which a significant amount of cobalt transport had occurred. For the one-phase experiments this temperature corresponds to the mean temperature of the specimen. However, for the two-phase experiments, this temperature is associated with the average temperature over only part of the sample as will be explained later. It should be noted here that in the single-phase experiments the solute concentration profiles could not be measured accurately enough to permit the determination of the effect of temperature on Q* from an individual experiment. Such a determination would require that the experimental concentration profile be precise enough to reveal a measurable curvature in the plot of ln c versus 1/T if Q* is temperature dependent.

The range of temperatures over which Q* could be determined in thorium using the single-phase steady-state technique was limited. This is due in part to the limited temperature range over which the α region exists (19). For example, for a cobalt concentration of 0.05 at.% Co the α region extends from 1100 to 1618 K where the upper temperature limit is the α to β transformation temperature. In addition, it was found that the hot and cold regions of the specimens had to differ by at least 300 K if reliable values for Q* were to be obtained. Therefore, for the 0.016 and 0.05 at.% Co alloy specimens used in the single-phase studies, the practical temperature range over which the mean specimen temperatures could be varied was about 1270 to 1470 K.

Two-Phase Nonsteady-State Technique

As indicated in the introduction, the studies of Okafor et al. (3) and Uz et al. (7) demonstrate that equation (4) describes the

thermotransport behavior of two-phase interstitial alloys very well. This forms the basis of a new technique, referred to herein as the two-phase nonsteady-state technique, whereby Q* can be determined for a given system. In this method a two-phase nonsteady-state experiment is performed and the solute concentration profile determined. Theoretical concentration profiles are then calculated on a computer for a series of Q* values and compared to the experimental profile. The computed curve which best matches the experimental data indicates the value of Q*.

In this study the theoretical cobalt concentration profiles were calculated using equations (1) and (4) in an explicit single-step finite difference method similar to that of Marino (8), Okafor *et al.* (3) and Uz *et al.* (7). The temperature profiles of the specimens were calculated by a seventh order polynomial which was fit to the experimentally determined temperatures. The diffusion coefficient, D, solid solubility limit, c_s, and the area fraction, a, were calculated according to the following equations:

$$D = 7.2 \times 10^{-7} \exp(-83.7 \text{ kJ mol}^{-1}/RT) \text{ m}^2/\text{s} \quad (7)$$

$$c_s = 7044 \exp(-110.5 \text{ kJ mol}^{-1}/RT) \text{ at.\%} \quad (8)$$

$$a = (c_{Th_7Co_3} - c)/(c_{Th_7Co_3} - c_s) \quad (9)$$

where c is the at.% Co at a given position and $c_{Th_7Co_3}$ is the at.% Co in the Th_7Co_3 phase. The diffusion data were obtained from Axtell and Carlson (20) and the solubility data from Axtell *et al.* (19). A detailed

description of this calculation method is given in the doctoral thesis of Uz (21). The computer program used in this investigation is listed in the appendix.

As mentioned earlier, Q* for a given experiment was correlated with the average temperature over that part of the specimen in which a significant amount of cobalt had been transported. For the two-phase experiments the cobalt is essentially immobile at the specimen ends, therefore, the average temperature was determined over only a portion of the sample. It was difficult to decide over which portion of the sample the temperatures should be averaged. This was because of the difficulty in deciding what constitutes a "significant amount of transport". It was finally decided that the boundary between that part of the specimen where a significant amount of cobalt transport occurred and that where it didn't is located at the position where a maximum cobalt build-up occurs. This position was chosen because, although the cobalt is mobile beyond this point, the relative mobility is so low that a concentration peak is produced.

RESULTS

Thermotransport in Single-Phase Alloys

Dilute alloys of two cobalt concentrations (0.05 and 0.016 at.%) were heated in three different temperature ranges. The results of these experiments are summarized in Table 1.

The plots of temperature and cobalt concentration versus distance for the 0.05 at.% Co alloy specimen heated at a mean temperature of 1458 K is shown in Fig. 2. Similar profiles were obtained for the 0.05 at.% Co alloy at 1380 K and the 0.016 at.% Co alloy at 1283 K. It will be noted that both the temperature and concentration profiles are parabolic in shape with the same symmetry axis. The heat of transport was determined from a linear least squares analysis of the plot of ln c versus 1/T, as shown in Fig. 3. For the 0.016 at.% Co alloy, the reported value for Q* is the average of two such analyses, as two SLMS measurements were made on this sample. As can be seen from Table 1, Q* is negative over the temperature range 1283 to 1458 K. Based on the scatter in the analyses, Q* could not be determined to within 15%.

It should be pointed out here that about 3% of the 0.016 at.% Co alloy was in the two-phase region at the end of the experiment as was noted from a microscopic examination of the specimen at the conclusion of the experiment. Technically, this would be considered a two-phase experiment, however, Uz *et al.* found for the thermotransport of carbon in vanadium and niobium (6) no significant difference between the Q* values obtained for single-phase alloys and those obtained for alloys containing only a small amount of second phase.

Table 1. Summary of Single-Phase Thermotransport Results

Cobalt Content (at.%)	Time of Run (h)	Temperature Range (K)	Mean Temperature (K)	Q* (kJ/mol)
0.016	263	935 to 1435	1283	-58
0.05	25	1090 to 1491	1380	-59
0.05	28	1270 to 1560	1458	-61

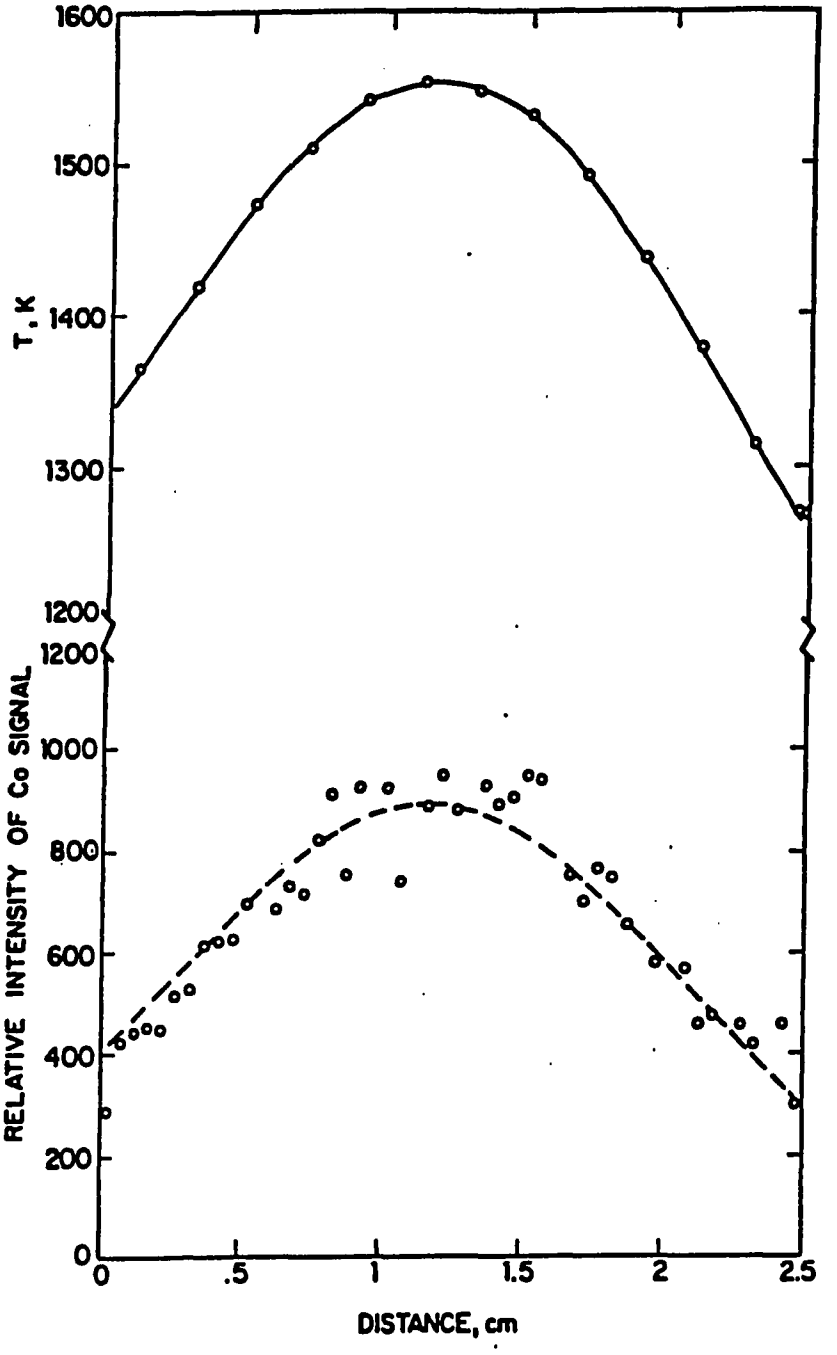

Figure 2. Temperature and concentration profiles for a Th-0.05 at.% Co thermotransport sample after heating for 28 h in the single-phase field

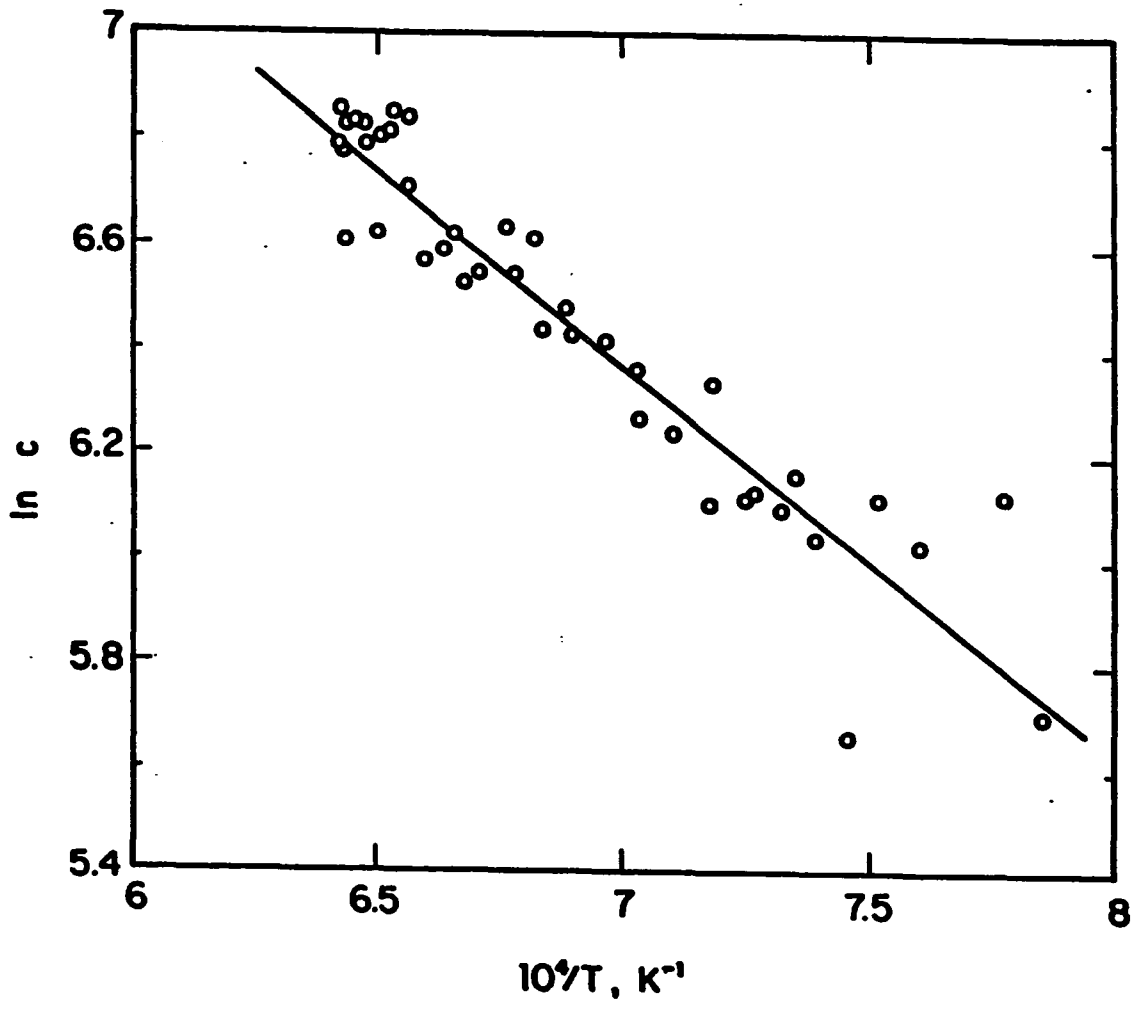

Figure 3. Plot of ln c versus reciprocal temperature for the Th-0.05 at.% Co sample

Thermotransport in Two-Phase Alloys

Two-phase experiments were performed on alloys of 0.24 and 0.56 at.% Co concentrations. A 0.56 at.% Co alloy was held in a temperature range such that the entire rod was in the two-phase region at the beginning of the experiment. The temperature range with respect to the solvus line and the cobalt concentration as a function of distance along the rod after heating for 120 h is shown in Fig. 4. The solubility data were obtained from Axtell et al. (19). It will be noted from Fig. 4(b) that the cobalt concentration over the middle portion of the specimen is relatively low and varies little with distance. A pronounced solute build-up is present in the regions of the specimen midway between the center and ends of the rod. At the ends of the rod the cobalt concentration is again relatively constant. This is because the temperature here was so low that the cobalt atoms were essentially immobile and, therefore, the cobalt concentration should be equal to the initial concentration of the alloy. The microscopic examination of this specimen indicated that a one-phase condition existed at the middle of the rod at temperature while the ends were in a two-phase condition. The boundary between the one- and two-phase regions was observed to be in the vicinity of the sharp discontinuity in the cobalt concentration. In the regions where a large solute build-up was detected, a relatively large volume fraction of equilibrium second-phase particles were observed. The micrographs in Fig. 5 show the microstructure at the middle of the specimen and of one of the regions where the large solute pile-up was observed. It will be noted that the plate-like metastable phase

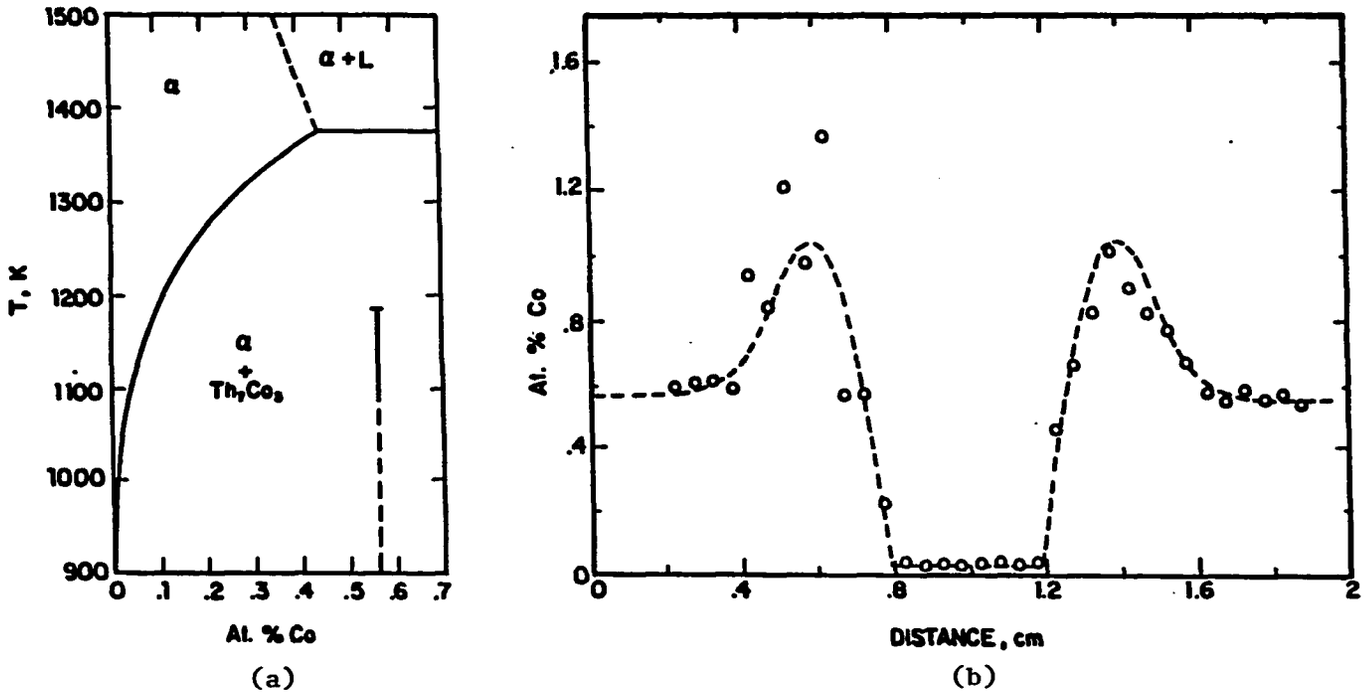

Figure 4. Data for a Th-0.56 at.% Co sample after heating for 120 h; (a) temperature range with respect to the solvus boundary and (b) concentration profile

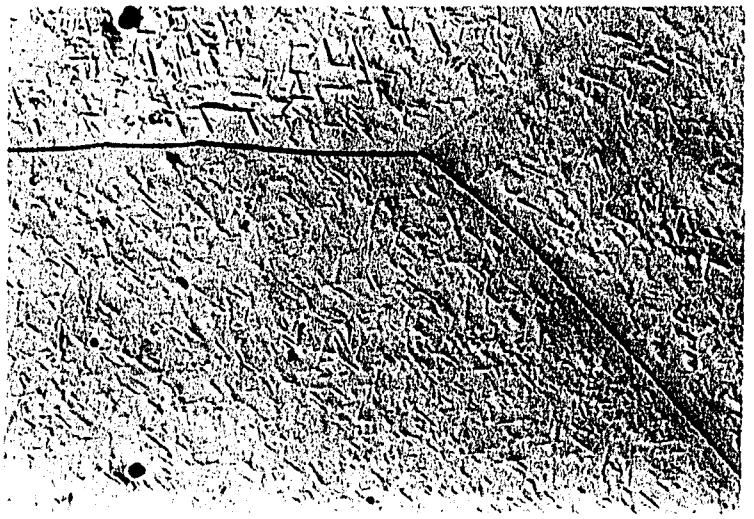

(a)

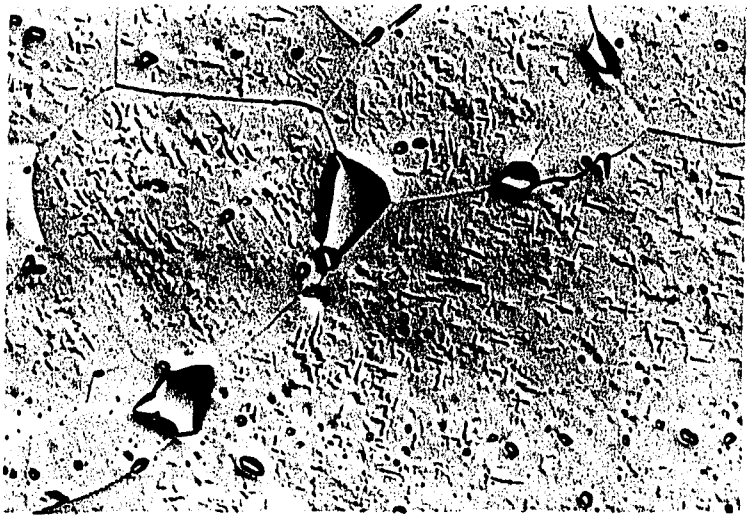

(b)

Figure 5. Microstructure of 0.56 at.% Co alloy; (a) single-phase structure at temperature near the center of the specimen and (b) two-phase structure at temperature at a portion of the sample where a solute pileup occurred. Electropolished, 500X DIC

identified in Section I of this thesis is present in both of these micrographs. This phase formed during the rapid cooling of the specimen at the conclusion of the experiment.

A somewhat different concentration profile was obtained for the 0.24 at.% Co alloy. As will be noted from Fig. 6(a), this sample was held in a temperature range where the central portion of the specimen was in the one-phase region while the cold ends were in the two-phase field. This concentration profile after 9 h (Fig. 6(b)) is similar to that for the 0.56 at.% Co alloy except that the solute build-up in the two-phase region is more pronounced and a broad maximum is present in the one-phase region. A microscopic examination of this specimen confirms the assumption that the interphase boundary is in the vicinity of the abrupt change in the cobalt concentration. The one- and two-phase microstructures were found to be similar to those observed for the 0.56 at.% Co alloy.

Theoretical concentration profiles for the 0.24 and 0.56 at.% Co alloys were calculated for a series of Q* values and compared with those determined experimentally. The calculated profiles for the 0.24 at.% Co alloy for three different Q* values are shown superimposed on the experimental profile in Fig. 7(a). Similar data for the 0.56 at.% Co alloy are shown in Fig. 7(b). It will be noted from these figures that, for the 0.24 at.% Co specimen, a Q* value of -30 kJ/mol provides the curve with the best fit to the experiment profile, whereas for the 0.56 at.% Co alloy, 20 kJ/mol provides the curve with the best fit. For these specimens, Q* could be conservatively estimated to within ± 20

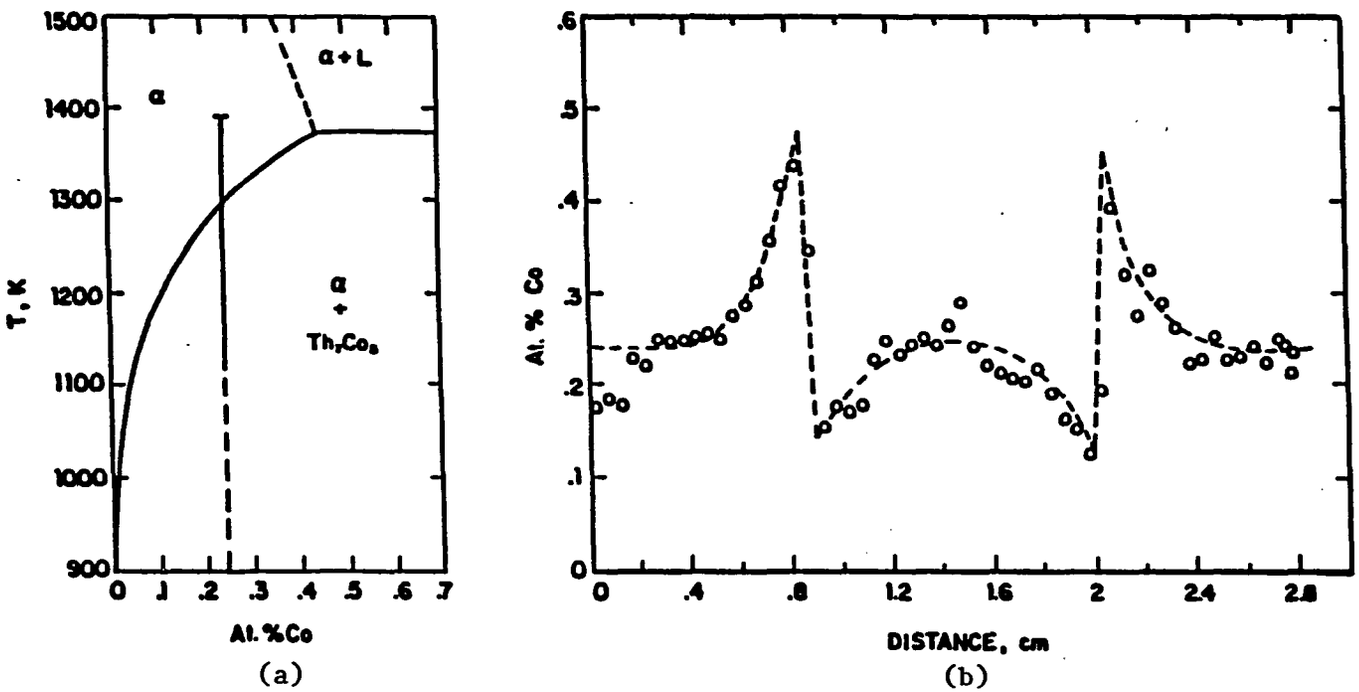

Figure 6. Data for a Th-0.24 at.% Co sample after heating for 9 h; (a) temperature range with respect to the solvus boundary and (b) concentration profile

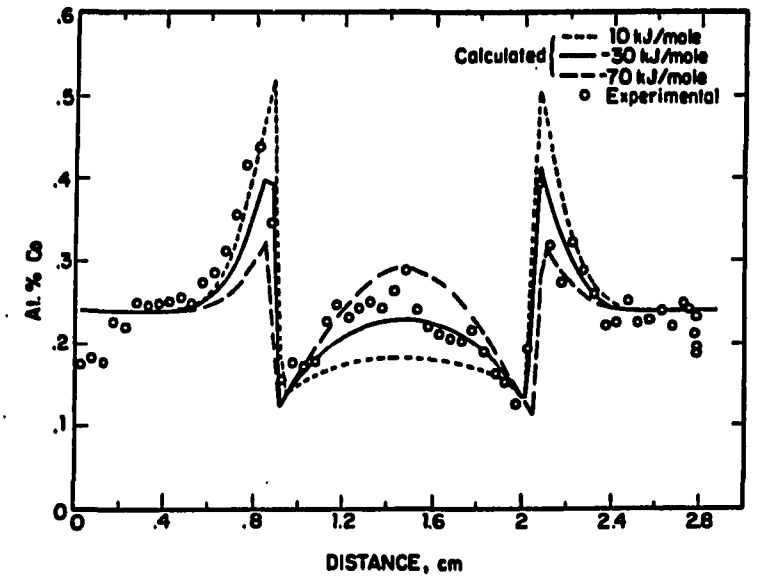

(a)

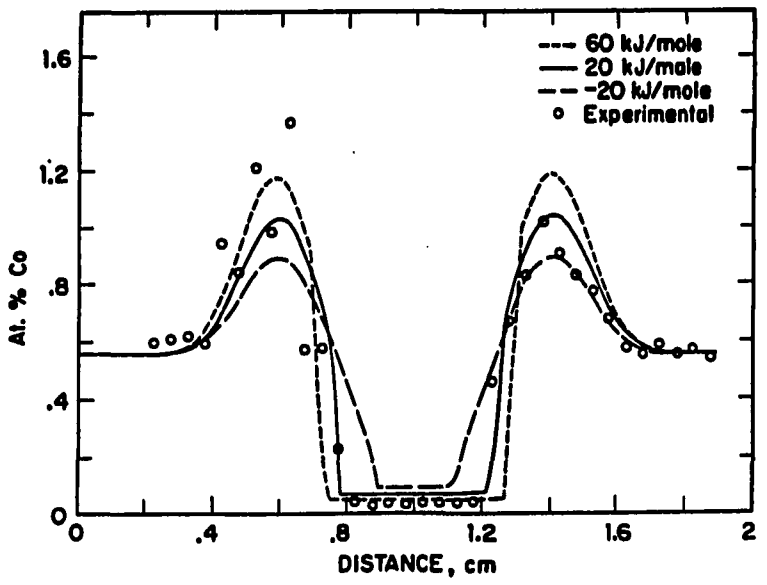

(b)

Figure 7. Calculated and experimental concentration profiles for (a) 0.24 at.% Co and (b) 0.56 at.% Co samples

kJ/mol. The mean temperatures at which the Q* values are reported for the 0.24 at.% Co alloy and the 0.56 at.% Co alloy are 1245 and 1125 K, respectively.

Q* Versus Temperature

The variation of Q* with the average temperature of the one- and two-phase alloys is shown in Fig. 8. It will be noted from the figure that Q* decreases with increasing temperature, decreasing from 20 kJ/mol at 1125 K to -61 kJ/mol at 1458 K. If a simple linear relationship between Q* and T is assumed, a linear least squares fit to the data indicates that Q* for cobalt in thorium may be described by

$$Q^* = 274 - 0.24\ T \text{ kJ/mol} \qquad (10)$$

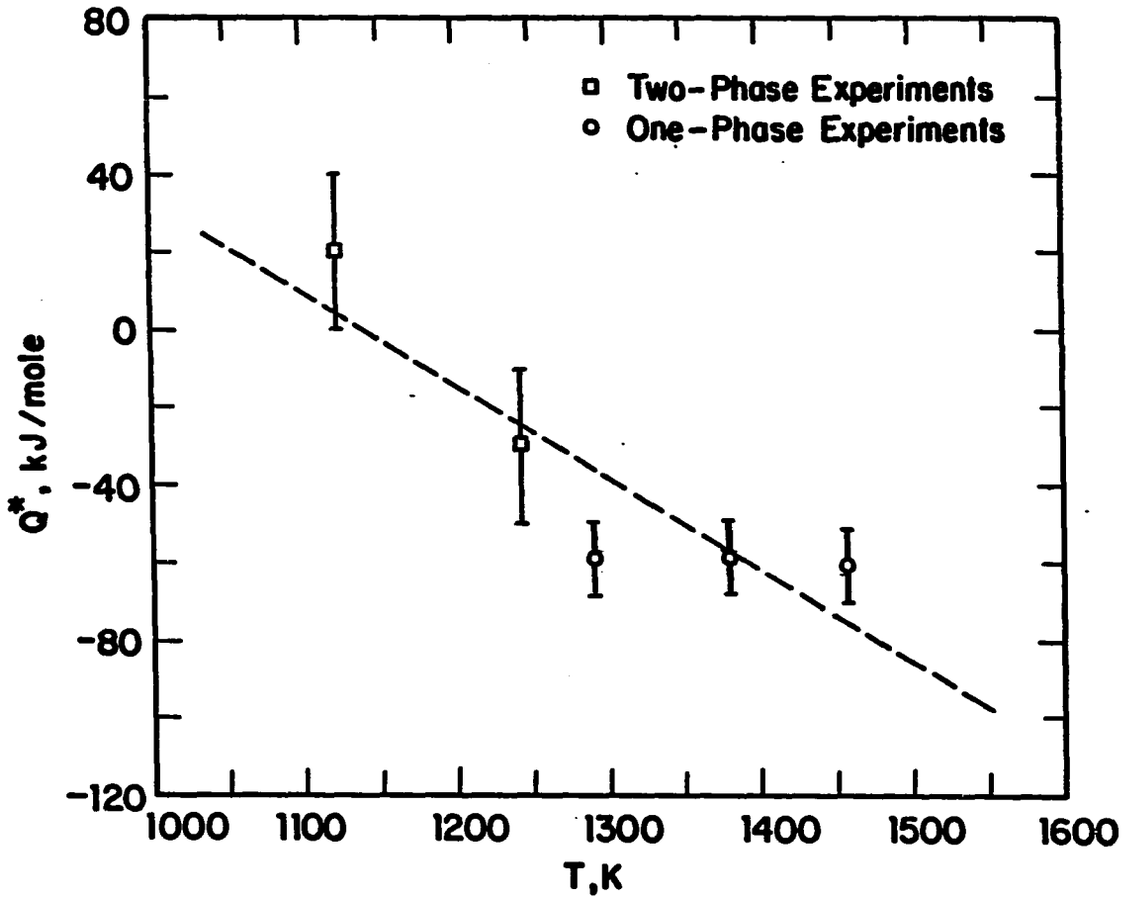

Figure 8. Plot of Q* versus mean temperature for one-phase and two-phase experiments

DISCUSSION

The validity of equation (10) may be tested by comparing the experimental concentration profiles of some of the one- and two-phase alloy specimens with those generated by a computer assuming that Q* is given by this relationship. In order for these calculations to be made, however, equations (1) and (4) must be modified to take into account a temperature dependence of Q*. The modified equations would be

$$J = - D \frac{dc}{dX} - \frac{Q^*(T)cD}{RT^2} \frac{dT}{dX} \tag{11}$$

for the flux in the single-phase field and

$$J = - \frac{Dca}{RT^2} (\Delta\bar{H} + Q^*(T)) \frac{dT}{dX} \tag{12}$$

for the flux in the two-phase field where Q*(T) is given by

$$Q^*(T) = a + bT + cT^2 + \ldots \tag{13}$$

and a, b, c, etc., are constant coefficients. In our calculations, however, Q* was assumed to be given by the linear relation

$$Q^*(T) = a + bT \tag{14}$$

A second order polynomial was considered, but, the theoretical concentration profiles which were calculated using that expression did not match the experimental profiles.

Theoretical concentration profiles for the 0.24 and 0.56 at.% Co two-phase alloys and the 0.016 single-phase alloy, which were calculated for Q^* given by equation (10), are shown in Fig. 9 along with the experimental data. The computed and experimental profiles are in very good agreement. This seems to substantiate that Q^* is temperature dependent over the temperature range investigated and is described by equation (10).

An examination of the atomistic mechanisms that have been associated with the thermotransport of solutes in metals may provide an explanation for the observed temperature dependence of Q^* for cobalt in thorium. According to Huntington (22), Q^* may be considered to be the sum of three contributions, i.e., an intrinsic contribution Q^*_{in}, phonon contribution Q^*_{ph} and electronic contribution Q^*_{el}, such that

$$Q^* = Q^*_{in} + Q^*_{ph} + Q^*_{el} \tag{15}$$

The intrinsic contribution arises from the difference in the jump frequencies of atoms lying on adjacent planes perpendicular to the temperature gradient. The electron and phonon contributions arise from the interaction of the solute atoms with phonons and electrons. Hehenkamp (23) has shown that Q^*_{el} may be given by

$$Q^*_{el} = - S_i(T) \cdot Z^*_i (T,N_i) \cdot T \tag{16}$$

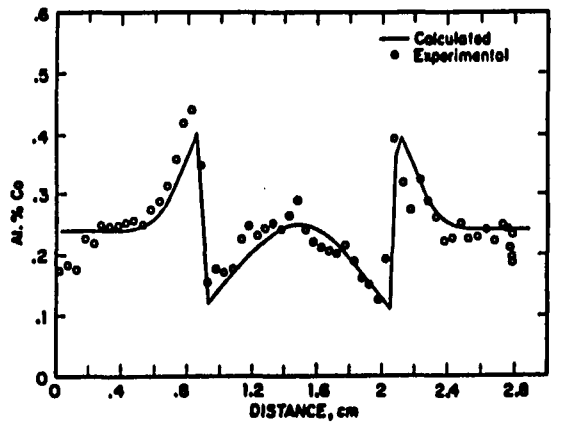

(a)

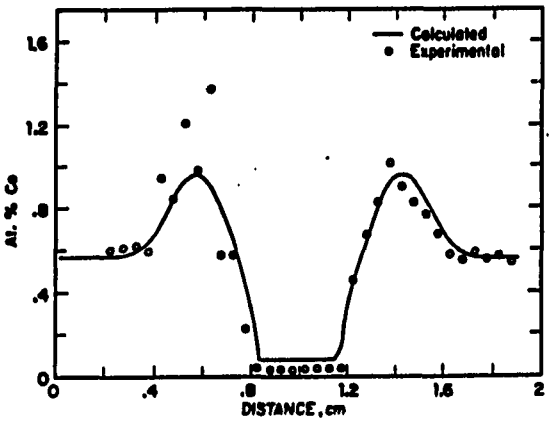

(b)

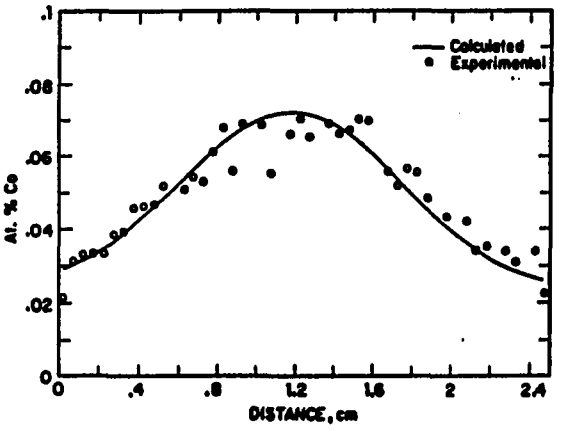

(c)

Figure 9. Calculated and experimental concentration profiles for (a) 0.24, (b) 0.56 and (c) 0.016 at.% Co samples

where S_i is the specific thermoelectric power, Z_i^* is the effective valence, N_i is the concentration of the diffusing species and T is the absolute temperature. This equation suggests that the electronic contribution to Q*, and therefore Q* itself, may be temperature dependent. The results of this investigation are, therefore, consistent with Hehenkamp's model of thermotransport.

CONCLUSIONS

1. The heat of transport of cobalt in thorium, as determined by the single-phase steady-state technique and a new technique referred to as the two-phase nonsteady-state technique, was observed to be temperature dependent, decreasing from 20 kJ/mol at 1125 K to -61 kJ/mol at 1458 K and is described by the relation $Q^* = 274 - 0.24\ T$ kJ/mol.
2. The observed temperature dependence of Q^* is consistent with a model for the electronic contribution to Q^*.

REFERENCES CITED

1. D. T. Peterson and M. F. Smith, Met. Trans. 13A, 821 (1982).

2. P. G. Shewmon, Trans. TMS-AIME 212, 642 (1958).

3. I. C. I. Okafor, O. N. Carlson and D. M. Martin, Met. Trans. 13A, 1713 (1982).

4. A. Sawatzky and E. Vogt, Trans. TMS-AIME 227, 917 (1963).

5. A. Sawatzky, J. Nuc. Mater. 2, 321 (1960).

6. J. M. Markowitz, Trans. Met. Soc. AIME 221, 819 (1961).

7. Mehmet Uz, D. K. Rehbein and O. N. Carlson, Met. Trans. 17A, 1955 (1986).

8. G. P. Marino, Nucl. Sci. Eng. 49, 93 (1972).

9. W. K. Warburton and D. Turnbull, in Diffusion in Solids: Recent Developments, edited by A. S. Nowick and J. J. Burton (Academic Press, New York, NY, 1974), p. 171.

10. A. D. LeClaire, J. Nuc. Mater. 69 & 70, 70 (1978).

11. C. Herzig, in DIMETA-82. Diffusion in Metals and Alloys, edited by F. J. Kedves and D. L. Beke (Trans Tech Publications, Switzerland, 1983) p. 23.

12. G. A. Sullivan, S. Larsson and P. T. Thermquist, Z. Naturforsch. 27a, 138 (1972).

13. E. Stracke and C. Herzig, Phys. Stat. Sol. (a) 66, 189 (1981).

14. C. Herzig and E. Stracke, Phys. Stat. Sol. (a) 27, 75 (1975).

15. E. Stracke and C. Herzig, Phys. Stat. Sol. (a) 47, 513 (1978).

16. W. N. Weins and O. N. Carlson, J. Less-Common Metals 66, 99 (1979).

17. S. R. deGroot, Physica 9, 699 (1942).

18. R. J. Conzemius, F. A. Schmidt and H. J. Svec, Anal. Chem 53, 1899 (1981).

19. S. C. Axtell and O. N. Carlson, Department of Materials Science and Engineering, Iowa State University, and Ames Laboratory, Ames, Iowa and A. J. Bevolo, Ames Laboratory, Ames, Iowa, 1988 (Section I in this thesis).

20. S. C. Axtell and O. N. Carlson, Department of Materials Science and Engineering, Iowa State University, and Ames Laboratory, Ames, Iowa, 1988 (Section II in this thesis).

21. Mehmet Uz, Ph.D. thesis, Iowa State University, 1985.

22. H. B. Huntington, Thin Solid Films 25, 265 (1975).

23. T. Hehenkamp, in Electro- and Thermotransport in Metals and Alloys, edited by R. E. Hummel and H. B. Huntington (AIME, Inc., New York, 1977), p. 68.

SUMMARY AND DISCUSSION

This investigation of the fast transport behavior of cobalt in thorium consisted of two primary studies and a supportive study. The primary studies included 1) a study of the mechanism of fast diffusion of cobalt in thorium using diffusion and internal friction experiments and 2) a study of the thermotransport behavior of cobalt in thorium. The results of the diffusion/internal friction study were supportive of either the host-solute diplon mechanism or the interstitial mechanism. It was indicated that the observed internal friction peak is more likely due to a substitutional-interstitial pair. The results of the thermotransport study indicate that Q* is temperature dependent, decreasing with increasing temperature. A highlight of the thermotransport study was the employment of a new technique to determine the heat of transport in a system.

The third study, which was supportive to the primary studies, was the investigation of the metastable $ThCo_x$ phase and the solid solubility of cobalt in thorium in dilute thorium-cobalt alloys. The results of this investigation indicate that the terminal solubility of cobalt in thorium is 0.45 at.% at 1373 K. In addition, it was observed that a metastable plate phase, possibly having an fcc crystal structure, a lattice parameter of 5.63 Å and a stoichiometry of $ThCo_{0.08}$, forms in alloys containing greater than 0.004 at.% Co that are quenched from the single-phase field. Upon aging above 773 K, the plate phase transforms to a rod-like equilibrium Th_7Co_3 phase.

The Th-Co system is only one of several systems that have been observed to exhibit fast diffusion. Other systems of more practical interest that exhibit this diffusion behavior are those of iron, nickel and cobalt in titanium and niobium. Studies of these systems may lead to improvements in alloys for aerospace and nuclear applications. In particular is the possible improvement of the strength of titanium and niobium alloys through the solid solution strengthening of the fast diffusion elements. In several of the lead-based fast diffusing systems it has been observed that the solid-solution strengthening is much greater than that observed in substitutional systems.

As indicated earlier, a new technique was used in the determination of Q^* for cobalt in thorium. It would be desirable to use this technique to determine Q^* for other systems. In particular, it would be useful for those systems in which the extent of the single-phase field is relatively small. This technique would also be valuable in studying the temperature dependence of Q^* in different systems. In this way the temperature range over which Q^* can be measured could be extended.

ACKNOWLEDGEMENTS

I would like to express my deep appreciation to Dr. O. N. Carlson for his excellent guidance and critical analysis in the course of this study. I would like to extend special thanks to F. A. Schmidt for the preparation of the thorium metal. Special thanks goes to L. P. Lincoln for his excellent technical assistance. Thanks are due to H. H. Baker for his metallographic work; F. Laabs and A. R. Pelton for their assistance with the transmission electron microscopy work; A. J. Bevolo for his scanning electron and scanning Auger microscopy work; and R. J. Conzemius, R. Z. Bachman and R. J. Hofer for their analytical work. I would also like to extend my appreciation to C. V. Owen for his assistance with the internal friction machine and M. E. Thompson, J. T. Wheelock, L. K. Reed and C. R. Ness for their technical assistance. Finally, I would like to thank my wife, Signe, for her untiring patience and constant support over the past 6 years.

APPENDIX

The following is a listing of the Pascal computer program

TRANSPORT:

```
PROGRAM TRANSPORT (INPUT,OUTPUT);
USES TRANSCENDS;

CONST  RC = 1.987;      {UNIVERSAL GAS CONSTANT USING CALORIES}
       RJ = 8.314;      {UNIVERSAL GAS CONSTANT USING JOULES}
       PI = 3.14159;

TYPE ATOM = ARRAY[0..100] OF REAL;

VAR  TSA,J,T,TG,CONC : ATOM;
     NUMBER,L,M,N,O,F,NS,NI : INTEGER;
     SAMPLE: STRING;
     RE, RE2,RE3,RE4,RE5,RE6,RE7,LE,LE2,LE3,LE4,LE5,LE6,LE7 : REAL;
     P,P2,P3,P4,P5,P6,P7,PA,PA2,PA3,PA4,PA5,PA6,PA7 : REAL;
     PB,PB2,PB3,PB4,PB5,PB6,PB7 : REAL;
     DIAMETER,LENGTH,SL,SV,DIFCOEF,DO,QDIFF,QSTAR,QSTARO,CO,HSOL : REAL;
     CSOLVUS,SC,QSTARC,QSTART,QSTARTG,A,B,C,D,X,Y,Z,XX,YY,ZZ : REAL;
     XXX,YYY,ZZZ,ETOTAL,SC1,SC2,TEMPA,TEMPB,XMAX,C2PHASE : REAL;
     FRACTION,C1,C2,CIF,CG,T1,T2,CAVG,TIME,XDIST,TI,TTE,TS : REAL;
     ITS,E,EFIELD,EVALENCE,JDT,JE,FC,G,H,I : REAL;
     FI : TEXT;

PROCEDURE INITVAR;      {INITIALIZE VARIABLES}
   BEGIN
      FOR F:= 0 TO 100 DO
         BEGIN
            TSA[F]:=0; J[F]:=0; T[F]:=0; TG[F]:=0
         END;
      SL:=0; SV:=0; DIFCOEF:=0; QSTAR:=0; QSTARC:=0; QSTART:=0;
      QSTARTG:=0; TEMPA:=0; TEMPB:=0; P:=0; PA:=0; PB:=0;
      CSOLVUS:=0; C2PHASE:=0; EVALENCE:=0
   END;    {END OF PROCEDURE INITVAR}

PROCEDURE SAMPLEDATA;          {ENTER SAMPLE DATA}
   BEGIN
      WRITELN ('****** SAMPLE DATA ******');
      WRITELN; WRITELN; WRITELN;
      WRITELN ('WHAT IS THE SAMPLE ALLOY?');
      WRITELN; WRITELN;
      READLN (SAMPLE);
      WRITELN; WRITELN; WRITELN;
      WRITE ('WHAT ARE THE SAMPLE LENGTH AND DIAMETER');
```

```
      WRITELN (' IN CENTIMETERS?');
      WRITELN; WRITELN;
      READLN (LENGTH,DIAMETER);
      WRITELN; WRITELN; WRITELN;
      WRITELN ('HOW MANY SECTIONS WILL THE SAMPLE BE DIVIDED INTO?');
      WRITELN; WRITELN;
      READLN (NS);
      SL:=LENGTH/NS;
      SV:= PI * SQR(DIAMETER/2) * SL;
      NI:= NS-1;
      WRITELN; WRITELN; WRITELN;
      WRITE ('WHAT IS THE TIME INCREMENT IN MINUTES AND TOTAL TIME ');
      WRITELN ('OF EXPERIMENT IN HOURS?');
      WRITELN; WRITELN;
      READLN (TI,TTE);
      TI:= TI/60     CONVERTS TIME INCREMENT TO HOURS
   END;    {END OF PROCEDURE SAMPLEDATA}

PROCEDURE CONCENTRATIONS;        {INITIALIZES CONCENTRATION OF SAMPLE}

   PROCEDURE ONE;
      BEGIN
         WRITELN; WRITELN;
         WRITE ('WHAT IS THE SOLUTE CONCENTRATION FOR ALL OF THE ');
         WRITELN ('SEGMENTS?');
         WRITELN; WRITELN;
         READLN (SC);
         FOR F:= 0 TO NS DO
            BEGIN
               TSA[F]:= SC * SV;
               CONC[F]:= SC
            END
      END;        {END OF PROCEDURE ONE}

PROCEDURE TWO;
   BEGIN
      WRITELN; WRITELN;
      WRITELN ('WHAT IS THE SOLUTE CONCENTRATION OF THE FIRST HALF');
      WRITELN ('AND THE SECOND HALF OF THE SAMPLE?');
      WRITELN; WRITELN;
      READLN (SC1,SC2);
      FOR F:=1 TO (NS DIV 2) DO
         BEGIN
            TSA[F]:= SC1 * SV;
            CONC[F]:= SC1
         END;
      FOR F:=((NS DIV 2) + 1) TO NS DO
         BEGIN
            TSA[F]:= SC2 * SV;
            CONC[F]:= SC2
```

```
        END
    END;        {END OF PROCEDURE TWO}

PROCEDURE THREE;
    BEGIN
       WRITELN; WRITELN;
       WRITELN ('WHAT IS THE CONCENTRATION OF SECTION ONE AND THE ');
       WRITELN ('CONCENTRATION OF THE REMAINING SECTIONS?');
       WRITELN; WRITELN;
       READLN (SC1,SC2);
       TSA[1]:= SC2 * SV;
       CONC[1]:= SC1;
       FOR F:= 2 TO NS DO
          BEGIN
             TSA[F]:= SC2 * SV;
             CONC[F]:= SC2
          END
    END;        {END OF PROCEDURE THREE}

PROCEDURE FOUR;
    BEGIN
       WRITELN; WRITELN;
       FOR F:= 1 TO NS DO
          BEGIN
             WRITELN ('WHAT IS THE CONCENTRATION OF SEGMENT ',F,'?');
             WRITELN; WRITELN;
             READLN (SC);
             TSA[F]:= SC * SV;
             CONC[F]:= SC
          END
    END;        {END OF PROCEDURE FOUR}

BEGIN
    WRITELN; WRITELN;
    WRITELN ('HOW DO YOU WISH TO SPECIFY THE SEGMENT CONCENTRATIONS?');
    WRITELN;
    WRITELN ('   1.  THE SAME CONCENTRATION FOR ALL SEGMENTS');
    WRITELN;
    WRITELN ('   2.  ONE HALF OF THE SEGMENTS AT ONE CONCENTRATION');
    WRITELN ('       AND THE OTHER HALF AT ANOTHER CONCENTRATION');
    WRITELN ('       (DIFFUSION COUPLE)');
    WRITELN ('   3.  THE FIRST SEGMENT AT ONE CONCENTRATION AND THE');
    WRITELN ('       REMAINING SEGMENTS AT ANOTHER CONCENTRATION');
    WRITELN ('       (RADIOACTIVE TRACER TECHNIQUE FOR DIFFUSION)');
    WRITELN ('   4.  SPECIFY EACH SEGMENT CONCENTRATION INDIVIDUALLY');
    WRITELN;
    WRITELN ('ENTER A NUMBER');
    WRITELN;
    READLN (NUMBER);
    CASE NUMBER OF
```

```
      1: ONE;
      2: TWO;
      3: THREE;
      4: FOUR;
   END          {CASE}
END;          {END OF PROCEDURE CONCENTRATIONS}

PROCEDURE TEMPPROFILE;
   BEGIN
      WRITELN; WRITELN; WRITELN;
      WRITE ('WHAT ARE THE COEFFICIENTS IN THE TEMPERATURE EQUATION?');
      WRITELN ('(A,B,C,D,E,G,H,I)');
      WRITELN; WRITELN;
      READLN (A,B,C,D,E,G,H,I);
      WRITELN; WRITELN; WRITELN;
      WRITELN ('AT WHAT POSITION ALONG THE SAMPLE IS THE TEMPERATURE');
      WRITELN ('A MAXIMUM?  (FOR EXAMPLE--SAMPLE MIDDLE: 0.5');
      WRITELN; WRITELN;
      READLN (XMAX);
      WRITELN; WRITELN; WRITELN;
   END;          {END OF PROCEDURE TEMPPROFILE}

PROCEDURE DIFFDATA;
   BEGIN
      WRITELN ('****** DIFFUSION DATA ******');
      WRITELN; WRITELN;
      WRITELN ('WHAT IS THE ACTIVATION ENERGY FOR SOLUTE DIFFUSION');
      WRITELN ('IN CAL/MOLE ?');
      WRITELN; WRITELN;
      READLN (QDIFF);
      WRITELN; WRITELN; WRITELN;
      WRITELN ('WHAT IS THE DIFFUSION CONSTANT IN SQUARE CENTIMETERS');
      WRITELN ('PER SECOND ?');
      WRITELN; WRITELN;
      READLN (D0);
      WRITELN; WRITELN; WRITELN
   END;          {END OF PROCEDURE DIFFDATA}

PROCEDURE THERMDATA;
    BEGIN
      WRITELN ('****** THERMOTRANSPORT DATA ******');
      WRITELN; WRITELN;
      WRITELN ('WHAT IS THE QSTAR CONSTANT IN CAL/MOLE ?');
      WRITELN; WRITELN;
      READLN (QSTAR0);
      WRITELN; WRITELN; WRITELN;
      WRITELN ('WHAT ARE THE COEFFICIENTS IN THE EQUATION FOR THE ');
      WRITELN ('CONCENTRATION DEPENDENCE OF QSTAR ? (X,Y,Z)');
     .WRITELN; WRITELN;
      READLN (X,Y,Z);
```

```
      WRITELN; WRITELN; WRITELN;
      WRITELN ('WHAT ARE THE COEFFICIENTS IN THE EQUATION FOR THE ');
      WRITELN ('TEMPERATURE DEPENDENCE OF QSTAR ? (XX,YY,ZZ)');
      WRITELN; WRITELN;
      READLN (XX,YY,ZZ);
      WRITELN; WRITELN; WRITELN;
      WRITELN ('WHAT ARE THE COEFFICIENTS IN THE EQUATION FOR THE ');
      WRITELN ('TEMPERATURE GRADIENT DEPENDENCE OF QSTAR ?');
      WRITELN (' (XXX,YYY,ZZZ) ');
      WRITELN; WRITELN; WRITELN;
      READLN (XXX,YYY,ZZZ)
   END;     {END OF PROCEDURE THERMDATA}

PROCEDURE ELECTRODATA;
   BEGIN
      WRITELN ('****** ELECTROTRANSPORT DATA ******');
      WRITELN; WRITELN; WRITELN;
      WRITELN ('WHAT IS THE ELECTRIC FIELD IN V/CM AND');
      WRITELN ('EFFECTIVE VALENCE ?');
      WRITELN; WRITELN;
      READLN (EFIELD,EVALENCE)
   END;       {END OF PROCEDURE ELECTRODATA}

PROCEDURE SOLDATA;
   BEGIN
      WRITELN ('****** SOLUBILITY DATA ******');
      WRITELN; WRITELN; WRITELN;
      WRITELN ('WHAT IS THE CONCENTRATION CONSTANT IN AT.% AND THE');
      WRITELN ('HEAT OF SOLUTION IN CAL/MOLE ?');
      WRITELN; WRITELN; WRITELN;
      READLN (CO,HSOL);
      WRITELN; WRITELN;
      WRITELN ('WHAT IS THE CONCENTRATION OF THE SECOND-PHASE ');
      WRITELN ('COMPOUND ?');
      WRITELN; WRITELN; WRITELN;
      READLN (C2PHASE)
   END;       {END OF PROCEDURE SOLDATA}

PROCEDURE ENDTEMP;
   BEGIN
      LE:= -XMAX * LENGTH;
      RE:= (1-XMAX) * LENGTH;          TEMPERATURE OF ROD ENDS}
      LE2:=LE*LE; LE3:=LE*LE*LE; LE4:=LE*LE*LE*LE; LE5:=LE*LE*LE*LE*LE;
      LE6:=LE*LE*LE*LE*LE*LE; LE7:=LE*LE*LE*LE*LE*LE*LE;
      RE2:=RE*RE; RE3:=RE*RE*RE; RE4:=RE*RE*RE*RE; RE5:=RE*RE*RE*RE*RE;
      RE6:=RE*RE*RE*RE*RE*RE; RE7:=RE*RE*RE*RE*RE*RE*RE;
      T[0]:=A+B*LE+C*LE2+D*LE3+F*LE4+G*LE5+H*LE6+I*LE7;
      T[NS]:=A+B*RE+C*RE2+D*RE3+F*RE4+G*RE5+H*RE6+I*RE7;
   END;         {END OF PROCEDURE ENDTEMP}
```

```
PROCEDURE IFTANDTG;
   BEGIN
      FOR F:=1 TO NI DO
        BEGIN
           P:=(F*SL) - (XMAX*LENGTH);
           PB:=(P-(SL/2));
           PA:=(P+(SL/2));
           P2:=P*P; P3:=P*P*P; P4:=P*P*P*P; P5:=P*P*P*P*P;
           P6:=P*P*P*P*P*P; P7:=P*P*P*P*P*P*P;
           PA2:=PA*PA; PA3:=PA*PA*PA; PA4:=PA*PA*PA*PA;
           PA5:=PA*PA*PA*PA*PA; PA6:=PA*PA*PA*PA*PA*PA;
           PA7:=PA*PA*PA*PA*PA*PA*PA;
           PB2:=PB*PB; PB3:=PB*PB*PB; PB4:=PB*PB*PB*PB;
           PB5:=PB*PB*PB*PB*PB; PB6:=PB*PB*PB*PB*PB*PB;
           PB7:=PB*PB*PB*PB*PB*PB*PB;
           T[F]:=A+B*P+C*P2+D*P3+E*PB4+G*PB5+H*PB6+I*PB7;
           TEMPB:=A+B*PB+C*PB2+D*PB3+E*PB4+G*PB5+H*PB6+I*PB7;
           TEMPA:=A+B*PA+C*PA2+D*PA3+E*PA4+G*PA5+H*PA6+I*PA7;
           TG[F]:=(TEMPA-TEMPB)/SL
        END
   END;                {END OF PROCEDURE IFTANDTG}

PROCEDURE VALUES;
   BEGIN
      CSOLVUS:= C0 * EXP(-HSOL/(RC*T[M]));
      DIFCOEF:= D0 * EXP(-QDIFF/(RC*T[M]));
      QSTARC:=X*CONC[M]+Y*(CONC[M]*CONC[M])+Z*(CONC[M]*CONC[M]*CONC[M]);
      QSTART:=XX*T[M] + YY*(T[M]*T[M]) + ZZ*(T[M]*T[M]*T[M]);
      QSTARTG:=XXX*TG[M] + YYY*(TG[M]*TG[M]) + ZZZ*(TG[M]*TG[M]*TG[M]);
      QSTAR:= QSTAR0 + QSTARC + QSTART + QSTARTG;
      T1:= (T[M-1] + T[M])/2;
      T2:= (T[M] + T[M+1])/2;
      C1:= C0 * EXP(-HSOL/(RC*T1));
      C2:= C0 * EXP(-HSOL/(RC*T2));
      ETOTAL:= HSOL + QSTAR
   END;     {END OF PROCEDURE VALUES}

PROCEDURE CALCFLUX;
   BEGIN
      FC:=96500.0  {FARADAY CONSTANT FOR ELECTROTRANSPORT COMPUTATIONS}
      FOR M:= 1 TO NI DO
         BEGIN
            VALUES;
            IF (CONC[M] =C1) AND (CONC[M+1] =C2)
               THEN BEGIN
                 CAVG:= (CONC[M] + CONC[M+1])/2;
                 FRACTION:= (C2PHASE-CAVG)/(C2PHASE-CSOLVUS);
                 JDT:=(-DIFCOEF*CSOLVUS*FRACTION*ETOTAL*TG[M])/(RC*
                      SQR(T[M]));
                  JE:=(-DIFCOEF*CSOLVUS*FRACTION*FC*EVALENCE*
```

```
                    EFIELD)/(RJ*T[M]);
                J[M]:= JDT + JE
             END;
          IF (CONC[M] C1) AND (CONC[M+1]) C2)
             THEN BEGIN
                CIF:= (CONC[M] + CONC[M+1])/2;
                CG:= (CONC[M+1] - CONC[M])/SL;
                JDT:=-DIFCOEF*(CG + (QSTAR*(CIF)*
                     TG[M])/(RC*SQR(T[M])));
                JE:=(-DIFCOEFD*CIF*FC*EVALENCE*EFIELD)/(RJ*T[M]);
                J[M]:= JDT + JE
             END;
          IF (CONC[M] C1) AND (CONC[M+1] C2)
             THEN BEGIN
                CIF:= (CONC[M] + C2)/2;
                CG:= (C2-CONC[M])/SL;
                JDT:= -DIFCOEF*(CG + (QSTAR*(CIF)*TG[M])/(RC*
                      SQR(T[M])));
                JE:= (-DIFCOEF*CIF*FC*EVALENCE*EFIELD)/(RJ*T[M]);
                J[M]:= JDT + JE
             END;
          IF (CONC[M] C1) AND (CONC[M+1] C2)
             THEN BEGIN
                CIF:= (C1 + CONC[M])/2;
                CG:= (CONC[M+1] - C1)/SL;
                JDT:= -DIFCOEF*(CG + (QSTAR*(CIF)*TG[M])/(RC*
                      SQR(T[M])));
                JE:= (-DIFCOEF*CIF*FC*EVALENCE*EFIELD)/(RJ*T[M]);
                J[M]:= JDT + JE
             END
       END
   END;                {END OF PROCEDURE CALCFLUX}

PROCEDURE NEWCONC;
   BEGIN
      FOR NF:= 1 TO (NS) DO
         BEGIN
            TSA[N]:=TSA[N]+(J[N-1]-J[N])*TI*PI*3600*SQR(DIAMETER/2);
            CONC[N]:=TSA[N]/SV;
            IF CONC[N] 0 THEN CONC[N]:=1E-10
         END
   END;     {END OF PROCEDURE NEWCONC}

PROCEDURE PRINTDATA;
   BEGIN
      REWRITE (FI,'CONC.TEXT');
      WRITELN (FI,'SAMPLE: ',SAMPLE);
      WRITELN (FI,'SAMPLE LENGTH: ',LENGTH:5:2,' cm');
      WRITELN (FI,'NUMBER OF SECTIONS: ',NS:3);
      WRITELN (FI,'TIME INTERVAL: ',TI*60,' min');
```

```
      WRITELN (FI,'TOTAL SIMULATED TIME: ',TTE:4,' h');
      WRITELN (FI,'ELECTRIC FIELD: ',EFIELD:6:3,' V/cm');
      WRITELN (FI,'EFFECTIVE VALENCE: ',EVALENCE:4:1);
      WRITELN (FI); WRITELN (FI);
      WRITE   (FI,'SEGMENT #   X(CM)      CONC    ln(CONC)    T(K)');
      WRITELN (FI,'    1/T(K)');
      FOR O:= 1 TO (NS) DO
         BEGIN
            TS:= (T[O] + T[O-1])/2;
            ITS:= 1/TS;
            XDIST:= (O*SL)-(0.5*SL);
            CSOLVUS:= CO * EXP(-HSOL/(RC*TS));
            WRITE (FI,O:8,XDIST:10:4,CONC[O]:10:4,LN(CONC[O]):10:4);
            WRITELN (FI, TS:10:2,ITS:10,CSOLVUS:10:4)
         END;
      CLOSE (FI,LOCK)
   END;     {END OF PROCEDURE PRINTDATA}

BEGIN            {****** MAIN PROGRAM *******}
   INITVAR;
   SAMPLEDATA;
   CONCENTRATIONS;
   TEMPPROFILE;
   DIFFDATA;
   THERMDATA;
   ELECTRODATA;
   SOLDATA;
   ENDTEMP;
   IFTANDTG;
   TIME:=TI;
   WHILE TIME = TTE DO
      BEGIN
         CALCFLUX;
         NEWCONC;
         TIME:= TIME + TI
      END;
   PRINTDATA
END.          {****** END OF PROGRAM TRANSPORT ******}
```